Abstracts of the Annual Meeting of Planetary Geologic Mappers, Greenbelt, MD 2011

Edited by:

Leslie F. Bleamaster, III
Planetary Science Institute, Tucson, AZ

James A. Skinner, Jr.
U. S. Geological Survey, Flagstaff, AZ

Kenneth L. Tanaka
U. S. Geological Survey, Flagstaff, AZ

Michael S. Kelley
NASA Headquarters, Washington, DC

NOTE: This is a preliminary posting in advance of the final volume to be published as a NASA Conference Paper. Abstracts in this volume can be cited using the following format:

Graupner, M. and Hansen, V.L., 2011, Structural and Geologic Mapping of Tellus Region, Venus, *in* Bleamaster, L. F., III, and others, eds., Abstracts of the Annual Meeting of Planetary Geologic Mappers, Flagstaff, AZ, June 21-24, 2011.

Report of the Annual Meeting of Planetary Geologic Mappers
NASA Goddard Space Flight Center
Greenbelt, Maryland
June 21 to 24, 2011

The construction of cartographic products to illustrate the surface characteristics of planetary bodies beyond our own has historically been met with particular challenges. These challenges can be overcome through innovative adaptation to burgeoning data sets and analytical technologies as well as a focused forum within which to present, critique, and discuss both technical approaches and scientific results. To assist, the Annual Meeting of Planetary Geologic Mappers (PGM) provides a unique forum for planetary scientists to address these challenges through the exchange of ideas and experiences relating to the creation, publication, and promotion of planetary geologic maps. PGM 2011 was convened by NASA's Planetary Geology and Geophysics (PGG) program Geologic Mapping Subcommittee (GEMS) Chair Les Bleamaster (Planetary Science Institute (PSI) and Trinity University), USGS Geologic Map Coordinator Ken Tanaka (U.S. Geological Survey (USGS) Astrogeology Science Center), and PGG Program Scientist Mike Kelley (NASA Headquarters) on June 21 to 24, 2011. Scott Mest (PSI and NASA Goddard Space Flight Center (GSFC)) hosted the meeting at GSFC in Greenbelt, Maryland. This volume contains summaries of PGM 2011 events and discussions, a schedule of presentations, submitted abstracts (attending and *in absentia*), and the 2011 Planetary Geologic Mappers' Handbook (including updates since prior annual versions).

The meeting began with a one-day Geographic Information System (GIS) "round-table" presentation, discussion, and question-answer session on Tuesday, June 21, which was attended by 12 people. The informal event was led by Trent Hare, Corey Fortezzo, and Jim Skinner (all of USGS) and focused primarily on digital data set acquisition and display, vector editing, and updates/changes in recent GIS program releases. As in past years, the goal of the GIS round-table was to help promote digital mapping, review, and publication standards, as recommended by USGS and required by PGG.

Science, programmatic, and technical presentations were held on Wednesday, June 22 and Thursday, June 23. Presentations began with welcoming comments by Les Bleamaster, logistical points by Scott Mest, an update on the status of mapping projects and publications by Ken Tanaka, and a summary of the current state of the PGG program generally and PGG-funded map projects specifically by Mike Kelley. Programmatic presentations were followed by a technical presentation by Trent Hare, who reminded the community of the resources available to planetary mappers, including the USGS Photogrammetry Lab, the (newly-funded) Mapping, Remote Sensing, Cartography, Technology, and Research (MRCTR) GIS Lab, and an upcoming submission and tracking website to assist with the review and publication of NASA-funded geologic maps.

Twenty six abstracts were submitted this year (15 Mars, 5 Venus, 3 Lunar, 1 Io, 1 Mercury, and 1 technical). From these, 19 were scheduled for presentation, focusing on ongoing, variously scaled map-based science investigations. Detailed discussions of particular projects were promoted by accompanying hard-copy maps and posters, which were viewed along the walls of the presentation hall during scheduled break-out sessions.

Presentations on Wednesday, June 22 focused on Io, the Moon, Mercury, and Venus, each at a variety of map scales. A reception and group dinner was organized by Scott Mest at the NASA GSFC recreation center on Wednesday evening. Presentations on Thursday, June 23 focused exclusively on Mars and ranged from global (1:20,000,000) to local (1:24,000) map scales using a variety of data sets.

Science presentations on Thursday were followed by a discussion on various aspects of the current state of the mapping program. Les Bleamaster announced that he will be stepping down as GEMS chair and that, after a few months of programmatic transition, Jim Skinner will take over responsibilities in late 2011. Discussions also included general and specific approaches to reinforce the publication, promotion, and use of geologic maps as contextual scientific products within the planetary science community. Of particular relevance was a discussion regarding the means by which funds are allotted for USGS review and publication, particularly in light that several NASA programs (other than PGG) allow for the production of PGG-funded geologic maps. There was broad consensus that the mapping community requires clarity on how the health of the planetary geologic mapping program can not only be sustained but improved. The meeting ended with a guided tour of NASA GSFC spacecraft testing facilities on Friday, June 24.

SCHEDULE OF PRESENTATIONS

Tuesday, June 21

Time		Topic
10:00 am		Arrive/Setup
10:30		General GIS project discussion
12:00 pm	LUNCH	
1:00		General GIS project discussion
2:00		Editing in Arc 10
3:30	ADJOURN	

Wednesday, June 22

Time	Planet/Body	Topic
8:30 am		Arrive/Setup
9:00		Welcome (L. Bleamaster)
9:10		Meeting logistics (S. Mest)
9:15		Map Coordinator update (K. Tanaka)
9:30		NASA PGG update (M. Kelley)
9:50		GIS Techniques and Resources (T. Hare)
10:10	POSTER SESSSION/BREAK	
10:30	Io	Io Global Map (D. Williams)
10:50	Moon	Aristarchus Plateau Region (T. Gregg)
11:10	Moon	W. South Pole-Aitken Basin (W. Yingst)
11:30	LUNCH (GEMS Meeting)	
1:30 pm	Mercury	Caloris Basin (D. Buczkowski)
1:50	Venus	Quads V-2, V-57 (J. Head)
2:20	Venus	Quad V-18 (E. McGowan)
2:50	Venus	Quads V-50, V-29 (L. Bleamaster)
3:10	POSTER SESSION/BREAK	
3:30	ADJOURN	
4:30 – 7:00	GROUP DINNER (GSFC Recreation Center)	

Thursday, June 23

Time	Planet/Body	Topic
8:30		GIS Toolset (T. Hare)
8:50	Mars	Global Map (K. Tanaka)
9:10	Mars	Candor Chasma Structure (C. Okubo)
9:30	Mars	Medusae Fossae (J. Zimbelman)
9:50	POSTER SESSION/BREAK	
10:40	Mars	Tharsis Montes (J. Bleacher)
11:00	Mars	Olympus Mons (D. Williams)
11:20	Mars	Hellas Region (D. Crown)
11:40	Mars	Scandia Region (K. Tanaka)
12:00	LUNCH	
1:30	Mars	Libya Montes Geology (J. Skinner)
1:50	Mars	Libya Montes Composition (D. Rogers/K. Seelos)
2:10	Mars	Mawrth Vallis/Nili Fossae (L. Bleamaster)
2:30	POSTER SESSION/BREAK	
2:50	Mars	Margaritifer (S. Wilson)
3:30	Mars	Arabia/Noachis Boundary (C. Fortezzo)
3:50	GROUP DISCUSSION	
5:00	ADJOURN	

Friday, June 24

Time	Topic
10:00 – 11:30	GSFC Tour

CONTENTS *(sorted by body, then alphabetically by author)*

Io

Other

Appendix

MAPPING AND ANALYSIS OF THE INTRA-EJECTA DARK PLAINS OF CALORIS BASIN, MERCURY. D.L. Buczkowski and K.D. Seelos, Johns Hopkins University Applied Physics Laboratory, Laurel, MD 20723, Debra.Buczkowski@jhuapl.edu.

Introduction: Two Mercury quadrangles based on Mariner 10 data cover the Caloris basin (Fig. 1): H-8 Tolstoj [1] and H-3 Shakespeare [2]. The dark annulus identified in MESSENGER data corresponds well to the mapped location of certain formations [3], primarily the Odin Formation. The Odin Formation is described in the quadrangle maps as a unit of low, closely spaced knobs separated by a smooth, plains-like material and was interpreted as ejecta from the Caloris impact. Schaber and McCauley [1980] observed that the intra-ejecta plains in the Odin Formation resemble the Smooth Plains unit that was also prevalent in the H-8 and H-3 quadrangles outside of Caloris. They state that these plains were included as part of the Odin Formation for mapping convenience.

Crater counts based on MESSENGER imagery indicate that the Odin intra-ejecta plains are younger than the Caloris floor plains within the basin [4,5]. This is inconsistent with the intra-ejecta plains being Caloris ejecta but is consistent with the plains being fingers of the smooth plains unit embaying the Odin ejecta knobs.

However, the intra-ejecta plains are not the same color as the smooth plains in Mercury Dual Imaging System (MDIS) data [3]; while the smooth plains are bright, the intra-ejecta plains are the same dark color as the ejecta knobs. A possible explanation is that the Odin knobs and intra-ejecta dark plains represent two facies of dark basement material excavated by the Caloris impact. Alternately, the intra-ejecta plains could represent a dark volcanic flow, distinct from the bright smooth plains volcanic flow; however, it would have to be a volcanic flow restricted to a region circumferential to the basin. A third possibility is that the intra-ejecta dark plains are a pre-Caloris smooth material (possibly the Intercrater Plains unit) darkened by a thin layer of superposed dark Odin material.

This abstract outlines the progress associated with a new mapping project of the Caloris basin, intended to improve our knowledge of the geology and geologic history of the basin, and thus facilitate an understanding of the thermal evolution of this region of Mercury.

Previous Caloris basin mapping: A detailed analysis of the Odin Formation performed by [5] noted that the unit is easily recognizable circum-Caloris in the MESSENGER data and concluded that the Odin Formation knobs are Caloris ejecta blocks that have been mostly embayed and buried by younger volcanic deposits. They found that MDIS color data supported this hypothesis and divided the formation into two sub-units: knobby plains and smooth plains.

High-resolution mapping of the intra-ejecta dark plains: We are using the new high resolution (200-300 m/p) imaging data from the MDIS instrument to create a new geomorphic map of the dark annulus around the Caloris basin. We also utilize a principle component map [3] to distinguish subtle differences in the color data. In the principle component map green represents the second principle component (PC2), which reflects variations between light and dark materials. Meanwhile, red is the inverted PC2 and blue is the ratio of normalized reflectance at 480/1000 nm, which highlights fresh ejecta.

We are mapping all contacts between bright and dark materials within the intra-ejecta plains, as determined in the principle component map, as sub-units of the Odin Formation (Fig 2a). All knobs are mapped individually and their color (either dark or bright) is noted (Fig 2b). Ejecta blankets from local craters (both extent and color) are mapped separately (Fig 2a).

All craters are mapped according to a newly devised crater classification scheme. The crater classification used in the Tolstoj and Shakespeare quadrangles [1,2] and formalized in 1981 [6] was based on degree of crater degradation. Our classification scheme includes both degradation state and level and type of infilling. Current classifications include: 1) blue and pristine, 2) fresh but not blue, 3) intact rim and superposed, 4) intact rim and embayed, 5) degraded rim and superposed, 6) degraded rim and embayed, 7) very degraded and superposed, 8) very degraded and embayed and 9) little to no rim. We expect these classifications will change as mapping continues.

We continue to look for unequivocal evidence of volcanic activity within the dark annulus and the Odin Formation, such as vents and flow lobes. To date we have been utilizing MDIS fly-by data; as orbital data becomes available we will enhance our search for these features with the newer, higher-resolution imagery.

Preliminary Observations: The Odin Formation shows two distinct sub-units: a dark sub-unit and a (relatively) bright sub-unit. The dark sub-unit has a higher concentration of knobs, knobs that are both bright and dark and craters that are both embayed and superposed. Meanwhile, the bright sub-unit has a lower concentration of knobs, knobs that are predominantly bright and craters that are fresh and/or superposed. Outcrops of the bright material can be associated with crater ejecta blankets, but are not always.

There is an inherent difficulty in determining if there is an age difference between the dark and bright sub-units. Crater counts on sub-units may be affected by the relatively small size of craters (< 20 km). Recent work by [7] indicates that secondary craters on Mercury can be as large as 25 km. More of the Caloris intra-ejecta dark plains need to be mapped, to provide a large enough area and crater population for viable counting. However, the observation that dark sub-unit craters encompass all crater classifications while bright sub-unit craters are almost uniformly fresh and superposed does imply that the bright sub-unit is younger.

Ongoing work: We will continue to identify all craters within the dark annulus surrounding the basin in the MESSENGER MDIS data. Each primary crater will be assigned a classification, as discussed earlier. Secondary craters, which usually have morphologies distinct from primary craters and they tend to occur in either clusters or chains, will be mapped separately.

Craters identified while mapping will be compared to the resultant geomorphic units. The diameters of craters superposed on each individual surface unit will be measured and counted, and the area covered by each geomorphic unit will be determined. Crater counts will be normalized to a common area of one million square kilometers in order to gener-

ate a crater size-frequency distribution (SFD) for each geomorphic unit. The SFDs are plotted on a log-log graph with crater diameter against the normalized cumulative crater count. Younger surfaces have SFDs that plot to the left and below older surfaces and so the relative ages of multiple units can be determined. Statistical uncertainties and plotting techniques will follow the form outlined by the Crater Analysis Techniques Working Group [8].

Present mapped stratigraphy of the Caloris basin does not take into account the nature of the Odin Formation intra-ejecta dark plains. If these plains are in fact lava flows younger than the Odin ejecta and distinct from the smooth plains unit, then this needs to be reflected in both the cross-section and a stratigraphic column. Similarly, the cross-section should more clearly reflect the stratigraphy of the Caloris units if the Odin Formation is comprised of multiple facies (hummocks and plains) of excavated dark basement material. If the intra-ejecta dark plains are smooth plains material embaying the ejecta, this too should be somehow reflected in any stratigraphic analysis of the basin.

Our new crater counts will help determine the timing relations between the units identified while mapping. We can then refine the stratigraphy of the Caloris basin units.

References: [1] Schaber and McCauley (1980) USGS Map I-1199. [2] Guest and Greeley (1983) USGS Map I-1408. [3] Murchie et al. (2008) *Science 321*, 73-76. [4] Strom et al. (2008) *Science 321*, 79-81. [5] Fasset et al. (2009) *Earth Planet. Sci Lett 285*, 297-308. [6] McCauley et al. (1981) *Icarus 47*, 184-202. [7] Strom et al. (2011) LPSC abs 1079. [8] Crater Analysis Techniques Working Group (1979) *Icarus 37*, 467-474.

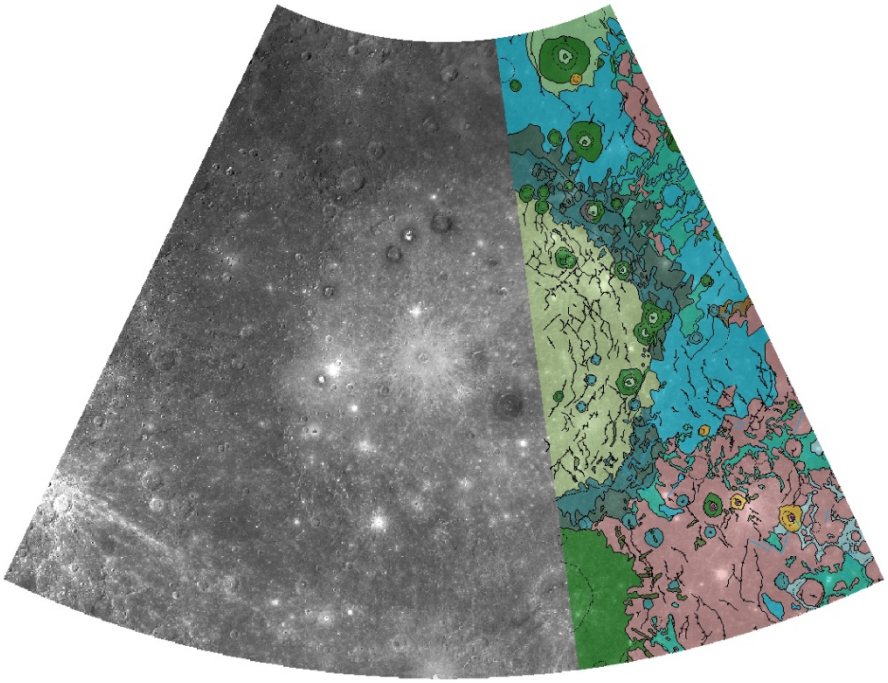

Figure 1. MESSENGER mosaic of the Caloris basin overlain by portions of the H-8 Tolstoj [1] and H-3 Shakespeare [2] quadrangles. Odin Formation is light blue; Smooth Plains are pink.

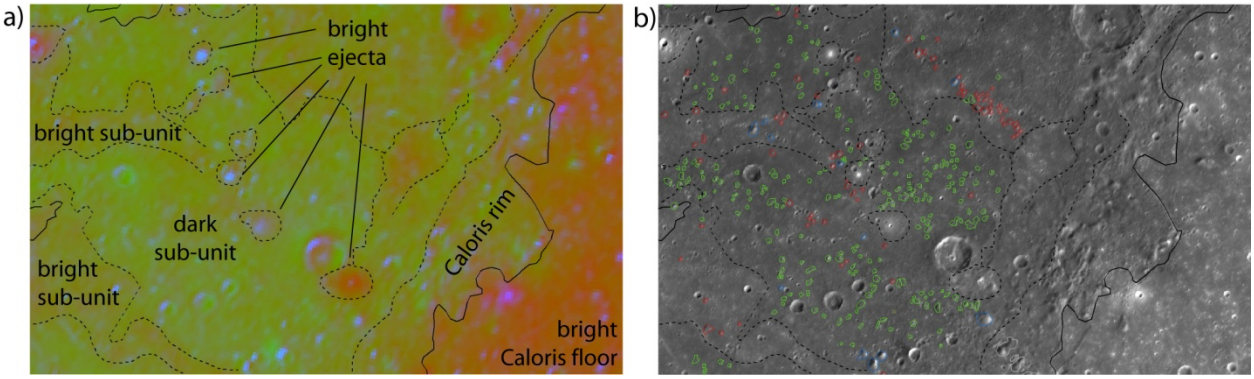

Figure 2. Part of Caloris dark annulus used as Odin Formation example in [5]. a) Principle component map, to demonstrate how bright and dark sub-units were mapped. Sub-units are labeled. b) Odin Formation knobs, shown with sub-unit contacts (dashed lines). Green knobs are dark in the MDIS principle component map; red are light. Note that the majority of knobs are identified in the dark sub-unit.

VOLCANIC RESURFACING STYLES OF THE BETA-ATLA-THEMIS (BAT) PROVINCE, VENUS. RESULTS FROM GEOLOGIC MAPPING STUDIES OF THE ISABELLA (V-50) AND DEVANA CHASMA (V-29) QUADRANGLES. L.F. Bleamaster, III[1,2], [1]Planetary Science Institute, 1700 E. Ft. Lowell Rd., Suite 106, Tucson, AZ, 85719, [2]Trinity University Geosciences Department, One Trinity Place #45, San Antonio, TX, 78212; lbleamas@psi.edu.

Introduction: The BAT (Beta-Atla-Themis) region on Venus is of particular interest with respect to evaluating global paradigms regarding Venus' geologic history, tectonic and thermal evolution, and resurfacing styles considering it is "ringed" by volcano-tectonic troughs (Parga, Hecate, and Devana Chasmata) and has an anomalously high-density of volcanic features with concentrations 2-4 times the global average [1; Figure 1]. The BAT is also spatially coincident with relatively "young terrain" as shown by Average Surface Model Ages (ASMA) [2,3]. Of late, specific locations within and surrounding the BAT have been recognized as potential sites of active volcanism based on newly acquired VIRTIS emissivity data, geophysical modeling, and geologic mapping (Imdr Regio [4] and Shiwanokia Corona [5,6,7]).

Two 1:5 million-scale quadrangles, Isabella (V-50) and Devana Chasma (V-29), are located on opposite sides of the BAT region and present mapping provides a means to compare the styles and sequence of materials and processes that have occurred.

Data Sets & Methodology: Aiming to discover the types of processes that have shaped the Venusian surface, geologic mapping started with the demarcation of major structural and morphologic features (lava flow boundaries, shield fields and edifices, radial and concentric deformation zones) and followed with the formal delineation of geologic map units. Stratigraphic, embayment, and crosscutting relationships as well as crater morphology and crater halo degradation [8] are used to determine the relative ages of map units. All data used were acquired during NASA's Magellan mission (operational 1989-1994) and includes: Synthetic Aperture Radar (SAR; basemap provided by the US Geological Survey at 75 meter/pixel), altimetry and reflectance (~10 x 10 km footprint), and emissivity (~20 x 20 km footprint). Mapping is facilitated with the use of a georeferenced digital synthetic stereo (red-blue anaglyph, which merges SAR and altimetry). ESRI ArcGIS software is used along with a WACOM 21 inch interactive monitor and digitizing pen. Location features and linear features are mapped at a scale of 1:200,000; geo-contacts are mapped at a scale of 1:300,000. The accuracy of line work is controlled using streaming (500 map units) and snapping tolerances (250 map units). Upon completion of mapping, the geodatabase within ArcGIS will allow for efficient data analysis.

Devana Chasma: The V-29 quadrangle is situated over the northeastern apex of the Beta-Atla-Themis (BAT) region and includes the southern half of Beta Regio, the northern and transitional segments of the Devana Chasma complex, the northern reaches of Phoebe Regio, Hyndla Regio, Nedolya Tesserae, and several smaller volcano-tectonic centers and impact craters. Devana Chasma is a narrow (~150 km), 1000 km long segmented topographic trough (1-3 km deep with respect to the surrounding terrain), which accommodates 3 to 9 kilometers of extension [9]. Devana Chasma is one of three radiating arms from Beta Regio and trends south. This topographic trough marks a physiographic divide (although discovered to be very subtle with respect to broad material units) between the relatively young Beta-Atla-Themis region to the west and the surrounding older highlands and plains to the east in Guinevere Planitia. Approximately midway down the map area from Beta Regio, Devana Chasma's lineament density decreases and changes trend to the southeast meeting with a north trending set of lineaments. This same mid-section is also marked by merging flows that emanate from volcanic centers located along the rift axis. Distinct relative timing markers are sparse, however when present, they often convey synchronous timing relations. Thus temporal constraints between the north and south lineament segments and/or flows are mostly unconstrained, but relations likely indicate that propagation of the north and south segments overlapped in time and are now in a period of rift-tip linkage as the stress fields responsible for each segment merge [9].

Local resurfacing is dominated by flows from Beta Regio, Tuulikki Mons, and a number of small shield clusters. The east/west division is most clear with respect to tesserae (dominant in the east; absent to the west) and the shield populations (the west, or region within the BAT, displays twice the spatial density of shields [10]). This could be related to elevated heat flow presumed to exist within the relatively youthful BAT region resulting in a greater number of isolated point source partial melts [11,12] being produced.

Isabella Quadrangle: The V-50 quadrangle, in contrast, has very little tessera or highland material and is dominated by a regional plains unit that covers much of the area (blue unit). These regional plains continue to the south in the Barrymore Quadrangle V-59 [13] and extend to the north towards Parga Chasmata (southeastern margin of the BAT). Additional coronae and small volcanic centers (paterae) contribute only to local resurfacing and a few flows from Imdr Regio spill into the quad in the southeastern corner. The flows from Imdr may correlate with the active

resurfacing as proposed by Smrekar [4], but this is the only "recent" flow activity in the region. The remainder of V-29 is dominated by focused (Aditi and Sirona Dorsa) and distributed (penetrative north-south trending wrinkle ridges) contractional deformation and the formation of Isabella crater itself (northeast corner).

This marks a dramatic resurfacing difference between the two regions despite their relative proximity to the BAT region and relatively young and comparable ASMA ages. Deformation, extension in Devana and contraction in Isabella are likely very similar in age (even contemporaneous) and related to general BAT-centric stresses. However, north-south trending contraction features in V-50, in response to, and accommodating extensional strain from, both Atla Regio and Parga Chasmata indicate lithospheric conditions unfavorable for producing significant melt and/or pathways for that melt, thus precluding widespread volcanism as seen in and near Devana Chasma.

References: [1] Head, J.W. et al. (1992) *J. Geophys. Res.*, *97*(E8), p. 13,153–13,197. [2] Phillips, R.J. and Izenberg, N.R. (1995) *Geophys. Res. Lett.*, *22*, p. 1517-1520. [3] Hansen, V.L. and Young, D.A. (2007) GSA Special Paper 419, p. 255-273. [4] Smrekar, S.E. et al. (2010) Science 328, p. 605-608. [5] Dombard A. et al. (2007) *J. Geophys. Res.*, *112*, E04006, doi:10.1029/2006JE002731. [6] Bleamaster III, L.F. (2007) *LPSC XXXVIII*, abstract 2434. [7] Stofan, E.R. et al. (2009) *LPSC XL*, abstract 1033. [8] Basilevsky, A.T. et al. (2003) *Geophys. Res. Lett. 30*, doi:10.1029/ 2003GL017504. [9] Keifer, W.S and Swafford, L.C. (2006) *J. Struct. Geo.*, *28*, p. 2144-2155. [10] Tandberg, E. and Bleamaster, L.F. (2010) Ann. Meet. Planet. Geo. Mappers, NASA/CP-2010-217041. [11] Hansen, V.L. and Bleamaster, L.F. (2002) *LPSC XXXIII*, abstract 1061. [12] Hansen, V.L. (2005) *GSA Bull. 117*, p. 808-822. [13] Johnson, J.R. et al. (1999) *USGS Geo. Inv. Sers. I-2610*.

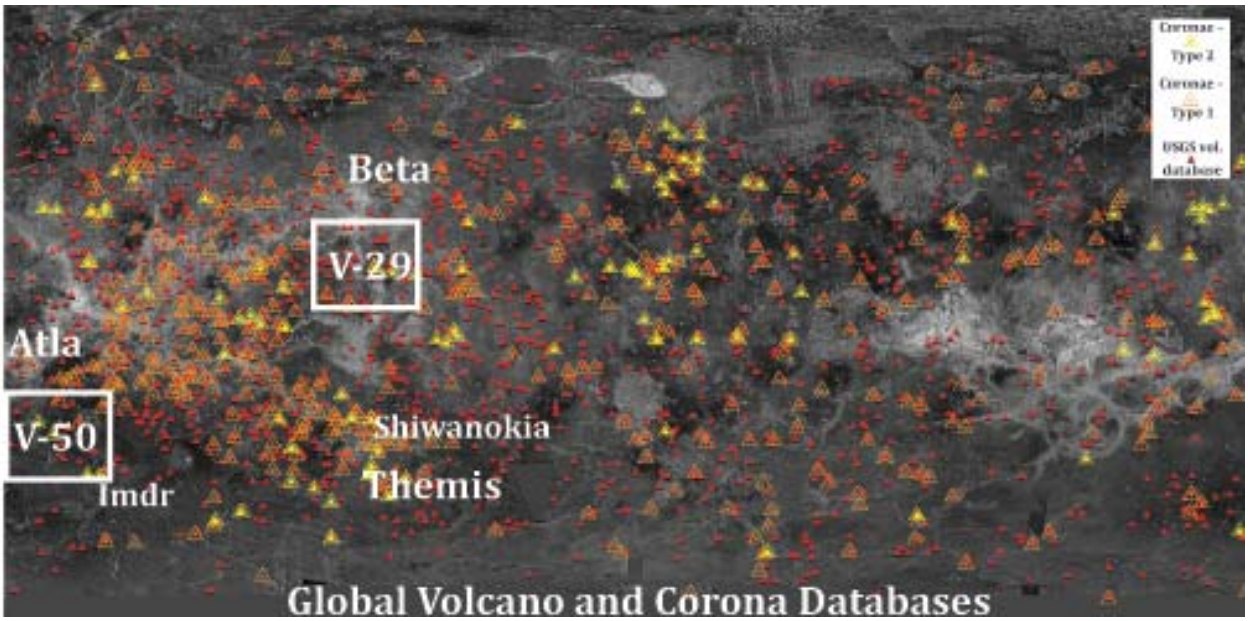

Figure 1 (above). *Global SAR context map showing distribution of coronae and volcanic centers.*
Figure 2 (below). *Isabella (V-50; left) and Devana Chasma (V-29; right) Quadrangles with generalized sequence of unit charts. V-50 is complete and is currently being converted to GIS for final submission; V-29 contacts and unit descriptions are being finalized.*

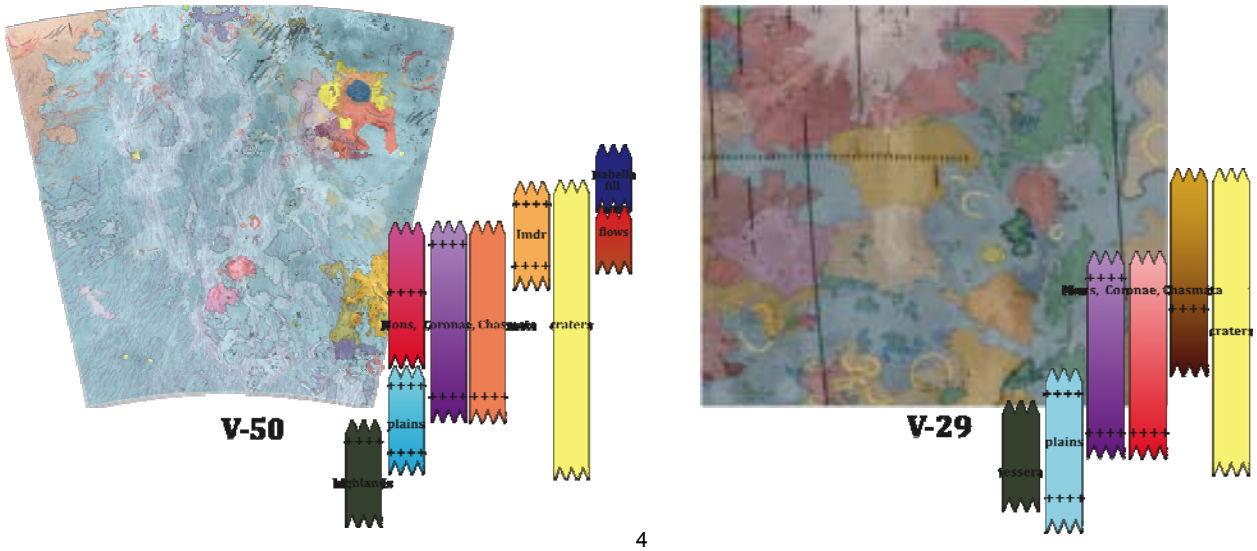

GEOLOGY OF THE FORTUNA TESSERA (V-2) QUADRANGLE: FORMATION AND EVOLUTION OF TESSERA AND INSIGHTS INTO THE BEGINNING OF THE RECORDED HISTORY OF VENUS. M.A. Ivanov[1,2], and J.W. Head[1], [1]Vernadsky Institute, RAS, Moscow, Russia, mikhail_ivanov@brown.edu, [2]Brown University, Providence, RI, USA, james_head@brown.edu.

Introduction: The V-2 quadrangle (50-75°N, 0-60°E) shows a large portion of Fortuna Tessera, which is among the largest tesserae on Venus [1] and is a good representative of this class of terrain. Tesserae are laterally extensive areas of dense tectonic deformation [2-4] that occurred near the beginning of the observable portion of the geologic history of Venus [5-9]. As such, tesserae provide clues for understanding the broad-scale tectonic regimes at these times and, thus, put important constraints on a variety of geodynamic models of Venus [10-14].

The geological mapping in the V-2 quadrangle is aimed to address several questions about the tessera formation. *Age:* (1) When did tessera form and what are its upper and possible lower stratigraphic limits? (2) Does tessera continue to deform after its fundamental structure is established? *Morphologic and topographic characteristics:* (1) What are the major facies and units of tessera? (2) How do they correlate with topography and can it be related to crustal thickness? (3) What do the boundaries of tessera tell us about the origin of this terrain? *Mechanisms of formation:* (1) What is the sequence of contractional and extensional structures in tessera? (2) What processes, convergent or divergent (or both), played the major role in tessera formation? (3) What is the evidence for formation of tessera by accretion of crustal blocks?

In this study we address some of these questions through investigation of the regional setting of Fortuna Tessera and characterization of its topographic configuration, internal structure, and relationships with the surrounding terrains.

Stratigraphic framework and regional settings: Global survey of relationships among the major units on Venus [15] reveals their consistent relative ages. Tessera appears as the oldest unit, ridge belts and groove belts postdate it. Vast plains units (the older shield plains, psh, and the younger regional plains, rp) superpose the tectonized units and are embayed by younger lobate plains. Fortuna Tessera and the belts form regional highs and separate basins that are filled by the vast plains. Shield plains are exposed closer to the basin edges and regional plains occur in the basin interiors. This correlation of stratigraphy and topography of the units implies that the major topographic features (the highs and the basins) formed before emplacement of regional plains and that the principal topographic pattern has not changed significantly since that time.

Topographic characteristics: A topographic map of the V-2 quadrangle shows that Fortuna Tessera is divided into three major regions. *(A) Western Fortuna* near Maxwell Montes forms a very broad and high standing (3-4 km) arc-like plateau around the eastern edge of Maxwell. A zone of lower topography occurs at the transition from Maxwell to Western Fortuna. The plateau shows significant (~1 km) high-frequency topographic variations and is disrupted by several topographic depressions that correspond to closed basins. The N edge of Fortuna represents a high (~1.5. km) regional scarp between the tessera and the lowlands of Snegurochka Planitia. *(B) Zone of Chasmata* displays deep (1-2 km) canyons that outline the western and eastern edges of the zone and separate the western and eastern regions of Fortuna. *(C) Eastern Fortuna* represents a lower (1-2 km) plateau with less prominent high-frequency topographic variations. The surface of Eastern Fortuna is slightly tilted northward.

Variations of the structural pattern: Near Maxwell Montes, ridges of the tessera (15-20 km wide) are sub-parallel to each other and to the eastern edge of Maxwell (N-S direction). At the E edge of Western Fortuna, the structural pattern of the tessera consists of shorter ridges and mounds that frequently change their width and orientation. Chaotically oriented ridges characterize the Zone of chasmata. Large regions within Eastern Fortuna consist of relatively narrow (5-10 km), long (a few hundred km), straight or curvilinear ridges that are oriented parallel to elongation of the tessera (W-E direction).

Structural facies and plains units: In Western Fortuna there are angular blocks with crisp-looking short and narrow ridges and scarps. A tessera matrix with softer morphology completely surrounds the blocks and overlaps their structures. This pattern resembles the augen-like structure of gneiss and suggests that the blocks may represent older fragments of more resistant materials involved in the formation of tessera. Elongated features with rounded edges in Western Fortuna represent shallow topographic depressions, the interiors of which display stacks of imbricated slabs. The surfaces of the slabs are morphologically smooth suggesting that they represent fragments of deformed lava plains. Zone of chasmata shows a series of troughs covered by plains that morphologically resemble those outside the tessera region. The plains are mildly deformed and embay structures of the tessera suggesting that they formed in topographic depressions on a tectonically stabilized region.

Relationships of structures and structural zones: In places where relatively old intratessera plains occur, they firmly establish age relationships between contractional (ridges) and extensional (graben) structures of tessera. The plains embay tessera ridges and are cut by a variety of extensional structures, which mean that the ridges are older.

Narrow (10-20 km) and long (100s km) zones divide Fortuna Tessera into a number of structural domains with different structural patterns. The zones usually represent prominent topographic depressions. The easternmost portion of Fortuna Tessera displays a large structure outlined by a series of bent troughs and ridges. The structure consists of two tongue-like features oriented in opposite N-S directions and extending for ~300 km. The syntaxis-like structure in Eastern Fortuna is similar by the structural pattern and the scale to the structures on Earth on both sides of the Indian plate where it collides with the Eurasian plate.

Northern edge of Fortuna: Segments of short ridges that are arranged en-echelon occur on the floor of Snegurochka Planitia to NW of Fortuna [16]. The edges of the segments are bent and turned to each other. This pattern of deformation suggests a strong shear component and may indicate lateral movements of lithospheric slabs relative to each other. Along the N edge of Fortuna there are several places where ridge belts within Snegurochka Planitia are terminated by the edge of the tessera. In some instances, the ridges are bent near the contact with the tessera suggesting stresses oriented parallel to the strike of the ridges. Vast plains units (rp) are not deformed and broadly embay both the tessera and the ridges. These relationships indicate that the deformation of the ridges ceased before emplacement of the plains.

Summary and Conclusions: The results of our study show the following.

(1) Fortuna Tessera formed as a large crustal block before emplacement of vast plains units (shield and regional plains) in the surrounding lowlands.

(2) There is little evidence for contemporaneous formation of the short-wavelength tessera structures and structures of groove and ridge belts along the S edge of Fortuna. At the N edge fragments of ridge belts may have been accreted to the main block of Fortuna.

(3) The surface of regional plains along the S edge of Fortuna is mostly tilted away from the tessera. The same is observed along the N edge of the Eastern Fortuna. Along the NW edge of Western Fortuna the adjacent plains display a moat-like topographic depression. The tilt of the plains can be attributed to a passive, long-wavelength epeirogenic uplift due to gravitational readjustment of a large crustal block of the tessera. The moat at the NW edge of Fortuna may be related to either recent or continued dynamic process (e.g., underthrusting [17]).

(4) Ridges and graben form the surface of tessera [3,4,18,19]. In places where local stratigraphic markers exist (the older intratessera plains [20]) they provide unambiguous evidence that the ridges are primary structures that have been cut and disrupted by the graben.

(5) The topographic characteristics and variations of the structural patterns in Fortuna indicate that the tessera consists of three major sub-regions with different arrangements of major structures: Western Fortuna, Zone of chasmata, and Eastern Fortuna. Four features of Western Fortuna indicate its possible mode of origin. (a) In this region, both the tessera-forming ridges and broader structural domains are aligned parallel to the outer edge of Maxwell Montes and are elongated in a N-S direction. (b) The N portion of Western Fortuna contains augen-like relicts and imbricated basins. (c) The relationships of the relicts with the surrounding tessera indicate that they are fragments of older and more resistant blocks incorporated into the tessera. (d) The topography and structure of the imbricated basins suggest that they represent deformed regions of intratessera plains. These features suggest that Western Fortuna may represent a site of convergent processes.

In the S half of Eastern Fortuna, both the short-wavelength tessera ridges and the larger structural domains are elongated in the same (E-W) direction. The syntaxis structure occurs at the easternmost edge of Fortuna and a series of elongated and triangle-shaped domains characterize the N edge of the region. The orientation and arrangement of structures in Eastern Fortuna is consistent with a model in which the southward displacement of the northern domains imparted stresses toward the southern portions of Eastern Fortuna and caused formation of long parallel ridges there. The structure of the syntaxis is consistent with such a model and may represent a feature similar to those that form on both sides of the India plate [21-23].

Deep troughs that interrupt the tessera structures characterize Zone of chasmata. The troughs, thus, are younger structures that cut the crustal block of Fortuna. Mildly deformed plains on the floor of the troughs indicate that little deformation occurred since the emplacement of the plains.

(6) The abruptly terminated and bent ridges at the contact of Snegurochka Planitia with Eastern Fortuna may suggest that the ridges have been partly underthrust under the crustal block of Fortuna Tessera. Sets of structures and units and their topographic configuration at the NW edge of Fortuna were interpreted as evidence for the underthrusting of the floor of Snegurochka Planitia under Western Fortuna [24]. These observations and interpretations are supported by the unusual arrangements of ridges on the floor of Snegurochka Planitia, which suggest the lateral displacement of lithospheric slabs within the planitia. Thus, Western Fortuna and Eastern Fortuna probably were affected by the southward displacements of lithospheric blocks of Snegurochka Planitia and their underthrusting under Fortuna.

In summary, our study of Fortuna Tessera reveals evidence for significant lateral displacement of crustal/lithospheric slabs, which may be related to either the upwelling [e.g., 4] or downwelling models [e.g., 12] of tessera formation.

References: 1) Ivanov, M.A. and J.W. Head, JGR, 101, 14861, 1996; 2) Sukhanov, A.L. In: Venus GGG, Barsukov, et al. eds., UAP, 82, 1992; 3) Solomon, S.C., et. al., JGR, 97, 13199, 1992; 4) Hansen, V.L. and J.J. Willis, Icarus, 123, 296, 1996; 5) Ivanov, M.A. and A.T. Basilevsky, GRL, 20, 2579, 1993; 6) Basilevsky, A.T. and J.W. Head, EMP, 66, 285, 1995; 7) Basilevsky, A.T. and J.W. Head, PSS, 43, 1523, 1995; 8) Basilevsky, A.T. and J.W. Head, JGR, 103, 8531, 1998; 9) Ivanov, M.A. and J.W. Head, JGR, 106, 17515, 2001; 10) Parmentier, E.M. and P.C. Hess, GRL, 19, 2015, 1992; 11) Turcotte, D.L., JGR, 98, 127061, 1993; 12) Head, J.W., et. al., PSS, 42, 803, 1994; 13) Phillips R.J. and V.L. Hansen, Science, 279, 1492, 1998; 14) Brown, C.D. and R.E. Grimm, Icarus, 139, 40, 1999; 15) Ivanov, M.A. and J.W. Head, PSS, 2011, submitted; 16) Hurwitz D. and J.W. Head, USGS Map V-1, 2011, in edit; 17) Solomon, S.C. and J.W. Head, GRL, 17, 1393, 1990; 18) Gilmore, M.S., et. al., JGR, 103, 16813, 1998; 19) Ghent, R. and V. Hansen, Icarus, 139, 116, 1999; 20) Ivanov, M.A. and J.W. Head, LPSC131, #1233, 2000; 21) Grosfils, E.B. and J.W. Head LPSC-21, 439, 1990; 22) Tapponier, P., et. al., In: Collision Tectonics, Coward and Reis, eds., Geol. Soc. Spec. Pub., 19, 115, 1986; 23) Tapponnier, P., et. al., Science, 294, 1671, 2001; 24) Ivanov, M.A. and J.W. Head LPSC 38, #1031, 2007.

HISTORY OF LONG-WAVELENGTH TOPOGRAPHY IN THE FREDEGONDE (V-57) QUADRANGLE, VENUS. M.A. Ivanov[1,2] and J.W. Head[2], [1]Vernadsky Institute, RAS, Moscow, Russia, mikhail_ivanov@brown.edu, [2]Brown University, Providence, RI, USA, james_head@brown.edu.

Introduction: The Fredegonde quadrangle (V-57; 50-75°S, 60-120°E, Fig.1) at the NE edge of Lada Terra is characterized by a broad topographic zone transitional from the midland [1,2] portion (0-2 km; all elevations are relative to MPR) of Lada Terra to the lowlands (<0 km [1,2]) of Aino Planitia. In this respect the V-57 quadrangle resembles the region of V-4 quadrangle [3] that is in the transition from the midlands of eastern Ishtar Terra to the lowlands of Atalanta Planitia [4]. The main goals of our mapping within the V-57 area are: (1) definition of material and structural units that make up the surface in this region, (2) establishing the sequence of the major events based on crosscutting and embayment relationships, and (3) assessment of the topographic configuration of the units in order to unravel the history of topography within the map area.

The high surface temperature on Venus strongly inhibits water-related erosional processes and may also cause coupling between convective and/or diapiric flows in the mantle and lithosphere [e.g., 5]. The long-wavelength topographic features, thus, may reflect regimes of the mantle flow. Constraints on the timing of formation of these features are very important for understanding the mantle dynamics on Venus.

Topography within the map area: The territory of the V-57 quadrangle is flat at regional scale; the maximum topographic range is from ~-0.5 km to ~2 km (Fig. 1a). The lowest portion of the quadrangle is near its NE corner and represents a broad area (several hundreds of kilometers across) where the surface lies below the 0 km contour line. The highest elevations occur within relatively small (tens of kilometers across) elongated areas in the NW corner of the quadrangle. The most significant topographic feature of the map area forms a very wide (hundreds of kilometers across) and relatively low (~1 km) topographic ridge that extends from the NW corner of the quadrangle area to its central portion and then to the southern margin of the quadrangle. The NE flank of the topographic ridge merges with the lowlands of Aino Planitia. Broad (a few hundreds of kilometers) and shallow (< 1 km) basin-like features occur to the SW and E of the ridge.

Major morphologic features of the map area: The most prominent features in the V-57 quadrangle are linear deformational zones of grooves that connect several large coronae (Fig. 1b). The zones occur in the NW and central portions of the map area and spatially coincide with the wide topographic ridge that extends through the study area. Morphologically and topographically, these zones are similar to the groove belt/corona complexes at the western edge of Atalanta Planitia [3]. In this region, the belts extend along the edges of Atalanta Planitia, whereas in the V-57 quadrangle the belts are oriented at high angles to the general trend of elongated Aino Planitia. Mildly deformed regional plains cover the surface of the broad equidimensional basins on the flanks of the topographic ridge. By their dimensions and morphology of the surface, these basins resemble topographic features that occur within the V-3 quadrangle [4].

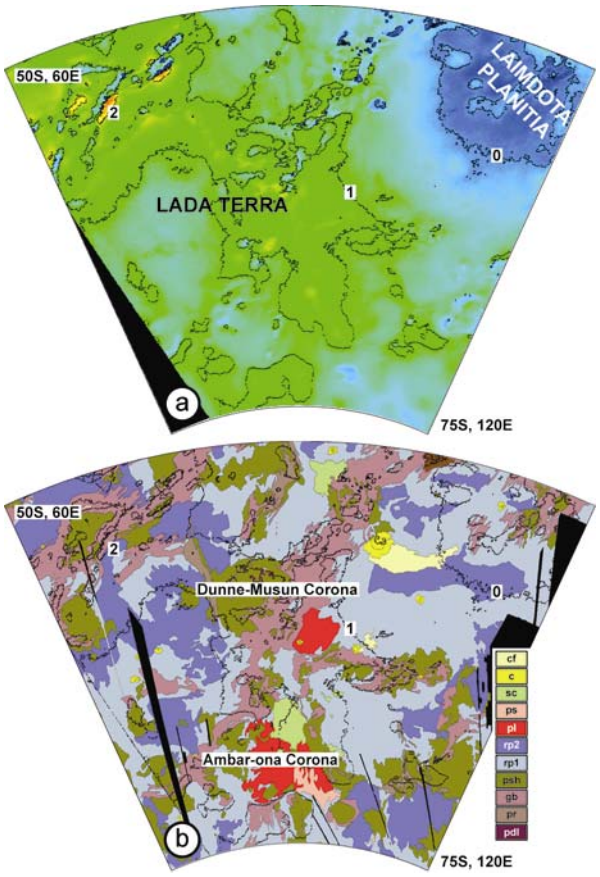

Fig. 1. Topographic and geologic maps of the V-57 area.

Material and structural units and their relationships: During our mapping we have defined the following material and structural units that demonstrate consistent relationships of embayment and crosscutting (Fig. 1b). *Densely lineated plains (pdl)* show a surface that is heavily dissected by narrow (a few hundred meters wide) and densely packed lineaments (fractures) that are several kilometers long. The low and flat surface of the pdl unit suggests that the unit represents volcanic plains, heavily deformed by extensional and/or shear structures. Type locality: 59.0°S, 85.2°E. *Ridged plains (pr)* have a morphologically smooth surface that is deformed by broad (5-10 km) and long (10s km) linear and curvilinear ridges with rounded and slightly undulating hinges. In one locality (Oshumare Dorsa), the ridges form prominent belts with elevated topography. Type locality: 57.1°S, 78.1°E. *Groove belts (gb)*

represent a structural unit that consists of swarms of linear and curvilinear lineaments. The lineaments are usually wide enough and show the morphology of fractures/graben. Within the V-57 quadrangle, groove belts form the most prominent structural and topographic zones, hundreds of km long and many tens of km wide and are often associated with coronae and corona-like features. Rims of most coronae in the map area consist of arcuate swarms of grooves. In the NE corner of the map area, groove belts form local highs within regional lowlands. Type locality: 58.8°S, 91.6°E.

Shield plains (psh) are characterized by numerous small (<10 km) shield-like features that are interpreted as volcanic edifices [6-8]. Materials of shield plains embay all previous units/structures and are mildly deformed by wrinkle ridges. Type locality: 59.4°S, 76.2°E. *Regional plains (lower unit, rp_1)* have a morphologically smooth surface with a homogeneous albedo pattern that can be locally mottled. The radar backscatter of the surface is relatively low. Wrinkle ridges deform the surface of the plains. This unit is the most abundant, makes up ~50% of the map area, and preferentially occurs on the floor of the broad basins. Type locality: 52.7°S, 107.9°E. *Regional plains (upper unit, rp_2)* show a morphologically smooth surface that is deformed by wrinkle ridges. The surface of the rp_2 unit is noticeably brighter than the surface of the rp_1 unit and displays flow-like features that extend down the regional slopes. Both units of regional plains embay shield plains. Type locality: 61.0°S, 74.6°E.

Shield clusters (sc) are morphologically similar to shield plains (psh) [9] but tectonically undeformed. Type locality: 69.7°S, 86.7°E. *Smooth plains (ps)* have a morphologically smooth, tectonically undisturbed, and featureless surface, which is usually dark. Within the V-57quadrangle, smooth plains occur in one small patch at 71.6°S, 92.5°E. *Lobate plains* display a morphologically smooth and undeformed surface that is made up by numerous radar bright and dark flow-like features that can be several tens of km long. Two occurrences of the unit within the quadrangle form equidimensional fields many tens of km across that are associated with Dunne-Musun and Ambar-ona Coronae. Lava flows of lobate plains follow the regional slope. Type locality: 62.0°S, 91.6°E. There is no good evidence to establish relative ages between shield clusters, smooth, and lobate plains. Materials that are related to impact craters consist of undivided impact crater materials (c) that include central peaks, floors, walls, rims, and continuous ejecta, type locality 56.2°S, 98.9°E, and *impact crater outflows (cf)*, type locality 57.0°S, 101.7°E.

Major events and correlation with topography: Results of the mapping in the V-57 quadrangle suggest the following sequence of major episodes in the geologic history of this region. Tectonic deformation dominated the earlier episodes of the geologic history. Regional extension (and perhaps shear) played the major role during this period and caused formation of prominent groove belts and coronae. The major topographic highs within the quadrangle coincide with the groove belt/corona chains and probably formed at the beginning of the observable geological record following tessera formation.

During the middle stages of geologic history, volcanism dominated and resulted in formation of vast plains units such as psh, rp_1 and rp_2. Tectonics played a secondary role and led to formation of small but abundant wrinkle ridges. Relatively older shield plains occur within slightly higher areas on regional slopes of the deformational belts and around the equidimensional basins. This suggests that the topographic distribution of the plains followed the regional topographic pattern established during earlier episodes of geologic history. The lower unit of regional plains is preferentially concentrated within the basins, and this implies that these topographic features formed before emplacement of the plains. The flows of the upper unit of regional plains also flow along the regional slope.

Volcanism related to local sources (lobate plains, shield clusters, and smooth plains at Dunne-Musun and Ambar-ona Coronae) continued during the final stages of the regional geologic history. The flows of lobate plains extend along the regional slopes from the broad ridges toward the floor of the basins.

Summary: The spatial association of the older material and structural units (pdl, pr, gb, psh) with the major positive topographic features and concentration of relatively younger (rp_1) materials within the basins suggest that the long-wavelength (hundreds of kilometers) pattern of topography within the V-57 quadrangle was established near the beginning of the regional geologic history prior to emplacement of the lower unit of regional plains (rp_1). The only exception is the area in the NE corner of the map area where the local highs of groove belts occur within the lowlands of Aino Planitia (below 0 km contour line, Fig. 1a,b). This suggests that either the general topographic pattern at the scale of thousands of kilometers (the midlands/lowlands scale) existed as a background pattern before formation of groove belts or that the surface of Aino Planitia continued to subside after formation of the belts. In either case, the flows of the upper unit of regional plains (rp_2) and lobate plains (pl), which extend along the regional slope, indicate that the principal topographic pattern in the study region did not change significantly subsequent to the emplacement of these units.

References: 1) Masursky, H., et al., *JGR*, 85, 8232, 1980; 2) Pettengill, G.H., et al., *JGR*, 85, 8261, 1980; 3) Ivanov, M. A. and J.W. Head, Geologic map of the Atalanta Planitia (V-4) quadrangle, *USGS Map 2792*, 2004; 4) Ivanov, M.A. and J.W. Head, *USGS Map 3018*, 2008; 5) Phillips, R.J. and M.C. Malin, In: Venus, Univ. Arizona Press, 159, 1983; 6) Aubele, J.C. and E.N. Slyuta, *EMP*, 50/51, 493, 1990; 7) Addington, E.A., *Icarus*, 149, 16, 2001; 8) Ivanov, M.A. and J.W. Head, *JGR*, 109, doi:10.1029/2004JE002252, 2004; 9) Ivanov, M.A. and J.W. Head, *USGS Map 2920*, 2006.

GEOLOGIC MAPPING OF V-19. P. Martin[1], E.R. Stofan[2, 3] and J.E. Guest[3], [1]Durham University, Dept. of Earth Sciences, Science Laboratories, South Road, Durham, DH1 3LE, UK, (paula.martin@durham.ac.uk), [2]Proxemy Research, 20528 Farcroft Lane, Laytonsville, MD 20882 USA (ellen@proxemy.com), [3]Department of Earth Sciences, University College London, Gower Street, London, WC1E 6BT, UK.

Introduction: A geologic map of the Sedna Planitia (V-19) quadrangle is being completed at 1:5,000,000 scale as part of the NASA Planetary Geologic Mapping Program, and will be submitted for review by September 2012.

Overview: The Sedna Planitia quadrangle (V-19) extends from 25°N - 50°N latitude, 330° - 0° longitude. The quadrangle contains the northernmost portion of western Eistla Regio and the Sedna Planitia lowlands. Sedna Planitia consists of low-lying plains units, with numerous small volcanic edifices including shields, domes and cones. The quadrangle also contains several tholi, the large flow-field Neago Fluctūs, the Manzan-Gurme Tesserae, and Zorile Dorsa and Karra-māhte Fossae which run NW-SE through the southwestern part of the quadrangle. There are six coronae in the quadrangle (Table 1), the largest of which is Nissaba (300 km x 220 km), and there are fourteen impact craters (Table 2). The geologic history of the quadrangle is dominated by multiple episodes of plains formation and wrinkle ridge formation interspersed in time and space with edifice- and corona-related volcanism. The formation of Eistla Regio to the southwest of this quadrangle postdates most of the mapped plains units, causing them to be deformed by wrinkle ridges and overlaid by corona and volcano flow units.

Mapped Units: Six types of materials have been mapped in the V-19 quadrangle: tessera, plains, volcanic edifice and flow, corona, crater, and surficial materials. All types of material units occur throughout the quadrangle, with the exception of tessera materials, which crop out only in the eastern part of the mapped region.

Highly deformed materials that have been mapped as tessera (unit t) range in size from < 50 km to several hundreds of kilometers across, and include the Manzan-Gurme Tesserae which are made up of several individual outcrops distributed along the eastern edge of this quadrangle.

Seven plains materials units have been mapped in V-19 (from oldest to youngest): Sedna deformed plains material (unit pdS), Sedna patchy plains material (unit ppS), Sedna composite-flow plains material (unit pcS), Sedna homogeneous plains material (unit phS), Sedna uniform plains material (unit puS), Sedna mottled plains material (unit pmS) and Sedna lobate plains material (unit plS). These seven units range from relatively localized, limited extent units (e.g. unit pdS) to regional plains units (e.g. unit phS).

Table 1. Coronae of V-19.

Name	Lat.	Long.	Max Width	Type
Ba'het	48.4	0.1	300 x 145	Concentric
Tutelina	29.0	348.0	180	Concentric
Purandhi	26.1	343.5	170	Concentric
Mesca	27.0	342.6	190	Type II
Nissaba	25.5	355.5	300 x 220	Concentric
Idem-Kuva	25.0	358.0	280	Concentric

Table 2. Impact Craters of V-19.

Name	Lat.	Long.	Diameter (km)
Ariadne	43.9	0.0	20.8
Veta	42.6	349.5	6.4
Jeanne	40.1	331.5	19.5
Unnamed	37.6	350.1	2.1
Zuhrah	34.7	357.0	6.6
Vassi	34.4	346.5	8.8
Al-Taymuriyya	32.9	336.2	21
Nutsa	27.5	341.8	4.2
Barton	27.4	337.5	50
Lachappelle	26.7	336.7	35.3
Roxanna	26.5	334.6	9.2
Kumba	26.3	332.7	11.4
Bakisat	26.0	356.8	7.4
Lilian	25.6	336.0	13.5

Each of the mapped plains units are composed of groups of many smaller plains units of varying age. These smaller plains units have been grouped into a mappable unit because of their similarity in appearance and stratigraphic position relative to other plains units. Similarly to other mapped quadrangles on Venus [1, 2], the V-19 quadrangle is dominated by regional-scale plains units: the northeastern half of the map is dominated by the homogenous plains material (unit phS); the southwestern half of the map is dominated by the composite-flow plains material (unit pcS). The remaining plains units, units pdS, ppS, puS, pmS and plS, tend to crop out as isolated patches of materials.

The V-19 quadrangle contains a variety of mappable volcanic landforms including two shield volcanoes (Evaki Tholus and Toci Tholus) and the southern portion of a large flow field (Neago Fluctūs). A total of sixteen units associated with volcanoes have been mapped in this quadrangle, with multiple units mapped at Sif Mons, Sachs Patera and Neago Fluctūs. An oddly textured, radar-bright flow is also mapped in the Sedna plains, which appears to have originated from a several hundred kilometer long fissure. The six coronae within V-19 have a total of eighteen associated flow units. Several edifice fields are also mapped, in which the small volcanic edifices both predate and postdate the other units. Impact crater materials are also mapped.

V-19 has common boundaries with four other quadrangles (V-7, V-8, V-18 and V-31), but a map has been published for only two of these (V-8 and V-31) [3 and 4 respectively], and therefore it is only possible to compare units mapped in V-19 with those mapped in V-8 and V-31 at this time.

There are a total of six units mapped in V-19 that are also mapped in V-8. The tessera is mapped as unit t in both V-8 and V-19. The Sedna homogeneous plains material (unit phS) and the Sedna composite-flow plains material (unit pcS) are both mapped as unit pr in V-8. The Sedna homogeneous plains material (unit phS) is also mapped as unit fs in two places in V-8, near Ba'het Corona. The Ba'het flow material (unit fB) mapped in V-19 is mapped variously as units pb, fcO_1 and pr in V-8. The Idem-Kuva Corona material member e (unit fl_e) is mapped as unit fG in V-8. Finally, the materials related to Ariadne crater are mapped as unit c, unit cf and unit cfi in V-8, but simply as unit c in V-19.

There are three plains units and a variety of flow units associated with Sif and Gula Montes that are mapped in both V-19 and V-31. The Sedna deformed plains material (unit pdS) is comparable with unit pd mapped in V-31, the Sedna composite-flow plains material (unit pcS) is mapped as unit plmG in V-31 and the Sedna homogeneous plains material (unit phS) is mapped as unit eG in the northwestern corner of V-31. Two of the Sif materials (units Si_a and Si_c) are collectively mapped as unit eS in V-31, a third Sif material (unit Si_b) is mapped as unit prG in V-31, and the final Sif material (unit Si_d) is mapped as unit vc in V-31, with the Gula material (unit fG) mapped as unit eG in V-31.

Conclusions: V-19 is comparable with our previously mapped quadrangles, V-31, V-39, V-46, V-28 and V-53 [4, 5, 6, 7 and 8]. V-19, V-39 and V-46 have a similar number of mapped plains units, whereas V-28 and V-53 have a greater number, and V-31 has fewer. V-19, V-28, V-31 and V-53 are similar to one another in that four quadrangles have very horizontal stratigraphic columns, as limited contact between units prevents clear age determinations. This does not mean that all units within each quadrangle formed at the same time. Rather, the stratigraphic columns reflect the limited nature of our stratigraphic knowledge in these quadrangles, allowing for numerous possible geologic histories. This uncertainty is illustrated by the use of hachured columns for each unit. Resurfacing in these quadrangles is on the scale of 100s of square kilometers, consistent with the fact that they lie in the most volcanic region of Venus.

References: [1] Bender, K. C. et al., 2000, Geologic map of the Carson Quadrangle (V-43), Venus. [2] McGill, G. E., 2000, Geologic map of the Sappho Patera Quadrangle (V-20), Venus. [3] McGill, G., 2004, Geologic map of the Bereghinya Planitia Quadrangle (V-8), Venus. [4] Copp, D. L. and Guest, J. E., 2007, Geologic map of the Sif Mons quadrangle (V-31), Venus. [4] Brian, A. W. et al., 2005, Geologic Map of the Taussig Quadrangle (V-39), Venus. [5] Stofan, E. R. and Guest, J. E., 2003, Geologic Map of the Aino Planitia Quadrangle (V-46), Venus. [6] Stofan, E. R. et al., 2009, Geologic Map of the Hecate Chasma Quadrangle (V-28), Venus. [7] Stofan, E. R. and Brian, A. W., 2009, Geologic Map of the Themis Regio Quadrangle (V-53), Venus.

STRATIGRAPHY OF THE LACHESIS TESSERA QUADRANGLE, V-18. E. M. McGowan[1] and G. E. McGill[2], [1,2]University of Massachusetts,[1]emcgowan@geo.umass.edu, [2]gmcgill@geo.umass.edu.

Introduction: The Lachesis Tessera quadrangle (V-18) of Venus is bounded by 300° and 330° east longitude, 25° and 50° north latitude. Lachesis is one of the 3 Fates in Greek mythology. The Lachesis Tessera occupies a very small section of the northwest quadrant of the quadrangle and is partially in the Beta Regio (V-17) quadrangle. The Lachesis Tessera quadrangle includes parts of Sedna and Guinevere Planitiae; regional plains cover approximately 80% of the quadrangle. In addition, the quadrangle includes two deformation belts and embayed fragments of one or two possible additional belts, 3 large central volcanoes, abundant small shield volcanoes and associated flow materials, 13 impact craters, 3 named coronae, and a number of corona-like features. The most interesting area of the Lachesis Tessera quadrangle is a linear grouping of a prominent structural belt, coronae, and corona-like features oriented northwest to southeast in the southern half of the quadrangle (fig. 1).

Stratigraphy of Linear Grouping: A prominent structural belt extends from the western boundary of the quadrangle at about 36° north latitude southeastward to near the southern boundary of the quadrangle at about 324° east longitude. This belt links Breksta Linea to Zemire and Pasu-Ava Coronae, and to smaller deformed regions aligned with this trend. It also includes a probable corona centered at about 323° east longitude, 28° north latitude. All but the eastern part of this putative corona is within the wide strip of no image coverage.

The highest elevation of this grouping is in the west adjacent to a fracture belt in the Beta Regio quadrangle (Basilevsky, 2008). Mapping of the structural belt found many of the lineations to be grabens. The age relationship between the fracture belt and two of the corona-like features is unclear since Breksta Linea appears to be younger than one corona-like feature yet older than another.

Lachesis Tessera Stratigraphy:

- The oldest materials in the Lachesis Tessera quadrangle are mapped into 3 units: tessera material (t), tessera-like material (tq), and bright material (mb).
- The dominant terrains of the Lachesis Tessera quadrangle are plains. About 80% of the area within the quadrangle is underlain by regional plains, which are subdivided into two members (pr1 and pr2). More local plains units include dark plains material (pd) and mottled plains material (pm). Unit pr1 appears to be the oldest plains unit, pr2, which is brighter, includes inliers of material with the same backscatter as pr1. The relative age of pb and pm to the regional plains themselves is uncertain.
- Deformation belts are characterized by fractures and faults, or by ridges, resulting in two map units: ridge belt material (br) and fracture belt material (bf). Ridge belt and fracture belts are both superposed on the regional plains.
- Structures and materials of at least four coronae are present in the Lachesis Tessera quadrangle. These are widely separated; consequently it is not possible to determine the relative ages of the coronae. The

structures of the coronae are superposed on the regional plains material and have both a younger and older relationship to structures in the br.

- Scattered around the quadrangle are exposures of various volcanic materials: isolated flows (f), materials of central volcanoes (mva, mvb), and materials of shield flows (fs, fsd). Isolated flows (f) are mostly moderately bright, relatively rare, digitate flows that generally do not have a resolvable construct at their source. Mva material is superposed on pr1 and pr2 while mvb material is superposed on pr1. The overall impression is that the miscellaneous shield flows can be considered a third member of the regional plains.
- The 13 impact craters in the Lachesis Tessera quadrangle range in diameter from 2.4 to 40 km. All thirteen of the impact craters are superposed on regional plains or on materials superposed on regional plains. Of the thirteen impact craters, only 2 are significantly degraded.

References: [1] Basilevsky, 2008, USGS Map #3023.

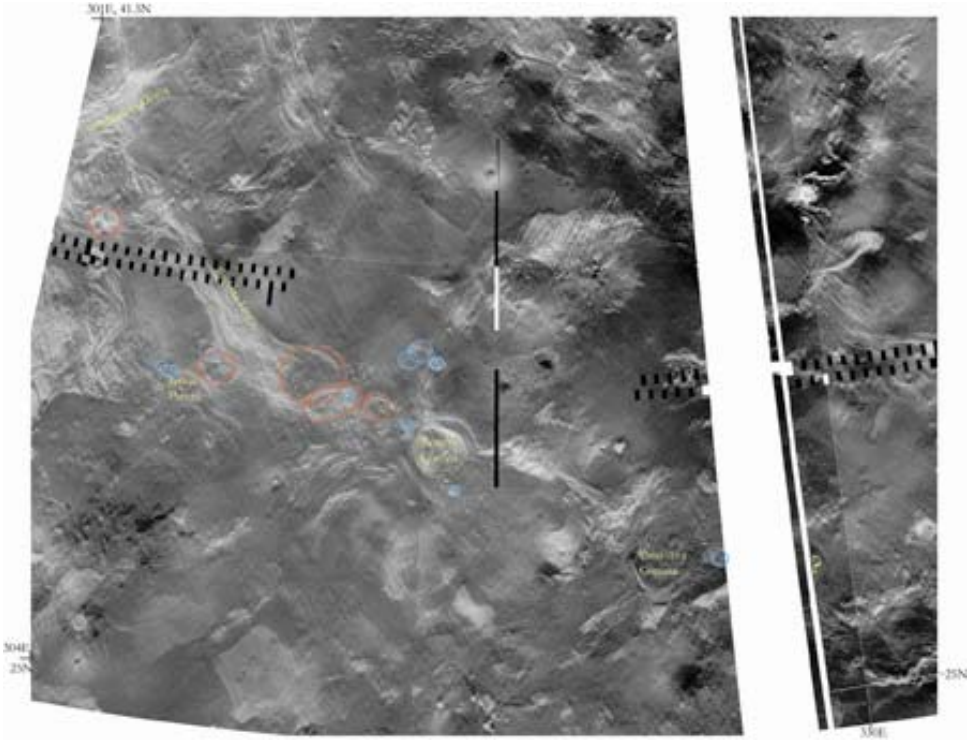

Figure 1. Linear grouping of structural features in Lachesis Tessera. Red circles are corona-like objects, question mark shows the location of possible corona, and blue circles indicate pancake domes.

DIGITAL RENOVATION OF THE LUNAR NEAR-SIDE, NORTH POLE, AND SOUTH POLE GEOLOGIC MAPS. C.M. Fortezzo and T.M. Hare, United States Geologic Survey, Astrogeology Science Center, 2255 N. Gemini Dr., Flagstaff, Arizona, cfortezzo@usgs.gov.

Introduction: In support of a NASA Planetary Geology and Geophysics-funded project to digitize existing lunar paper maps and because of the increasing emphasis on lunar studies from recent orbital data returns, we have renovated the digital versions of the lunar near-side, north, and south pole geologic maps [1-3]. The renovations used new topographic data and image mosaics to adjust the original linework and adjust the map boundary to the current ULCN2005 and the Lunar Reconnaissance Orbiter (LRO) Lunar Orbiter Laser Altimeter (LOLA) control networks [4,5].

These maps are not a reinterpretation of the original geologic units or relationships, but a spatial adjustment to make the original work more compatible with current digital datasets. This increased compatibility allows these maps to be compared and utilized with ongoing and future lunar mapping projects. This work represents the beginning of a project aimed at digitizing the original maps that made up the global view of the Moon [1-3,6-8].

Background: The 1:5M near-side map was a synthesis of 36 1:1M maps produced from Earth-based telescopic observations and Lunar Orbiter imagery [1]. The purpose of the synthesis was to produce a coherent and consistent near-side time-stratigraphy. The base image for the 1:5M map was generated by the United States Air Force Aeronautical Chart and Information Center (USAF-ACIC) in 1966 in an Orthographic projection. The irregular boundary for the map area follows the boundaries for the 36 1:1M maps and narrows in steps as it approaches the poles.

The near-side map delineated 43 geologic units that are broken down into the following major groupings: dark materials (5 units), circumbasin materials (7 units), crater materials (20 units), and terra plain, plateau, and dome materials (11 units). The units span the pre-Imbrium to the Copernican system. The only linear representations on the map are geologic contacts and basin rings. There is no distinction between contact types (e.g., certain, approximate, or concealed) used in the original map.

The lunar north pole map was generated in 1978 and delineated 34 units split into the following groups: crater materials (13), basin materials (9), other terra materials (9), and mare and other dark materials (3). These units span the pre-Nectarian through the Copernican system. The linear representations included approximate contacts, crests of buried crater rims, and certain and approximate crests of basin ring structures. The north pole map utilized a Polar Stereographic projected shaded-relief base map generated by the USAF-ACIC.

The lunar south pole map was generated in 1979 and delineated 37 units split into the following groups: materials of primary impact and their secondary craters (13), basin materials (11), probable basin related materials (8), and mare and other dark materials (5). These units span the pre-Nectarian through the Copernican system. The linear representations included certain and queried contacts, crests of buried crater rims, certain and approximate crests of basin ring structures, fissure and narrow fault grabens, sinuous ridges, and sinuous scarps. The south pole map utilized a Polar Stereographic projected shaded-relief base map generated by the Defense Mapping Agency in 1970. This map included a location near the pole where there was no photographic coverage, thus no units were mapped.

These maps were digitized the first time by the USGS in 2000 by tracing units on scanned versions of the maps. These original digital files were created in the orthographic and polar projections in ArcInfo Workstation and reprojected into a Simple Cylindrical projection for compatibility with global datasets. It was not possible to salvage these original files because they were registered to a hand-tied, airbrushed mosaic based on an out-dated control network. The renovation described herein has allowed us to correct flaws in the original digital product, including improving consistency in vertex spacing and adding (where appropriate) a level of vector smoothing to remove redundant vertices.

Datasets: Four orbital datasets were used to renovate the lunar near-side map (listed in order of utility): Lunar Orbiter global mosaic (~63 m/pix), Kaguya Digital Terrain Model (~2 km/pix), Clementine UVVIS (100 m/pix), and the Clementine Mineral Ratio (200 m/pix). The Lunar Orbiter global mosaic provides visible imagery of the lunar surface allowing for distinct delineation of the morphologic and geologic relationships. The Kaguya Digital Terrain Model (DTM) provided rough topography allowing for delineation of features that were less prominent in the Lunar Orbiter mosaic. The Clementine UV-VIS provided a tool for identifying the mare geologic units which make up 40% of the total map area [1]. The Clementine Mineral Ratio map was used

sparingly but was helpful in some locations where it was necessary to delineate ejecta blankets.

For the polar maps, we used 3 datasets: the Lunar Reconnaissance Orbiter (LRO) Lunar Orbiter Laser Altimeter (LOLA) DTM (100 m/pix), Lunar Reconnaissance Orbiter Camera wide-angle camera (WAC) mosaic (100 m/pix), and Lunar Orbiter global mosaic (~63 m/pix).

Methodology: The current renovation of the digital maps adhered to strict guidelines for vector generation and used recent datasets to spatially adjust the location of the geology and linework. This adjustment did not change the original geologic framework but sought to update the locations of the contacts and geology. These adjustments resulted in the omission of some discrete units by connecting areas that were previously mapped as isolated portions and, vice versa, isolated previously grouped units. The sole new addition to the map was the use of both certain and approximate contacts to indicate areas where (1) the geologic relationships were unclear to the digital author and (2) where the datasets did not provide adequate information for the interpretations of the original map.

The data sets discussed above were used in combination with ESRI's ArcMap Geographic Information System (GIS) software, to draw vectors on the Lunar Orbiter global mosaic. The vectors were drawn with a consistent vertex spacing of ~3 km at 1:1.5M scale, and were smoothed using a maximum allowable offset tolerance of ~16 km. The adjustments and adherence to these guidelines resulted in a product that increased the feature location accuracy at the 1:5M scale and makes the product more cartographically appealing.

Generating the polygons from the contact linework was an iterative process that involved ensuring that all polygons were properly accounted for, and making changes to the contacts as needed. Once all geology polygons were built, the contacts were smoothed and topology errors caused by the smoothing process were fixed by assigning topology rules in ArcMap. Geology polygons were generated from the smoothed contacts and attributed using the geologic attributes from the original digital files generated in 2000. The geologic attributes from the original digitization of the map were used because the original digital attributions were robust in their descriptions. These attributes were held in point data and included the unit symbol, unit name, major grouping designation, epoch of lunar time, and a brief description of the unit. These data were merged into the renovated geologic map when the remapped polygons were generated. Because of the lumping/splitting of units and the spatial adjustment, it was necessary to quality check each geology polygon and its associated attribute to ensure that the two features matched. Basin rings were digitized once editing of the contacts and geology was finished.

No nomenclature is included on the map because of the availability of digital nomenclature provided by the U.S. Geological Survey's IAU Gazetteer of Planetary Nomenclature website (http://planetarynames.wr.usgs.gov). This site allows users of the map to choose which features are displayed digitally and in paper copies they generate.

Results: Subtle changes to all the maps improved the location of units, contacts, and structures. For the south pole, the zone of "no-data" has been filled in with interpretations stemming from recent LOLA topographic coverage. This provides an update to the map that may prove helpful given the increased interest in the permanently shadowed craters at the lunar poles.

The renovated lunar near-side and polar geologic maps provide the community with a means to digitally view and analyze the data from the original map. The ability of GIS to analyze data reinvigorates the 30- to 40-year-old products and makes them viable products for a new generation of planetary scientists due to an increasing reliance on digital resources. Additionally, with a new influx of lunar data, it is important to preserve and extend the capabilities of this useful heritage map.

Future Work: This project will continue to digitally renovate the 3 remaining original lunar geologic maps. Next year, the focus will shift to the far-side of the Moon. Once all of the maps are completed, the feasibility of merging the maps will be assessed.

References: [1] Wilhelms, D.E. and J.F. MacCauley (1971) *Map I-703*. [2] Wilhelms, D.E., et al. (1979) *Map I-1162*. [3] Lucchitta, B.K. (1978) *Map I-1062*. [4] Archinal, B. et al. (2006) *Open-File Report 2006-1367*. [5] Smith, D. E. et al. (2008) NASA Goddard Space Flight Center. [6] Wilhelms, D.E. and F. El-Baz (1977) *Map I-948*. [7] Stuart-Alexander, D.E. (1978) *Map I-1047*. [8] Scott, D.H. et al. (1977) *Map I-1034*.

A TEST OF GEOLOGIC MAPPING TECHNIQUES IN THE ARISTARCHUS PLATEAU REGION, THE MOON. Tracy K.P. Gregg[1], T.A. Lough[1], and R. Aileen Yingst[2], [1]411 Cooke Hall, Geology Dept., University at Buffalo, Buffalo, NY 14260 (tgregg@buffalo.edu), [2]2420 Nicolet Dr., Natural and Applied Sciences, University of Wisconsin-Green Bay, WI 54311.

Introduction: Aristarchus plateau (centered at ~25ºN, 40ºW) is a volcanologically diverse region containing sinuous rilles, volcanic depressions, mare material and pyroclastic deposits [1-5]. Interpretations of the region's volcanic evolution have implications for the global history of lunar volcanism, the crustal and mantle development of the Moon, and may ultimately help support successful lunar exploration [6]. Here, we present preliminary mapping of a 13° x 10° area around Aristarchus plateau [7], and investigate differences between maps generated using different available datasets.

Background: The map area contains: mountainous highland terrain; impact craters; the highest concentration of sinuous rilles on the Moon; volcanic depressions and hills [1]; lava flows as young as 1.2 Ga to >3.4 Ga [2]; and a blanket of dark mantling material interpreted to be pyroclastic deposits [e.g., 3-5]. Kiefer [8] found positive gravitational anomalies on the eastern and southern margins of the plateau that may be caused by a magmatic intrusion. Radon detection around the region suggests it may still be degassing [8, 10]. The geologic diversity of this region led to the creation of geologic maps of the Aristarchus region using Apollo-era data [e.g., 11-13] as well as compositional maps from ground-based radar and orbital remote sensing data [e.g., 14-16].

Methods: The USGS provided orthorectified digital basemaps of the Lunar Orbiter (LO) and Clementine data sets and a geodatabase containing the features used to map the Copernicus Quadrangle [17]. We created 3 maps using these datasets. The "Morphologic Map" relied almost exclusively on the LO basemap, composed of mosaicked Lunar Orbiter (LO) IV and V images. These LO images were used because: 1) they are the highest resolution comprehensive dataset available (~1 to ~150 m/pixel); and 2) low sun angles highlight morphologic and topographic features. The "Compositional Map" was created using Clementine UV-VIS datasets as basemaps, specifically: 1) iron and titanium ratio maps [18]; and 2) a color composite image from LPI Clementine Mapping Project (hereinafter referred to as the "RGB Clementine image) [18]. The "Synthesized Map" was created using all available data for the region. Resulting maps are shown in Figure 1. Each map covers the same area ~390 km wide by ~300 km tall.

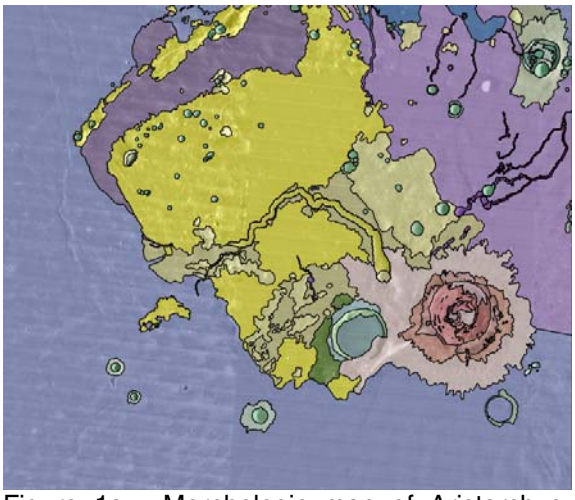

Figure 1a. Morphologic map of Aristarchus plateau region, using LO images as basemap. Upper left corner at (30°N, 58°W); lower right corner at (20°N, 45°W). Map width ~390 km.

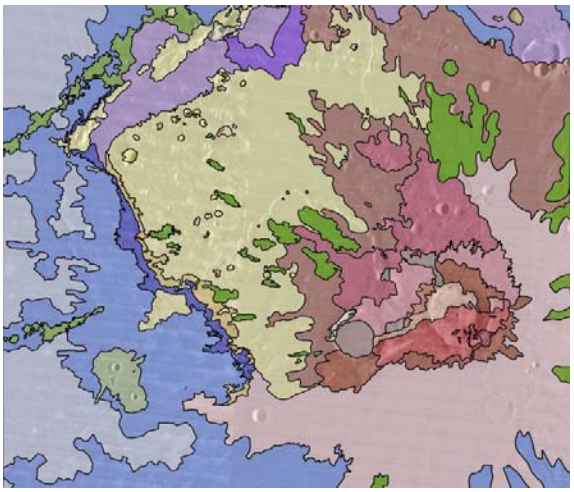

Figure 1b. Compositional map of Aristarchus plateau region, using Clementine data as basemap. Upper left corner at (30°N, 58°W); lower right corner at (20°N, 45°W). Map width ~390 km.

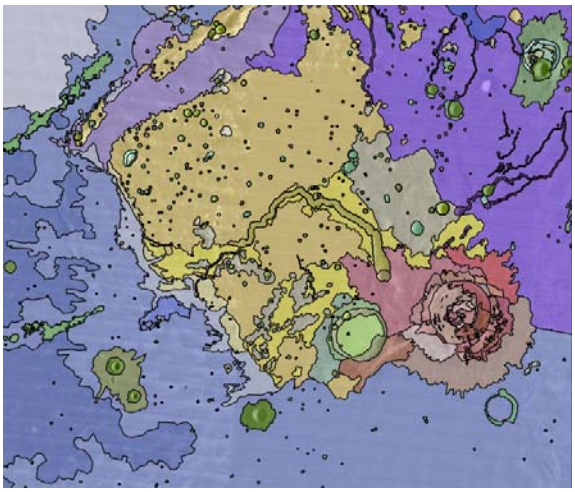

Figure 1c. Synthesized map of Aristarchus plateau region, incorporating all available datasets and using LO images as basemap. All primary impact craters with diameters >1 km are mapped. Upper left corner at (30°N, 58°W); lower right corner at (20°N, 45°W). Map width ~390 km.

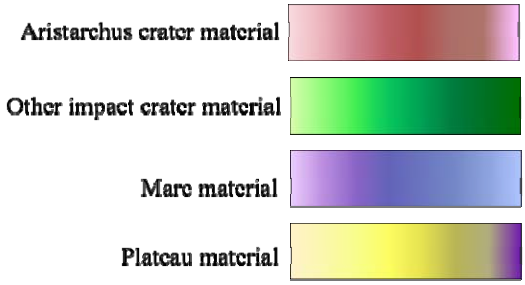

Figure 1d. Representative unit colors for all maps. Reds and browns are Aristarchus crater materials; purples and blues are mare materials; yellows and tans are Aristarchus plateau materials for all 3 maps.

Discussion: We have identified the following unit types in each of the three maps: Mare materials, Aristarchus plateau materials, Aristarchus crater materials, and other (i.e., non-Aristarchus crater) impact crater materials. However, the distribution of these units is distinct in each of the three maps. Although each map reveals important information, we interpret the "Synthesized Map" (Figure 1c) as telling the most comprehensive geologic story, because it reveals compositional information that influences the morphologic units, as well as the converse.

The "Compositional Map" (Figure 1b) is dominated by ejecta from Aristarchus crater. More mare units are shown here than in the "Morphologic Map" (Figure 1a) because variations observed in relative Ti and Fe abundances in the Clementine dataset were used locally to define mare boundaries. Additionally, the compositional data reveal regions of mixing along highland-mare boundaries that are defined as units within the "Compositional Map."

In contrast, the "Morphologic Map" hides the chemical complexity of the region, allowing structural and morphologic relations to be easily seen. For example, the "Morphologic Map" clearly shows the parallel NW trends of the Agricola mountains and the northern boundary of Aristarchus plateau.

We assert that the "Synthesized Map" (Figure 1c) transmits the most significant geologic information most efficiently, as compared with the other two maps. In this map, the compositional effect of Aristarchus crater ejecta is confined to within 1 crater radius, allowing the variations in mare composition to be revealed. Important structural features (such as the Agricola mountains) are shown, as are purely compositional phenomena (such as the NE-trending crater ray from the Glushko impact, mapped in green in the Synthesized Map and the Compositional Map).

Conclusions: This mapping effort demonstrates the importance of incorporating and evaluating all available datasets in the generation of lunar (and, by extension, Martian) geologic maps.

References: [1] Wilhelms (1987) *The Geologic History of the Moon*, USGS Prof. Paper 1348. [2] Hiesinger et al. (2000) *JGR, 105*, 29,239-29,275. [3] Adams et al. (1974) *Proc. Lunar Plan. Conf. 5, 1,* 171-186. [4] Gaddis et al. (1985) *Icarus, 61*, 461-489. [5] Weitz et al. (1998) *JGR 103*, 22,725-22,759. [6] NRC (2007) *The Scientific Context for Exploration of the Moon: Final Report*, http://www.nap.edu/catalog/-11954.html, 120pp. [7] Yingst et al. (2009) LPSC abstract #1319 [8] Kiefer (2009) *LPSC* # 1106. [9] Gorenstein and Bjorkholm (1973) *Science 179*, 792-794. [10] Lawson et al. (2005) *JGR, 110,* E09009, doi:10.-1029/2005JE002433. [11] Moore (1965) *USGS Misc. Inv. Ser. Maps* I-465. [12] Moore (1967) *USGS Misc. Inv. Ser. Maps* I-527. [13] Zisk et al. (1977) *Moon, 17,* 59-99. [14] Lucey et al. (1986) *JGR, 91*, D344-D354. [15] McEwen et al. (1994) *Science 266*, 1858-1862. [16] Chevrel et al. (2009) *Icarus,199*, 9-24. [17] Gaddis et al. (2006) *LPSC* abstract # 2135. [18] The LPI Clementine Mapping Project, http://www.lpi.usra.edu /lunar/tools/clementine/.

GEOLOGIC MAPPING OF JULES VERNE IN WESTERN SOUTH POLE-AITKEN BASIN, LUNAR QUADRANGLE 29. R. A. Yingst[1], D. Berman[1], F.C. Chuang[1] and S. Mest[1], [1]Planetary Science Institute, 1700 E. Ft. Lowell, Suite 106, Tucson, AZ 85719 (yingst@psi.edu).

Introduction: Lunar Quadrangle 29 (LQ-29) extends from -60° to -30° latitude and 120° to 180° longitude. This area encompasses the western portion of South Pole-Aitken basin (SPA), a region that has a diversity of volcanics and excavates deeply into the lunar lower crust, thus representing the thickest stratigraphic cross-section on the Moon. Our objectives in mapping LQ-29 are to (1) provide constraints on models of lunar volcanic generation and evolution by characterizing volcanic units in the unique bounding environment of western SPA; (2) provide constraints on the timing and sequence of impact-related surface materials and features found uniquely clustered in this region; and (3) characterize the extent and distribution of units important for future lunar missions. Here we present our mapping results from a subset of this area containing examples of most of the unique aspects of the quad, the region surrounding the crater Jules Verne.

Geologic Setting: LQ-29 (Figure 1) is dominated by the western portion of the pre-Nectarian South Pole-Aitken basin. The northwest rim of SPA mapped by [1] cuts across the quadrangle from the southwest to the northwest-northcenter. The south portion of the quad is nearly entirely covered by Poincaré and Planck basins, while the eastern part of the quad contains the basins Leibnitz and Von Kármán. In the north-center lies Jules Verne, and Mare Ingenii is to the east.

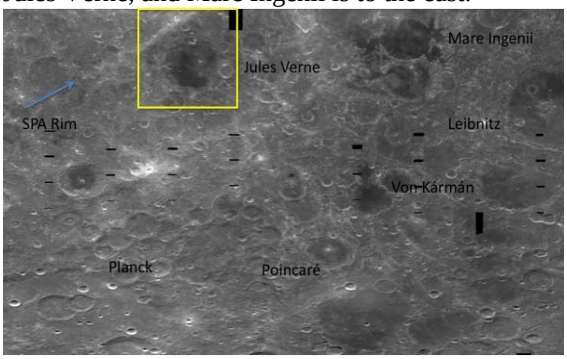

Figure 1. Clementine mosaic of LQ-29; the area mapped (yellow box) is shown in Figure 2.

Impact structures. The quadrangle is dominated by multiple, overlapping impact structures from sizes below resolution to over 600 km across, with ages ranging from pre-Nectarian to Copernican [1]. Other important basin or impact materials include the high-albedo swirls inside Mare Ingenii, and the unusual groove-and-mound terrain surrounding it. These features occur at the antipodal point of the Imbrium basin. Imbrian-aged impact melt deposits are scattered throughout the quadrangle, confined for the most part to crater floors. Finally, ancient, heavily-cratered highlands terrain exists in the far northwest corner of the quad.

Volcanism. Volcanic products in the region are Imbrian in age [1]. These products are primarily discrete, non-contiguous maria occurring within or breaching the rims of craters or basins [2, 3]. The Jules Verne crater floor is dominated by such a deposit. Based upon assessment of morphology [4] and composition [5-8], these ponds are likely basaltic, similar to the nearside maria, but low in Fe and Ti (possibly due to vertical or lateral mixing of non-mare soils beneath these thin, areally small deposits [9,10]). Cryptomare material (basaltic material buried or mixed into the regolith as a result of impact activity) [11,12] does not appear in previously-published maps.

Data Sets and Methods: Morphology was determined using Lunar Orbiter (LO) and Clementine images. Because resolution of LO images varies widely in this area, Clementine UVVIS 750 nm images were used as the basemap (Figure 1); these average 150-200 m/pxl for Jules Verne. Clementine data were also utilized to extract compositional information. Coverage is global and includes ultraviolet/visible (UVVIS; 5 bands between 415 and 1000 nm) and near-infrared (NIR; 6 bands between 1100 and 2780 nm) data. We measured the average reflectance in the "visible" (750 nm) band and examined band ratios 750/950 nm, 750/415 nm, and 415/750 nm. Albedo is an indicator of the mafic content of the soil because it depends strongly on dark-mineral (e.g., ilmenite) content. The 750/950 nm ratio indicates the FeO content; the deeper the absorption feature, the greater the FeO content. The other band ratios measure the “continuum slope”; the younger the soil, the flatter the slope. Data acquired by the Lunar Orbiter Laser Altimeter (LOLA) yields topographic data at 100 m/pixel [13]. This topographic dataset represents the most refined spatial and vertical (~1 m/pixel) resolutions acquired for the Moon.

Mapping results: Figure 2 shows the preliminary map for this subsection of LQ-29. Jules Verne is a ~140 km diameter crater lying at ~ 35°S, 147°E, near the north central rim of SPA. Jules Verne has been dated as Nectarian in age; we date the floor as ~3.8-3.9 Gyr using crater size-frequency statistics. The crater lies in heavily-cratered basin terrain; this terrain is ~4 Gyr, with a potential resurfacing event at ~3.9 Gyr. The rim of SPA is visible in the topographic and albedo data, and is mapped slightly south of the previously mapped rim [1]. The interior of Jules Verne displays arcuate fracturing along its E edge and significant portions of the floor have been flooded with

Imbrian-aged mare material that we dated at ~3.6 Gyr. Volcanic products never previously identified include a potential dome (d) and associated sinuous rille (sr), and at least two dark mantling deposits (DMD) that may be pyroclastic in origin (1 and 2 in Fig. 2). DMD 1 is associated with a W-E trending graben, while DMD 2 lies on the main fracture to the east.

Mineralogy around the crater is most similar to cratered highlands. Strong mafic spectral signatures within surrounding crater floors are associated with patches of smooth, less-cratered terrain previously mapped as Nectarian-aged "rolling terra" (local erosional debris and ejecta within surrounding craters); three such regions are labeled in Figure 2. Region A, in particular, has a spectral signature richer in FeO than a previously-mapped inter-crater mare deposit just north of Jules Verne (not shown). Based on the combination of smooth, dark surfaces and FeO-rich spectra, we mapped these as mafic floor material/cryptomaria.

Discussion: Our preliminary map indicates volcanic activity was more diverse in terms of mode of emplacement in Jules Verne than previously indicated. Association of pyroclastic deposits with fracturing might indicate a tectonic mechanism for emplacement; the graben associated with DMD 1 in particular may be the result of near-surface dike emplacement (e.g. [14]). An area at least 3 times greater than previously indicated [1] is covered by cryptomaria; if this ratio holds consistent for any significant portion of LQ-29, then this would place new constraints on our understanding of the global lunar thermal budget. We are refining crater frequency-derived ages to determine whether the period of volcanic activity in this area may be extended in time.

References: [1] Stuart-Alexander, D. (1978), *USGS, I-1047*. [2] Zuber, M.T. et al. (1994), *Science, 266*, 1839. [3] Wieczorek, M.A. and Phillips, R.J. (1999), *Icarus, 139*, 246. [4] Yingst, R.A. and Head, J.W. (1997) *JGR, 102*, 10,909. [5] Lucey, P.G. et al. (1998), *JGR, 103*, 3701. [6] Pieters, C.M. et al. (2001) *JGR, 106*, 28,001. [7] Yingst, R.A. and Head, J.W. (1999), *JGR, 104*, 18,957. [8] Lucey, P. et al. (2005), *LPSC 36*, 1520. [9] Li, L. and Mustard, J. (2003), *JGR, 108*, 7-1. [10] Li, L. and Mustard, J. (2005), *JGR, 110*. [11] Hawke, B.R. et al. (1990), *LPI-LAPST*, 5. [12] Head, J.W. and Wilson, L. (1992), *GCA, 56*, 2155. [13] Smith, D.E. et al. (2010), *GRL, 37*, L18204. [14] Head, J.W. and Wilson, L. (1994), *Science, 41*, 719.

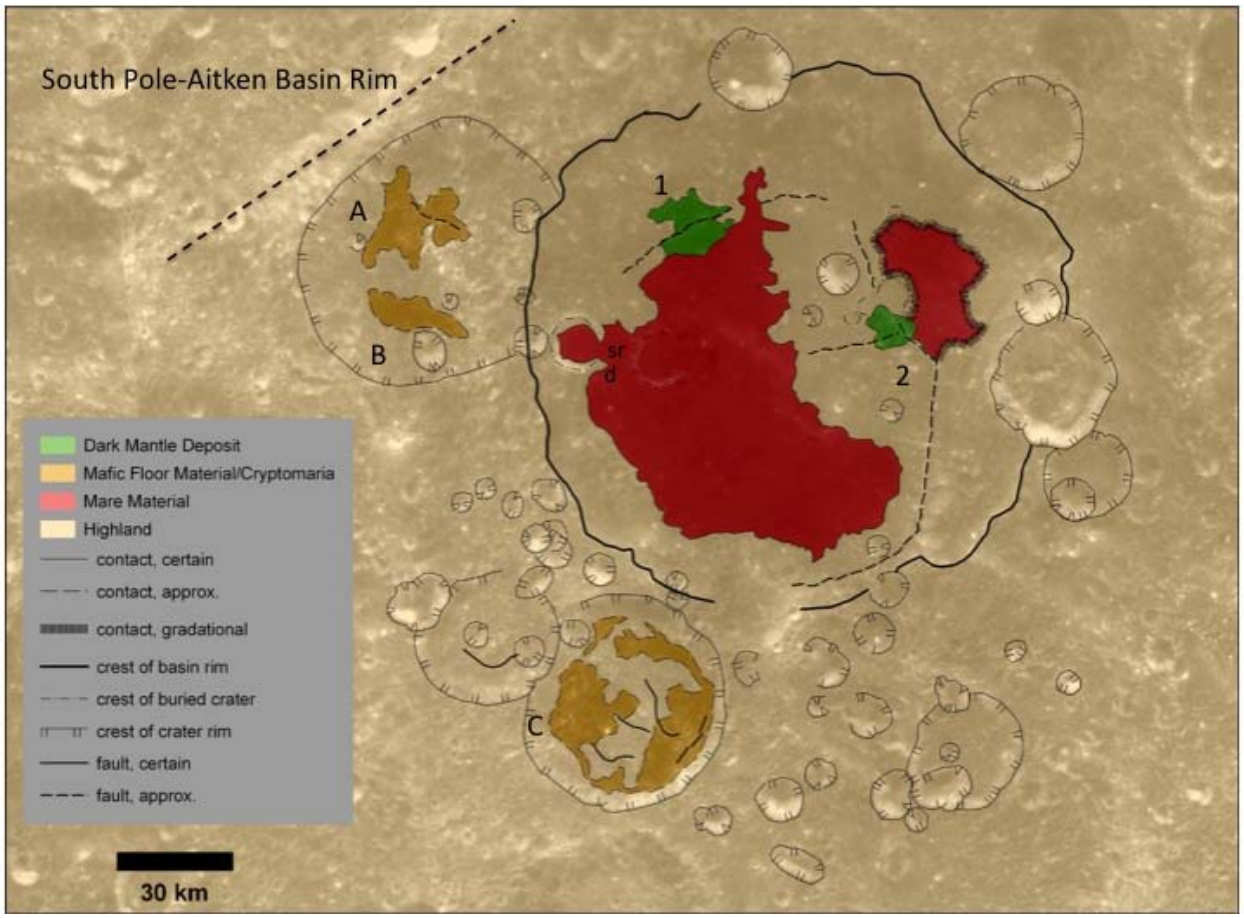

Figure 2. Geologic map of Jules Verne crater. Clementine 750 nm images provide the basemap.

UNRAVELING THE SPATIAL AND TEMPORAL HISTORIES OF MEMNONIA FOSSAE, SIRENUM FOSSAE, AND ICARIA FOSSAE, MARS. R.C. Anderson[1], J.M. Dohm[2], [1]Jet Propulsion Laboratory/California Institute of Technology, Pasadena, California (Robert.C.Anderson@jpl.nasa.gov), [2]University of Arizona, Tucson, AZ (jmd@hwr.arizona.edu).

Introduction: The formation of the Tharsis rise has influenced the geologic and tectonic histories of Mars, particularly evident in the Terra Sirenum region. The Terra Sirenum region is located to the southwest of Tharsis centered at 39.7°S and 210°E (Fig.1).

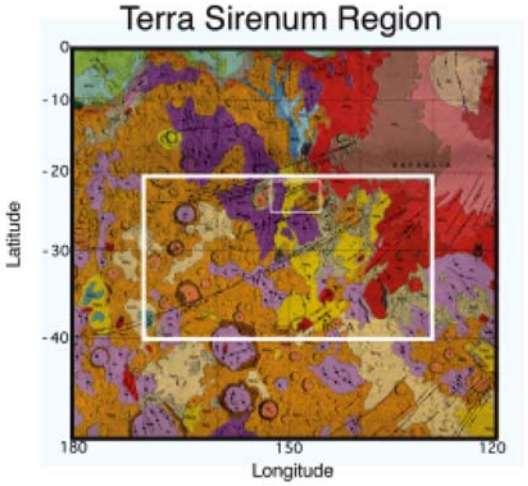

Fig. 1. Approximate map boundary of the proposed study region.

Due to its prime location, this region holds a significant key to improving our understanding of the timing of the major fault systems associated with the formation of the Tharsis rise. Five major fault systems are associated with the southwestern region of Tharsis. Of these five major fault systems, three have been identified within the Terra Sirenum region: Memnonia Fossae, Sirenum Fossae, and Icaria Fossae. Detailed examination of these structures within this region provides an excellent window into identifying and constraining the tectonic processes that influenced the geologic evolution of the western hemisphere region.

Objectives: Through the production of a geologic map of the Terra Sirenum region, our research objectives include: (1) reconstructing the temporal and spatial histories of the major fault systems located within the Terra Sirenum region, (2) determining the stratigraphic ages of tectonic features and comparing this paleotectonic information with centers of [1] (Fig. 2), and (3) identifying and time constraining any additional regional and local magmatic-tectonic events and ancient basins.

Preliminary results from the first year of mapping: In the first year of investigation, we have mapped thousands of faults (e.g., Fig. 3) and generated a preliminary stratigraphic map in GIS format for this region (Fig. 4).

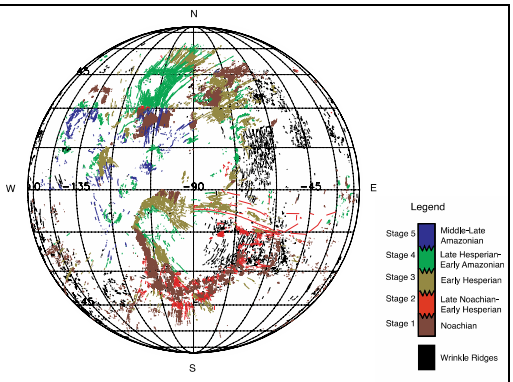

Fig. 2. Paleotectonic map of the western hemisphere of Mars [1]. Colors correspond to stratigraphic age of the tectonic features**.**

Continued effort and implications: We plan on completing the 1:5,000,000-scale geologic map of the Terra Sirenum region of Mars. This includes finalizing the stratigraphic map, compiling crater statistics, and completing structural mapping, which will include Tharsis-centered faults, large

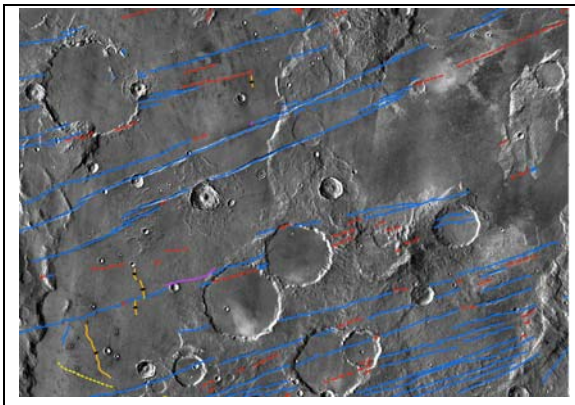

Fig. 3. Part of the Terra Sirenum map region exemplifying faults that have been identified and mapped. Narrow graben (blue lines), inferred faults (red lines), wrinkle ridges (orange lines), and unknown lineaments (yellow dashed lines) are shown. Our next step is to delineate, map, and characterize large (some several hundreds to over a thousand kilometers in length) north-trending faults.

structures (several with lengths exceeding 1,000 kilometers) not necessarily related to Tharsis, channels and valley networks, and wrinkle ridges. We will also perform spectroscopic/stratigraphic investigation, which includes construction of cross sections, and GIS-based statistical analysis and centers investigation.

In addition, we have identified and mapped large basins, many of which appear to be structurally controlled. Though the mapping is in preliminary phase, we are detailing what appears to be a significant relation among the basins, structures, magmatism, and hydrologic activity in places, as per objective #3 listed above.

The results of this comprehensive geologic mapping project will increase our knowledge of and have a direct bearing on 1) Terra Sirenum's tectonic history, 2) Terra Sirenum's erosional and sedimentary histories, 3) the geologic processes and events that have shaped the surface of Mars, and 4) understanding Mars' early climate history.

References: [1] Anderson, R.C., et al., *J. Geophys. Res.* 106, 20,563–20,585, 2001.

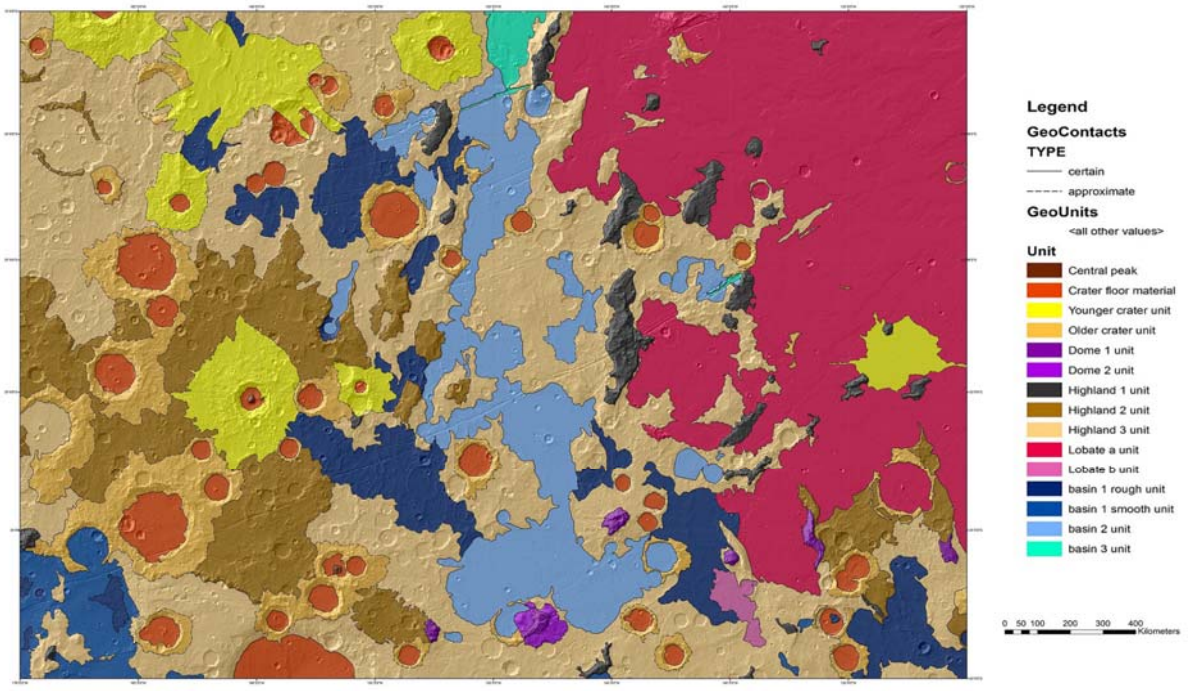

Fig. 4. Preliminary stratigraphic map of the Terra Sirenum region of Mars at 1:5,000,000-scale.

GEOLOGIC MAPPING OF THE OLYMPUS MONS VOLCANO, MARS. J.E. Bleacher[1], D.A. Williams[2], D. Shean[3], R. Greeley[2], [1]Planetary Geodynamics Laboratory, Code 698, NASA GSFC, Greenbelt, MD, 20771, Jacob.E.Bleacher@nasa.gov, [2]School of Earth & Space Exploration, Arizona State University, Tempe, AZ, 85282, [3]Malin Space Science Systems, Inc., San Diego, California.

Introduction/Background: We are in the second year of a three-year Mars Data Analysis Program project to map the morphology of the Olympus Mons volcano, Mars, using ArcGIS by ESRI. The final product of this project is to be a 1:1,000,000-scale geologic map. The scientific questions upon which this mapping project is based include understanding the volcanic development and modification by structural, aeolian, and possibly glacial processes.

The project's scientific objectives are based upon preliminary mapping by Bleacher et al. [1] along a ~ 80-km-wide north-south swath of the volcano corresponding to High Resolution Stereo Camera (HRSC) image h0037. The preliminary project, which covered ~20% of the volcano's surface, resulted in several significant findings, including: 1) channel-fed lava flow surfaces are areally more abundant than tube-fed surfaces by a ratio of 5:1, 2) channel-fed flows consistently embay tube-fed flows, 3) lava fans appear to be linked to tube-fed flows, 4) no volcanic vents were identified within the map region, and 5) a Hummocky unit surrounds the summit and is likely a combination of non-channelized flows, dust, ash, and/or frozen volatiles. These results led to the suggestion that the volcano had experienced a transition from long-lived tube-forming eruptions to more sporadic and shorter-lived, channel-forming eruptions, as seen at Hawaiian volcanoes between the tholeiitic shield building phase (Kilauea to Mauna Loa) and alkalic capping phase (Hualalai and Mauna Kea).

Methods: To address our science questions we are conducting flow morphology mapping on the Olympus Mons main flank at ~ 1:200,000 scale using the Context Camera (CTX) image mosaic as our base data. This scale enables a distinction between sinuous rilles and leveed channels, which is fundamental for interpreting abundances among, and changes between, tube- and channel-forming eruptions. We identify Channeled, Mottled, Hummocky, Smooth, Tabular, and Scarp Materials morphology units. We do not uniquely interpret a mapped unit as tube-fed flows as was done by [1]. Instead, we map sinuous rilles and chains of depressions as linear features. We identify fans as location features forming topographic highs surrounded by radiating flow patterns. We distinguish elongate topographic ridges as surface features. To assist in the identification of ridges and fans we derive local contour maps at 25, 50 and 75 meter intervals from the HRSC DTMs and MOLA DEMs.

Primary science issues driving this research project are identifying where the volcanic materials were erupted from, and determining if rift zones are present. In order to address these issues we separate the Channeled and Mottled units into 1) caldera-sourced, 2) fan-sourced, and 3) flank units. Often boundaries among these types of morphologic units are mapped as uncertain, and can eventually be combined if results do not provide any valuable insights into the development of the volcano. We also map as linear features boundaries between significant flow fields. Often we observe two distinctly different channelized flow fields that would be mapped singularly as the channeled unit. However, distinguishing between these flow fields might help distinguish between major eruptive episodes that could yield unique crater retention ages and estimates about the episodic nature of this volcano.

Current Results: We presented the results of our 1:1,000,000 structural mapping of the volcano at LPSC 41 [2]. We are now focused on the morphology mapping on the flank of the volcano. Our mapping effort is currently focused on the surface morphologies of the southern flank of Olympus Mons.

Our mapping of CTX data at ~ 6 m/pixel shows that surfaces that would have been mapped as lava tubes by [1] from coarser resolution HRSC data (12-20 m/pixel) can often be divided into several other units (typically Mottled, Smooth, and Channeled). This can be seen in Figure 1 where a topographic ridge with sinuous rille and fan that would have been mapped as a tube-fed flow by [1] is seen to be dominated by the mottled unit and some small channels. As such, we now infer the presence of tube-fed flows by a combination of at least two of the following criteria: rilles or pit chains, topographic ridges

with smooth or mottled surfaces, fans, and/or non-impact raised rim depressions. As such, a tube-fed flow can comprise several Olympus Mons morphologic units. These inferred criteria are also based upon field work funded by the Moon & Mars Analog Missions Activities Program and a Hawaiian analog is demonstrated in Figure 1. This discussion was presented at LPSC 42 [3] and is currently in preparation for submission to the Journal of Geophysical Research, Planets. We will likely conclude our morphologic mapping by interpreting which flow surfaces are tube-fed and adding this information as a surface feature.

Our current observations also suggest that an inference by [1] that tube-fed flows are embayed by younger channel-fed flows is not always consistent. Although this observation might be a result of a larger mapping area in this study, again the difference in resolution is aiding in the new interpretations. If in fact a number of major tube systems are observed to be the locally youngest flow features, then based on comparison with the Hawaiian volcanoes, Olympus Mons might be in an evolutionary stage similar to Kilauea and Mauna Loa (tholeiitic shield building) opposed to Hualalai and Mauna Kea (alkalic capping).

The Mottled and Hummocky units of [1] were noted as difficult to distinguish, in other words, a possible over-interpretation. The distinction between the units was based on surface roughness, Mottled being rough at the 10s-100s m scale and Hummocky at the 100s-1000s m scale. Both were interpreted, in part, as possible dust mantling over lava flows. The improved resolution of the CTX mosaic confirms that these two units are unique. The Mottled unit is now seen at the CTX resolution to involve the development, or near development, of small channeled flows (not detectable at the mapping scale of 1:200,000 but at full resolution), whereas the Hummocky unit appears to be a mantled lava flow surface, or a location where channels did not form near the caldera.

Ongoing Mapping: We have identified map units and features that appear to remain consistent across Olympus Mons and provide insight into the development of the volcano. We are currently continuing our mapping from the south flank, clockwise around the volcano. The northwest flank does show a surface mantle similar to that of the Hummocky unit near the summit [4]. This region might prove to require the addition of new map units. Otherwise, our preliminary unit identification and mapping efforts suggest that the current approach will be sufficient to complete the project and to provide new insight into the current science questions outlined in our proposal and the presentations of [2 and 3].

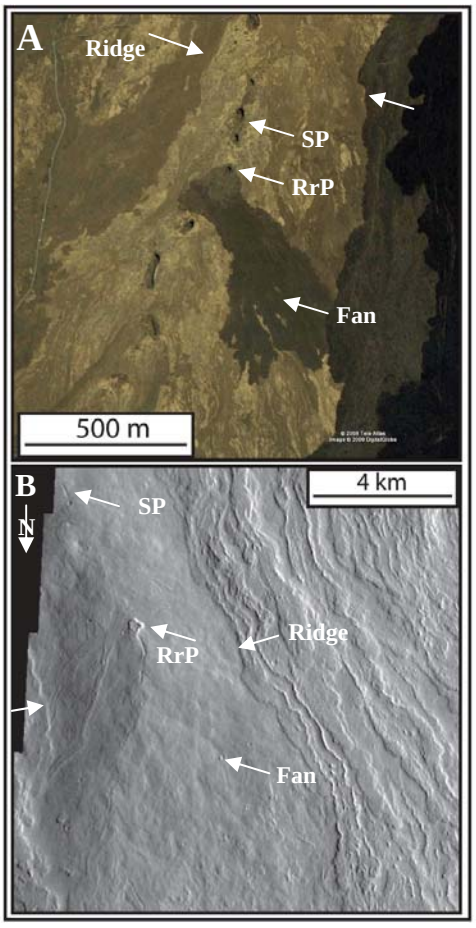

Figure 1. A) Landsat image (Google) showing the Pōhue Bay lava flow with several rimless pits that are sinuously aligned (SP) along the axis of a raised ridge (Ridge). Some pits also display raised rims (RrP), with one as the source for a ~750 m ʻaʻā flow (Fan). B) Themis image showing an Olympus Mons lava tube with rimless pits that are sinuously aligned (SP) along the axis of a ridge (between arrows marked "Ridge"). A raised rim pit (RrP) also is located at the apex of a lava fan (Fan). Although the ridge typically shows a mottled surface it also displays minor channels.

References: [1] Bleacher et al., (2007), JGRE 112, doi:10.1029/2006JE002826. [2] Williams et al., (2010), LPSC 41, #1053. [3] Bleacher et al., (2011), LPSC 42, #1805. [4] Basilevsky et al., (2005), Solar System Research, 39, 2, 85-101.

GEOLOGIC MAPPING OF MAWRTH VALLIS, MARS. L.F. Bleamaster, III[1,2], A.C. Wetz[1,2], F.C. Chuang[1], and D.A. Crown[1], [1]Planetary Science Institute, 1700 E. Ft. Lowell Rd., Suite 106, Tucson, AZ, 85719, [2]Trinity University Geosciences Department, One Trinity Place #45, San Antonio, TX, 78212; lbleamas@psi.edu.

Introduction: Geologic mapping at 1:1 million-scale of Mawrth Vallis and Nili Fossae (see Wetz and Bleamaster, this issue) is being used to assess geologic materials and processes that shape the highlands along the Arabia Terra dichotomy boundary. Placing these landscapes, their material units, structural features, and unique compositional outcrops into broad spatial and temporal context along the dichotomy (***Figure 1,*** red dashed line = topographic dichotomy) and with other highland-lowland transitions (***Figure 1,*** inset boxes) may help to: a) constrain paleo-environments and climate conditions through time, b) assess fluvial-nival modification processes related to past and present volatile distribution and their putative reservoirs (aquifers, lakes and oceans, surface and ground ice), c) address the influences of nearby volcanic and tectonic features on hydrologic systems and processes, including possible hydrothermal alteration, across the region and d) further evaluate the origin and subsequent modification of the Martian crustal dichotomy. The identification of broad geologic/geomorphic units (current mapping includes 12 map units for Mawrth Vallis (***Figure 2***) and 27 for Nili Fossae (see W&B, this issue; Figure 1) at scales significantly higher than previously available [1]) will help constrain the distribution, stratigraphic position, and crater model age of units across these areas providing regional and temporal context for larger-scale and more focused studies looking at mineralogic signatures from orbit (e.g., MSL landing site surveys).

Data and Methods: Datasets for geologic mapping include Viking and THEMIS day & night IR basemaps, MOLA topographic data (128 pixel/deg; ~462 m/pixel), HRSC, and CTX images. Mineralogy maps are derived from CRISM and OMEGA data and have been extracted from multiple literature sources [2,3, and references therein]. These mineralogy maps show outcrops and deposits of olivine, pyroxene, hydrated silicate, phyllosilicates, carbonate and sulfate detections. Using GIS and digital methods, manual geo-rectification of published mineralogy maps are being compared with the newly generated geologic maps of Nili Fossae and Mawrth Vallis.

Mawrth Vallis (MTM quadrangles 20022, 20017, 20012, 25022, 25017; ***Figure 2***) is one of the oldest outflow channels on the surface of Mars. This sinuous channel cuts across the western surface of the Arabia Terra plateau. This channel is a possible representation of past catastrophic outflow of a subterranean aquifer or persistent groundwater sapping. Few bed forms are preserved indicating the channel has undergone significant modification since its formation.

Unit Descriptions: (in order from oldest to youngest as constrained by **preliminary** N16 and N5 counts; ***Figure 3***). There are three primary units of Mawrth Vallis: the Noachian cratered terrain, Noachian/Hesperian channel floor materials, and Hesperian plains deposits near the northwest boundary of the Mawrth Vallis terminus.

Arabia Terra unit 1 (NAt1) **–** Plains with ridges ranging from straight to sinuous in planform shape with relatively constant widths that occasionally widen and narrow along their length; ridges appear as a simple step or a broad, flat-topped surface with relief; some ridge axes intersect at near right angles (i.e., near-perpendicular). *Interpretation:* Near-surface highland crust modified by tectonic forces producing ridges either by contraction and (or) upwards thrusting along a fault. For intersecting ridges, crustal shortening may have occurred as separate events along each ridge axis or as isotropic contraction activating structures of multiple orientations.

Mawrth Vallis, undivided (HNMvu) **–** Multiple smooth surfaces within the channel floor along the upper and middle reaches of Mawrth Vallis; surfaces have a low abundance of impact craters, are divided into larger polygonal sections in places, and are sometimes incised by one or more channels; darker material is exposed from below this unit in the middle reaches. *Interpretation:* Fluvially-modified surface during the formation of Mawrth Vallis with possible remnant bars and scour features.

Mawrth Vallis unit 1 (HNMv1) **–** Dark-toned surfaces with abundant knobs and smooth floors that are lower relative to other adjacent Mawrth Vallis units 2 and 3; few craters are observed. *Interpretation:* Heavily-modified plains material near Mawrth Vallis with exposure of underlying dark-toned unit that may be compositionally different from Arabia Terra unit. Mineral detections: phyllosilicates.

Mawrth Vallis unit 2 (HNMv2) **–** Dark and light-toned surfaces with some knobs and rough-textured floors that are higher relative to adjacent Mawrth plains 1 material, but possibly lower than adjacent Mawrth plains 3 material; craters are more abundant than on Mawrth plains 1 surfaces. *Interpretation:* Moderate to heavily-modified plains material near Mawrth Vallis that is transitional between Mawrth Vallis units 1 and 3. Mawrth Vallis unit 1 is an exhumed lower dark-toned unit that is interspersed with a lighter-toned unit or covered by the moderate-toned Mawrth 3 unit. Mineral detections: phyllosilicates.

Mawrth Vallis unit 3 (HNMv3) **–** Smooth moderate-toned surfaces that appear to be at the same relative elevation as Arabia Terra unit l; craters are more abundant than on Mawrth Vallis unit 1 surfaces. *Interpretation:* Plains material near Mawrth Vallis with little to no modification relative to Mawrth plains 1 and 2 units.

Arabia Terra unit 2 (HNAt2) **–** Smooth material with occasional ridges and abundant secondary craters and crater chains; areas near Mawrth Vallis appear etched where parts of the surface are stripped, exposing a possible lower surface unit. *Interpretation:* Highland crust modified by tectonic forces producing ridges, but in fewer numbers than Arabia Terra unit 1. Eolian deflation and (or) weathering processes have eroded the surface, creating rough, knobby-like regions, particularly near Mawrth Vallis.

Arabia Terra undivided (HNAtu) **–** Smooth material with few ridges and abundant secondary craters and crater chains; outcrops within Acidalia Planitia appear as remnant knobs and massifs. *Interpretation:* Highland crust modified by tectonic forces producing plateau and trough topography. Eolian deflation and (or) weathering processes have eroded the surface, creating rough, knobby-like regions, particularly near Acidalia Planitia.

Acidalia plains material (HAp) **–** Relatively smooth plains covering the lowlands beyond the dichotomy boundary;

many locales have clusters or individual polygonal blocks and knobs of highland material; several ridges similar to those in Arabia Terra units 1 and 2 are observed. *Interpretation:* Highland materials deposited into the low-lying northern plains by sedimentary processes that may include eolian, mass-wasting, and volcanic air fall deposits. Fluvially-deposited materials may be near the mouth of Mawrth Vallis.

Other units (unconstrained by crater counts):

Highly-degraded crater material (c1) – Partial to discontinuous rim with little or no relief relative to surrounding surfaces; little to no ejecta blanket; several craters have channels along the interior walls. *Interpretation:* Deposits exhibiting extensive degradation that form ejecta, rims, and floors of impact craters.

Moderately-degraded crater material (c2) – Continuous rim with minor relief relative to surrounding surfaces and continuous to semi-continuous ejecta blanket; several craters have channels along the interior walls. *Interpretation:* Deposits exhibiting moderate degradation that form ejecta, rims, and floors of impact craters.

Well-preserved crater material (c3) – Pronounced, continuous rim with significant relief relative to surrounding surfaces and continuous ejecta blanket; several craters with ejecta blankets have rampart margins. *Interpretation:* Deposits exhibiting little degradation that form ejecta, rims, and floors of impact craters.

Channel material (ch) – Smooth surfaces confined to the floor of large sinuous channels in Ridged Plains and Mawrth Plains materials. *Interpretation:* Sedimentary material deposited during channel formation.

Mineral Detections: Three principle clay types are located within the Mawrth Vallis units: Fe, Mg, and Al-rich smectites. The Al-rich phyllosilicates, in the form of montmorillonite clays, are located in eroded light-toned outcrops along the flanks of Mawrth Vallis unit 2 (royal blue map unit). The Al-rich unit is minimally hundreds of meters thick [4,5,6], layered down to the meter-scale [4-8] with moderate thermal inertia signatures [5,6], and is eroded into knobby and flat mesa-like cliff forms [7,8], typical of Mawrth Vallis unit 1 (dark blue map unit). In some locations along the walls of Mawrth Vallis, the Al-rich unit appears to lie stratigraphically between Fe or Mg-bearing smectite units (e.g., nontronite) [8,9]. A transitional unit with spectral signatures of both Al-bearing and Fe/Mg clays is also observed. The Al-bearing unit has meter-scale polygonally fractured surfaces while the darker-toned Fe/Mg-bearing clay units have larger polygonal surfaces that are tens of meters wide [5,10]. These surfaces may have formed as a result of thermal and/or desiccation contraction [5,10]. Other dark-toned materials present throughout the region are identified as pyroxene-rich materials (i.e., basaltic sand and dust) that mantle the surface (and clay-bearing units) [6,8,9]. The presence of clays in Mawrth Vallis is important as they imply a past aqueous environment in this region of Mars. It is argued, and supported here, that the clay-bearing units were formed early in the history of Mars (also prior to the formation of Mawrth Vallis) as aqueous deposits of sedimentary or pyroclastic materials, or a combination of both [4-11].

References: [1] Greeley and Guest (1987) *USGS Geo. Inv. Ser. Map 1802-B.* [2] Ehlmann et al. (2009) *JGR 114,* doi:10.1029/2009JE003339. [3] Noe DoBrea et al. (2010) *JGR 115,* doi:10.1029/2009JE003351. [4] Poulet et al. (2005) *Nature 438,* 623-627. [5] Loizeau et al. (2007) *JGR 112,* doi:10.1029/2006JE002877. [6] Michalski J.R. and Fergason R.L. (2009) *Icarus 199,* 25-48. [7] Bibring et al. (2006) *Science 312,* 400-404. [8] Michalski J.R. and Noe Dobrea E.Z. (2007) *Geology 35,* 951-954. [9] Bishop et al. (2008) *Science 321,* 830-833. [10] Wray et al. (2008) *GRL 35,* doi:10.1029/2008GL034385. [11] Howard A.D. and Moore J.M. (2007) *LPSC 38,* abstract #1339. [12] Chuang and Crown (2009) *USGS SIM #3079.* [13] Bleamaster and Crown (2010) *USGS SIM #3096.*

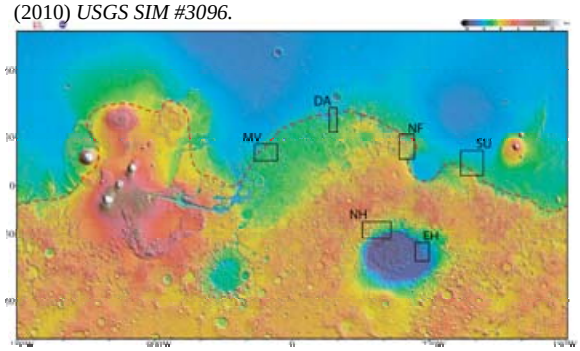

Figure 1. *Global MOLA map showing locations of various highland-lowland mapping efforts: MV=Mawrth Vallis, NF=Nili Fossae (see W&B, this issue), DA=Deuteronilus/Arabia [12], EH=Eastern Hellas [13], SU=Southern Utopia [Skinner et al., in prog.], NH=Northwest Hellas [Crown et al., in prog.].*

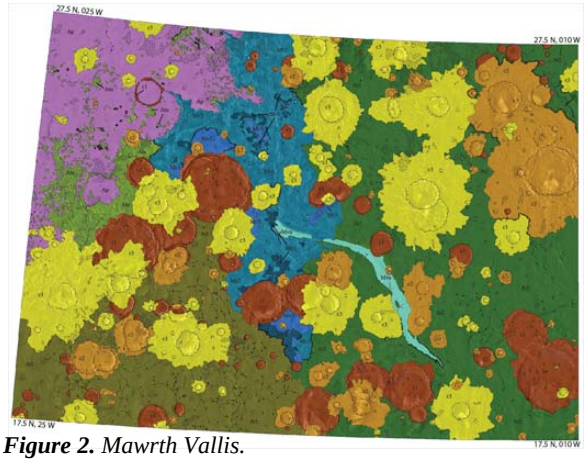

Figure 2. *Mawrth Vallis.*

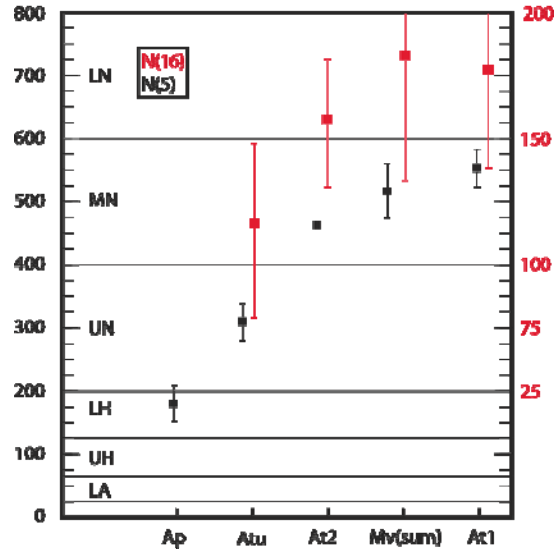

Figure 3. *N5 and N16 crater ages for major units.*

GEOLOGIC MAPPING INVESTIGATIONS OF THE HELLAS REGION OF MARS. David A. Crown, Scott C. Mest, and Leslie F. Bleamaster III, Planetary Science Institute, 1700 E. Ft. Lowell Rd., Suite 106, Tucson, AZ 85719; crown@psi.edu.

Introduction: At 2000+ km across and with elevations below -8200 m, Hellas basin is the largest well-preserved impact structure on Mars and its deepest depositional sink [e.g., 1]. The Hellas rim and adjacent highlands are of great significance for understanding the water and climate histories of Mars given the possibility of paleolakes on the basin floor [2-4], recent studies of potential localized fluvial/lacustrine systems in the Hellas region [e.g., 2, 5-8], and evidence for phyllosilicates around and within impact craters north of the basin [e.g., 9-12].

This abstract reports on three mapping investigations of the Hellas region: 1) a 1:1M-scale geologic map of four MTM quadrangles at the eastern margin of Hellas Planitia (MTM -40277, -45277, -40272, and -45272 [4]), 2) a 1:1.5M-scale geologic map of eight MTM quadrangles along Hellas' NW rim (-25312, -25307, -25302, -25297, -30312, -30307, -30302, -30297 [Crown et al., USGS, in prep.]), and 3) a 1:1M-scale geologic map of three MTM quadrangles covering the upper reaches of the Reull Vallis system (MTM -30247, -35247, and -40247 [Mest and Crown, USGS, submitted]).

Geologic Mapping of Eastern Hellas Planitia: This map area (37.5-47.5°S, 80-90°E) contains Hellas floor and rim materials, including extensive plains interpreted to be sedimentary in origin as well as parts of Dao and Harmakhis Valles. Key findings from this mapping study include recognition and characterization of widespread deposition on top of eroded highland terrain, including the presence of finely-layered outcrops along the basin margin [2, 4]. Sedimentary materials may have been deposited subaqueously in a standing body of water or along the margin of an ice-covered lake. If the plains above -5,800 m in elevation are partially lacustrine, then extensive Hellas paleolakes may have existed into the Early Hesperian Epoch; if the rim sediments are not lacustrine, then any Hellas paleolakes would have been more ancient and/or restricted to the basin floor. Development of channels across the Hellas east rim followed and resulted in the eventual formation of the larger valles through sapping and collapse. The Amazonian Period is dominated by local erosion and redistribution of material, including recent ice-rich mid-latitude mantling deposits.

Geologic Mapping of NW Hellas: This map region (22.5-32.5°S, 45-65°E) includes a transect across the cratered highlands of Terra Sabaea, the degraded NW rim of Hellas, and basin interior deposits of NW Hellas Planitia. Mapping of the NW Hellas rim initially involved production of geologic maps of two subregions of the larger map area in order to establish a scheme for delineation of geologic units. Research related to the geologic mapping investigation [13-18] has included general terrain characterization, evaluation of geomorphology and stratigraphic relationships, exploration of compositional signatures using CRISM, and investigation of impact crater distribution, morphometry, and interior deposits.

Geologic mapping and investigations of impact craters on the NW Hellas rim [13-18] show evidence for crater infilling and regional resurfacing along with widespread occurrences of phyllosilicates and Fe-bearing silicates in association with highland remnants, including depressions formed by retreat/erosion of plains. The NW Hellas region preserves the record of an extensively buried landscape with sedimentary deposition that extended beyond the topographic margin of Hellas basin and well into the surrounding highlands.

Geologic Mapping of Reull Vallis: This map area (27.5-42.5°S, 110-115°E) is centered on the upper reaches of the Reull Vallis canyon system, including the newly named Waikato Vallis that comprises the northerly segment of the Reull Vallis system. The map area includes eroded remnants of highland terrains surrounding Reull and Waikato Valles and a series of ridged, smooth, etched, and mottled plains units [Mest and Crown, USGS, submitted]. A key objective was analysis of the Reull Vallis system in its fluvial zone, where evidence for fluvial erosion is observed along with subsidence and collapse and where relationships to adjacent plains could be assessed. The southern part of the ridged plains pre-date the valles and show evidence for fluvial dissection and collapse as part of vallis formation. The regional landscape records a complex interaction of water with the cratered highlands, including dissection and modification of ancient crater rims and ejecta and infilling of local low-lying regions in intercrater zones and crater interiors. Lacustrine sediments may characterize part of the plains surrounding Reull Vallis. Scour marks and terraces characterize the uppermost parts of the Reull Vallis system, whereas ice-driven mass-wasting appears to dominate vallis wall and floor deposits closer to Hellas basin.

References: [1] Tanaka, K.L. and G.J. Leonard (1995), JGR, 100, 5407-5432. [2] Crown, D.A. et al. (2005), JGR, 110, E12S22, doi:10.1029/2005JE002496. [3] Moore, J.M. and D.E. Wilhelms (2001), Icarus, 154, 258-276. [4] Bleamaster, L.F. and D.A. Crown (2010), USGS Sci. Inv. Ser. Map 3096. [5] Ivanov, M.A. et al. (2005), JGR, 110, E12S21, doi:10.1029/2005JE002420. [6] Korteniemi, J. et al. (2005), JGR, 110, E12S18, doi:10.1029/2005JE002427. [7] Moore, J.M. and A.D. Howard (2005), JGR, 110, E04005, doi:10.1029/2004JE002352. [8] Wilson, S.A. et al. (2007), JGR, 112, E08009, doi:10.1029/2006JE002830. [9] Poulet, F. et al. (2005), Nature, 438, 623-627. [10] Bibring, J.-P. et al. (2006), Science, 312, 400-404. [11] Murchie, S. et al. (2007), JGR, 112, E05S03, doi:10.1029/2006JE002682. [12] Pelkey, S.M. et al. (2007), JGR, 112, E08S14, doi:10.1029/2006JE002831. [13] Crown, D.A. et al. (2007), EOS Trans. AGU, abstract P41A-0189. [14] Mest, S.C. et al. (2008), LPSC XXXIX, abstract 1704, LPI (CD-ROM). [15] Crown, D.A. et al. (2009), LPSC XL, abstract 1705, LPI (CD-ROM). [16] Crown, D.A. et al. (2010), in NASACP-2010-216680. [17] Crown, D.A. et al. (2010), LPSC XLI, abstract 1888. [18] Crown, D.A. et al. (2011), in NASA/CP-2010-217041.

Figure 1. Below) Geologic map of the eastern Hellas Planitia region [Bleamaster and Crown, USGS, 2010] showing sedimentary shelf along basin rim, floor deposits, and through-going channels and valles. Right) Geologic map of the upper reaches of the Reull Vallis system (including Waikato Vallis) [Mest and Crown, USGS, submitted] showing initiation within ridged plains and extension through cratered highlands.

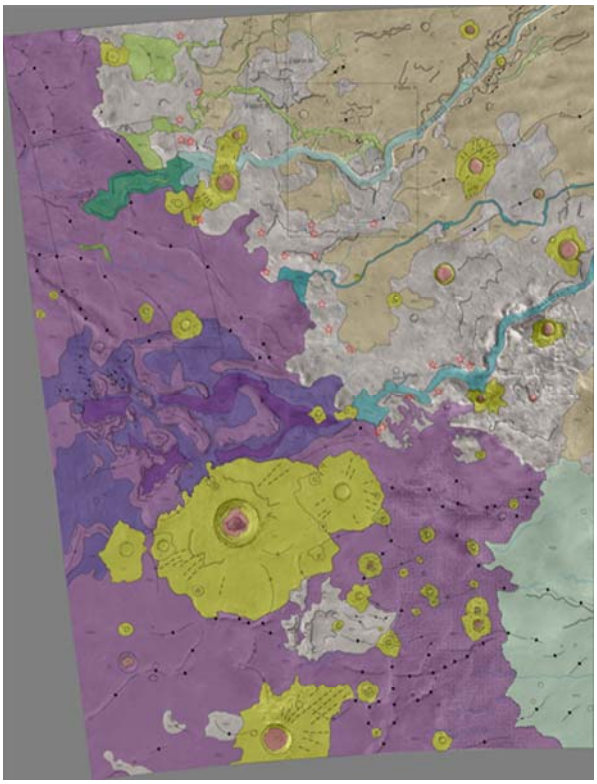

GEOLOGIC MAPPING INVESTIGATON OF THE ARGYRE AND SURROUNDING REGIONS OF MARS. J.M. Dohm, University of Arizona, Tucson, AZ (dohm@hwr.arizona.edu).

Introduction: Was the Argyre basin occupied by a large lake, and did this hypothesized lake source the Uzboi Vallis drainage system during the Noachian Period, as hypothesized during Viking-era investigation [1]? What was the extent of flooding and glaciation in and surrounding the ancient giant impact basin [e.g., 2]? How did the narrow ridges located in the southeast part of the basin form [e.g., 3]? What was the extent of Argyre-related tectonism and its influence on the surrounding regions [e.g., 4]? These and other significant questions concerning the geologic and paleohydrologic histories of the Argyre impact basin and surroundings are being investigated through a post-Viking-era geologic mapping investigation.

The primary objective of the investigation is to produce a geologic map of the Argyre basin and surrounding region at 1:5,000,000 scale that will detail the stratigraphic and crosscutting relations among rock materials and landforms (30°S to 65°S, 290°E to 340°E; **Fig. 1**); the most recent published geologic map of the Argyre basin and surroundings was based from Viking data [4,5]. The regional geologic mapping investigation includes the Argyre basin floor and rim materials, the transition zone that straddles the Thaumasia plateau, which includes Argyre impact-related modification, and the southeast margin of the Thaumasia plateau.

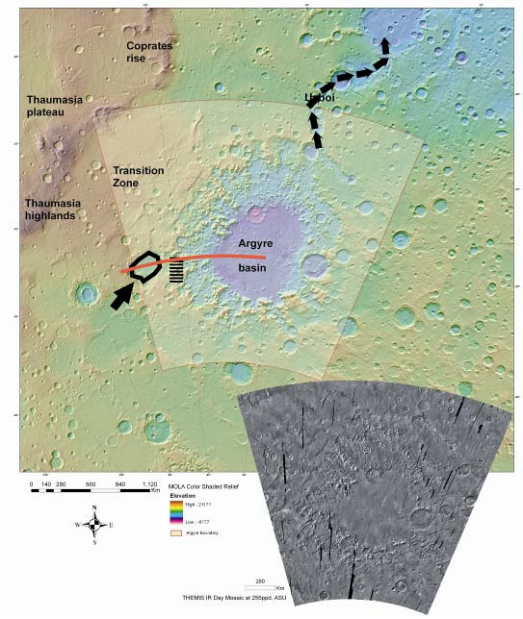

Fig. 1. MOLA color shaded relief map centered on the Argyre region (transparent outline). The image on the bottom right shows a 256 pixels/degree THEMIS IR day mosaic. The regional 1:5,000,000-scale mapping investigation includes the Argyre floor and rim, transition zone, and the southeast margin of the Thaumasia plateau [4].

Also shown is a possible paleolake basin (wide arrow) located on the western margin of the Argyre impact basin and the Uzboi drainage system (narrow arrows), referred to hereafter as the AWMP, possible spillway separating AWMP from the Argyre basin at a present-day topographic interval nearing 1.5km (dashed line), and a transect for the topographic profile shown in **Fig. 4** (red line).

Preliminary results from the initial phase of mapping: In the initial phase of the Argyre mapping investigation, general stratigraphic relations and tectonic and erosional structures have been mapped (**Fig. 2**). This information has been incorporated into the global geologic mapping effort of Mars led by Ken Tanaka [6].

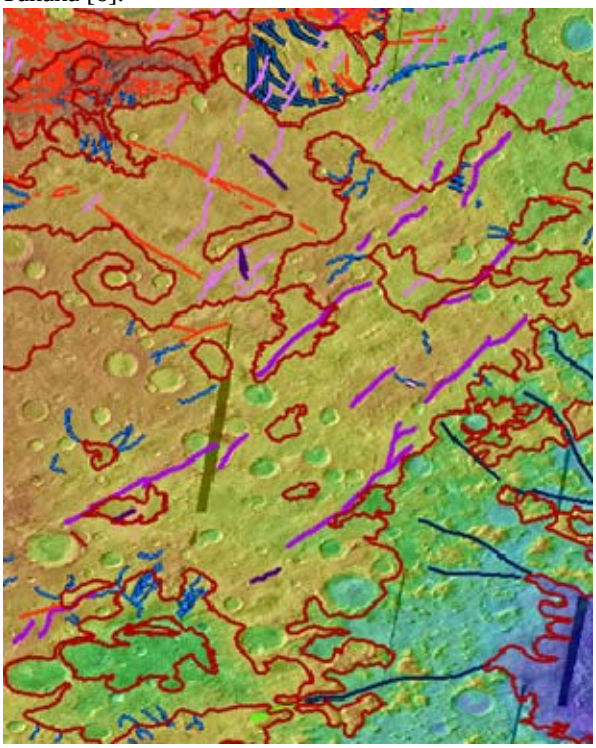

Fig. 2. The northwest part of the Argyre map region exemplifying mapped graben (red lines), large faults (hundreds of kilometers in length), several of which are related to the Argyre impact event (violet lines), erosional landforms such as valleys, many of which are influenced by the Argyre impact event (light and dark blue lines), wrinkle ridges (pink lines), and geologic contacts (red lines). North is at top and the scene is approximately 1,250 kilometers across.

In addition, large basins, many of which appear to be both the result of the Argyre impact event and occupied by lakes (**Figs. 3 and 4**), have been identified and mapped.

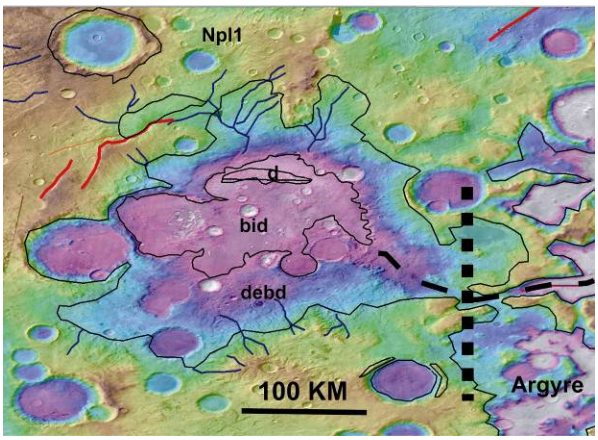

Fig. 3. MOLA color shaded relief map coupled with a THEMIS IR day mosaic highlighting AWMP. Argyre-induced tectonic structures (red lines), drainage systems that debouch into the basin (blue lines), a possible spillway, and from oldest to youngest, cratered highland materials (Npl1), dissected and etched basin deposits (debd), basin infill deposits (bid), and dune deposits (d), are highlighted. Note that the drainage systems terminate within a contour interval ranging from 0 to 1.5km (within debd which may mark a lake-related topographic bench), the latter elevation of which occurs at a possible spillway divide (thick black dashed line) at present-day topography.

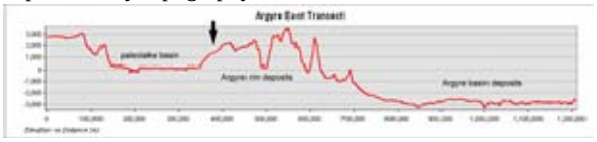

Fig. 4. Topographic profile transecting from west to east (see **Fig. 1** for transect location) through AWMP and the Argyre rim materials and basin deposits. Note that a topographic bench (arrow) occurs near an elevation of ~1.5km. Direct evidence of a paleolake is subdued, however, due to modification by processes such as periglacial and glacial activity [7].

Continued effort and implications: Completion of the geologic map of the Argyre region of Mars will include finalizing the stratigraphic map, compiling crater statistics, and completing structural mapping, which will include Argyre- and Tharsis-related faults, channels and valley networks, many of which are controlled by the growth of Tharsis and landscape deformation through the Argyre impact event, wrinkle ridges, and a diverse assemblage of glacial and periglacial features. This investigation will also include spectroscopic/stratigraphic investigation, which includes construction of cross sections [e.g., 8], and GIS-based statistical analysis of the rock stratigraphic units and structures.

A new regional geologic map of the Argyre region of Mars will have wide-ranging significance and application, including: (1) the establishment of a spatial and temporal geologic context for local to regional geologic, geophysical, geochemical, hydrologic, and climatic studies, (2) the refinement of the regional stratigraphic scheme for establishing chronology and estimating rates of geologic activity, and (3) spatial and temporal information for which to assess whether the Argyre basin contained lakes [1] (e.g., **Fig. 5**) and whether flooding and glaciation contributed significantly to the geologic and paleohydrologic records of the Argyre region [e.g., 2,9-11], and the extent of Argyre-related tectonism [4]. Furthermore, this geologic investigation could provide timely information to the Mars Science Laboratory (MSL) mission (i.e., regarding provenance, including a possible source region for the floodwaters and rock materials), if MSL performs reconnaissance in an impact crater along the Uzboi Vallis system [12]).

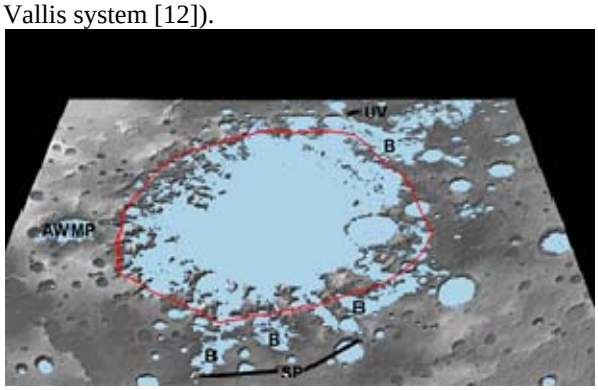

Fig. 5. Schematic paleolake map of the Argyre basin using a maximum topographic elevation of 0 km based on MOLA topography (regions in blue). An estimated extent of the putative Argyre lake based on geomorphologic and topographic analyses, as well as detailed geologic mapping is also shown (red line). In addition to the estimated extent, sapping valley systems, local basins which occur among the crater rim materials, and the Uzboi Vallis system correspond to the blue-highlighted region. The volume of the putative lake is estimated to be 1,899,337.0 km^3 based on Geographic Information Systems (GIS) calculation using MOLA. There is significant evidence of water-ice modification (e.g., glaciation) as shown by [e.g., 2,3,11]. Was there an interplay between lakes, ice sheets, glaciers, and ever changing conditions through time including waning water bodies? Continued detailed geologic investigation is warranted.

References: [1] Parker, T.J., and Gorsline, D.S. (1993) Am. Geophys. Union Spring Meeting, 1pp. [2] Kargel, J.S., and Strom, R.G., Ancient glaciation on Mars, Geology, 20, 3-7, 1992. [3] Banks, M.E., et al., 2008, J. Geophys. Res., 113, E12015, doi:10.1029/2007JE002994. [4] Dohm, J.M., et al., 2001a, USGS Map I-2650. [5] Scott, D.H., et al., 1986-87, USGS Map I-1802-A-C. [6] Tanaka, K.L., et al., this meeting. [7] Dohm, J.M., et al., 2011, Lunar Planet. Sci. XXXXII, Abstract #2255. [8] Buczkowski, D.L., S. Murchie, R. Clark, K. Seelos, F. Seelos, E. Malaret, C. Hash and the CRISM Team (in revision), Investigation of an Argyre basin ring structure using MRO/CRISM, J. Geophys. Res. [9] Hiesinger, H., and J.W. Head, 2002, Planetary and Space Sci. 50, 939-981, 2002. [10] Parker, T.J., et al., 2000, LPSC 31, abstract 2033. [11] Banks, M.E., et al., 2009, J. Geophys. Res. 114, E09003, doi:10.1029/2008JE003244. [12] Grant, J.A., et al., 2010, AGU.

GEOLOGIC MAPPING IN THE ARABIA AND NOACHIS TERRAE BOUNDARY REGION, MARS: MTM QUADRANGLES -20002, -20007, -25002 AND -25007. C.M. Fortezzo, United States Geological Survey, Astrogeology Science Center, 2255 N. Gemini Dr., Flagstaff, AZ, 86001, cfortezzo@usgs.gov.

Introduction: As part of a continuing study to understand the relationship between valleys and highland resurfacing through geologic mapping, I am finalizing 4 quadrangles at 1:1,000,000-scale in the Arabia and Noachis Terrae region for submission [1,2]. Results from this mapping have helped to constrain the regional role and extent of water. The MTM quads extend from 17.4º - 27.6ºS and -10.1º - 0.1ºE and abut SIM-3041 [3] along its western margin.

Methods: Over the past 5 years, I have used ESRI's ArcGIS software to build linework and geologic polygons. Using this digital environment, all digitization of lines (e.g., contacts, structures, etc.) and polygons (e.g., units and craters) is complete. Arc extensions provided robust tools for (1) analyzing spatial relationships across multiple data layers, (2) attributing and updating digital linework, (3) building, analyzing, and cleaning vector topologies, and (4) importing new data as they are released. To inspect and quantify stratigraphic relations, I am compiling crater counts in ArcGIS software using the CraterTools extension and plotting the counts using the CraterStats IDL program provided by the Freie Universität in Berlin, Germany [4,5]. These crater counting tools are specifically developed for planetary mappers and researchers.

Datasets: The proposed map base for this map was the MDIM 2.1 and MOLA (463 m/pixel) datasets. In 2008, I switched the map base to THEMIS daytime IR, when the coverage neared 100% of the map area. In 2010, the THEMIS team released a semi-controlled, tone matched, global mosaic of THEMIS daytime IR (100 m/pixel) which is now the USGS standard for all 1:1,000,000- and 1:500,000-scale Mars maps. This mosaic will be the final base map.

New high-resolution datasets from the Mars Reconnaissance Orbiter including CTX (~6 m/pix), and HiRISE (0.25 m/pix) images were incorporated into the project upon release. CTX provides both high-resolution, local details with regional context. The HiRISE images provide detail to further characterize the geomorphology and contacts of the units. HiRISE coverage is limited to small areas, so the HiRISE level descriptions are not available for all units.

Local Physiography: MTM quads -20002, -20007, -25002 and -25007 contain portions of Noachis and Arabia Terrae and lie on the eastern border of Margaritifer Terra. The area slopes down from southeast to northwest following the regional trend of the northwest portion of the circum-Hellas rise in the highlands. Two large impact basins, Newcomb crater and Noachis basin (informal name, centered at -22ºS and -5ºE), dominate the local topography. Valley orientation is controlled by local topography. In the west, valleys trend west towards Paraná basin (informal name, centered at -22ºS and -12.5ºE). In the south, valleys flow into the relatively flat-floored Noachis basin. In the north, valleys flow towards southern Arabia Terra, through the highland-midland transition zone (HMTZ).

The HMTZ is represented in MOLA as a northwest-facing, southwest northeast trending slope from the Holden crater region in the southwest to the western flank of the Terra Sabaea rise in the northeast. The transition zone appears less densely cratered than the adjacent Noachis and Arabia Terrae [6]. Based on the abundance of partially buried and flat-floored craters, the apparent younger age is likely due to resurfacing from deposited materials sourced from the Noachis Terra region highlands.

Changes to Map Unit Approach: In an attempt to conform to modernized planetary geologic mapping standards [7], units are delineated by their stratigraphy and emplacement type. The approach for this map uses the geologic principle of superposition creating a rift from traditional photogeologic geomorphic mapping and crater-dating techniques. For example, a denuded unit should display a more youthful crater-based age than an undisturbed stratigraphically younger unit. However, superposition dictates that the undisturbed material unit is stratigraphically younger, regardless of its crater density relative to a subjacent, denuded unit. I found that this principle could be applied fairly consistently throughout this map area. Thus, the units are labeled with a group designation and a number representing its interpreted stratigraphic level (e.g., h_1, where h is a highland unit and 1 is the lowest and subsequently oldest exposed and delineated unit). Using this technique, the units of this map area have been divided into the three groups: highlands, basins, and craters.

Highland Map Units: The highland group includes an upper and lower unit. The upper unit is a topographically high-standing, plateau-forming material characterized by wrinkle ridges, a relatively high density of impact craters and a muted, mantled appearance. The lower unit is a slope forming material located at the edge of the upper unit. The older material is exposed by incisions created by dense, well-integrated, and well-preserved valley systems. The highland units have unit names that represent their

stratigraphic location in this group: h_1 (lower) and h_2 (upper).

Basin Map Units: The basin group includes 6 units widely distributed over the map area. The oldest basin unit (b_1) is located on larger, older crater floors including Noachis basin and Newcomb crater. The unit is characterized by light-toned material with decameter-scale polygonal fractures. The fractures are frequently filled with a more resistant material, which remain when the surrounding material is eroded. Wrinkle ridges and eolian deposits are also present. This unit is overlain by the b_2 and b_5 units.

The next basin unit (b_2) forms characteristic "islands" of blocky, knobby, and etched materials within basins. Some locations include scarp margins, possibly dikes similar to those observed in unit b_1, which are more resistant to erosion than surrounding material. This unit is often in direct contact with the b_1 materials and is not overlain by any other units.

The b_3 unit includes materials deposited in the highland terrain through various processes (fluvial, impact, airfall, and/or eolian) and represent early basin infill. These materials have been denuded by downcutting of channels. This unit is different from the h_1 unit in that the number of valleys markedly decreases in both density and valley morphology appears muted. This supports that this material is less competent than unit h_1 and is, likely, unlithified or otherwise friable material. This material underlies the b_4 materials.

The b_4 unit consists of flat-lying, smooth early basin-infill materials that overlie the b_3 materials. This material was emplaced in the same manner as b_4 and is likely unconsolidated regolith, but less friable due to partial cementation (e.g., desert pavement formation). The crater age of this surface may provide an estimate of age of a significant drop in base level and the reactivation of both this unit and the materials of b_3. These materials overlie b_3 and are most often at the slope break of unit h_1, indicting at least one of its sources.

The b_5 materials are the deposits created by the remobilization of the b_3 and b_4 deposits as well as some components of h_1 and h_2 materials. These materials sit in the lowest parts of the basins and form broad, flat, deltaic-like deposits. The materials that are deposited in Noachis basin appear to be back-wasted, leaving behind a bright albedo material at the distal margin. From the medial to proximal extent, unit b_5 grades from knobs and mesas eroding into meter-scale boulders, to a coherent fan deposit. The presence of meter-scale "erratic" boulders near the high-albedo margin suggests the deposits once extended into this area but have since been eroded. The other deposits of this unit, in the northeast and northwest, are smooth, flat deposits of fairly nondescript materials. This unit overlies b_1 in Noachis basin and fills in lows adjacent to units h_1, b_3, and b_4.

The materials of b_6 are located solely in Peta crater--a loosely divided, dual impact crater--and are unique in the mapping area as having a very high olivine signal in CRISM data. The deposit is characterized as a flat, smooth surface, bounded in both circles by meter-scale, symmetrical ridges. The unit has a homogenous albedo except for areas where eolian processes have collected darker sediments. It is possible that these are flood lavas because of the absence of a volcanic edifice, a lack of a source outside of Peta crater, and a partition between the two crater floors.

Crater Map Units: There are 5 units in the crater units: The morphologic crater preservation states c_1, c_2, and c_3, undifferentiated crater floor material (unit cf), and a blanket of undifferentiated ejecta (unit ceu) in the northeastern Noachis basin.

The c_1 craters have partial, highly eroded rims of little to no relief. The c_2 craters typically have a complete rim although it may be breached by small valley systems but lack discernable margins of an ejecta blanket and have low to moderate relief. The c_3 craters often have bowl-shaped floors, high rim relief, and a discernable ejecta blanket. The crater floors are lumped into the cf unit unless designated as unit b_1.

The crater floor unit consists of undifferentiated materials filling the bottom of craters. These deposits are typically flat-lying, smooth deposits interpreted to have been deposited by intra-crater processes (e.g., slumping and gullying) and airfall. Some of the deposits have been reworked by eolian processes into dune and ripple forms.

The last unit, ceu, is an areally large deposit of smoothed materials in northeast Noachis basin. The ejecta have been deflated, buried, or reworked through eolian processes to a point where the source crater cannot be accurately detected. This material may also contain a portion of the Newcomb crater ejecta materials. This unit differs from the b_3 and b_5 adjacent materials because it appears to overlie those units and there is a paucity of drainages on this surface. This paucity suggests emplacement subsequent to widespread fluvial activity. This might also suggest a lack of access to fluid either meteoric and/or groundwater.

References: [1] Fortezzo, C.M. and K.K. Williams, (2009) Planet. Map. Mtg. (abst.). [2] Fortezzo, C.M., (2009) Master's Thesis, Northern Arizona University. [3] Grant, J.A,. et al., (2009) USGS SIM-Map, 3041. [4] Michael, G.G. and G. Neukum, (2010) *Earth and Planetary Science Letters*. [5] Kneissl, T., et al., (2010) *Planetary and Space Sciences*. [6] Anguita, F., et al., (1997) *Earth, Moon, and Planets*, 77. [7] Tanaka, K.L., et al., (2005) USGS Map 2888.

HIGH-RESOLUTION STRUCTURAL MAPPING OF LAYERED DEPOSITS IN WEST CANDOR CHASMA, MARS: INITIAL PROGRESS AND DISCOVERIES. C. H. Okubo, U.S. Geological Survey, 2255 N. Gemini Dr., Flagstaff, AZ, 86001, cokubo@usgs.gov.

Introduction: Much work has been directed toward understanding the geologic evolution of Valles Marineris and the layered sedimentary deposits that are exposed within its chasmata. The majority of this earlier work focused on structures and processes that operated at length scales of a few kilometers to thousands of kilometers. Although invaluable for establishing an initial framework for understanding the broader geologic history of this region, the finer details of these interpretations need to be further tested and refined through investigations at outcrop scales. Such insight can be gained through new, high-resolution structural mapping at length scales of 100 m or less using DEMs derived from HiRISE data.

While the interpretations of previous investigations imply many corollaries, there are several fundamental and tractable tests that need to be conducted at the HiRISE scale. For example, 1) the layered deposits should show evidence of normal faulting if chasma-related rifting occurred after their deposition, assuming negligible burial by post-deformation sediments, 2) if the layered deposits fill ancestral basins, they should show on-lap relationships with the wall rock of the basins, 3) evidence of syn-tectonic deposition and soft-sediment deformation would be expected if sedimentation were contemporaneous with rifting.

The motivation of this new PG&G-funded project is to use high-resolution structural information to test and refine current interpretations and their corollaries, address outstanding questions, and define new structural relationships, in the geologic history of the layered deposits and west Candor Chasma. The standards and procedures developed over the course of this project will also help to establish new protocols for the publication of future high-resolution maps.

This work aims to produce four high-resolution structural maps of selected sites in west Candor Chasma over a four year period. Mapping is being conducted using DEMs and orthorectified imagery derived from publicly-released stereo HiRISE observations. Two HiRISE DEMs and orthoimage pairs have been produced, PSP_001641_1735/ PSP_002063_1735 (map 1) and ESP_011372_1730/ ESP_012295_1730 (map 2), and mapping has begun on map 1. Both maps 1 and 2 are within MTM -05077.

Methods: The HiRISE DEMs are built following the methodology of [1], and as documented by [2], using the USGS/NASA Planetary Photogrammetry Guest Facility. The HiRISE red mosaics input to SOCET Set are dejittered (both halves), and the DEMs

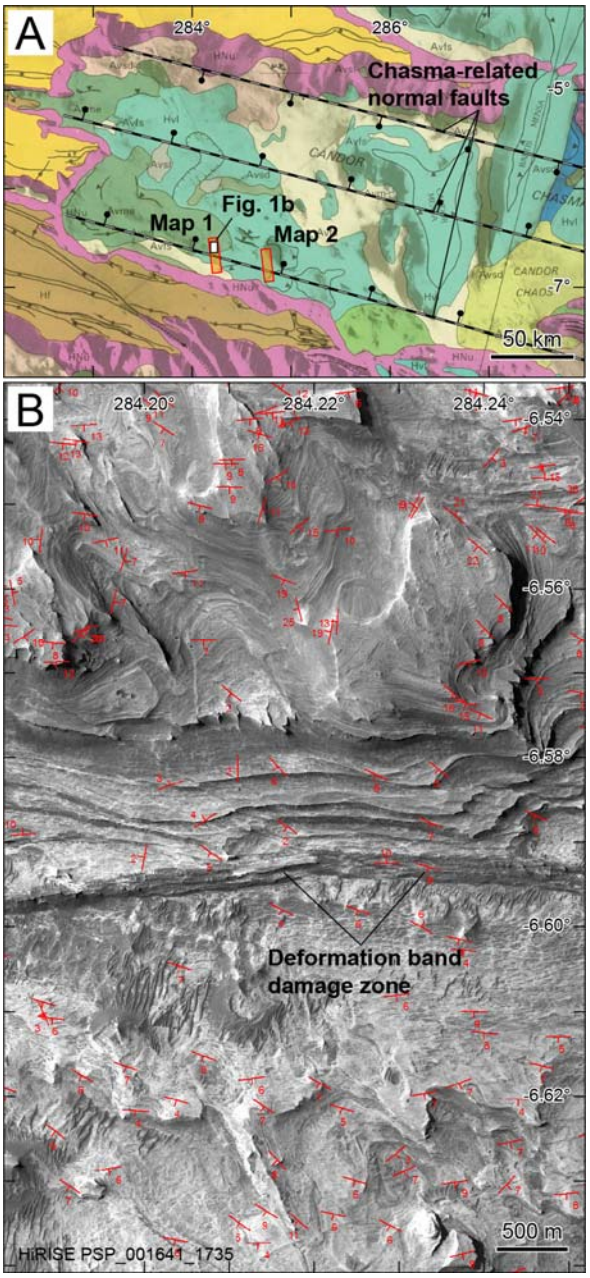

Figure 1. A) Location of maps 1 and 2 in west Candor Chasma. Basemap is from [3], and schematic locations of chasma-related normal faults are from [4]. B) Representative bedding orientation measurements showing typical attitudes in the local Avme (green colored unit in A) and Hvl (teal colored unit in A) for a small part of map 1. For these orientations, uncertainty in strike measurements is ~10° ± 6° and uncertainty in dip is ~2° ± 4°.

are tied to MOLA then hand-edited to minimize errors in stereo correlation. The resulting DEMs have 1 m/post spacings. The HiRISE image pairs are orthorectified using their corresponding DEMs and are output at both 0.25 m/pixel and 1 m/pixel.

Orientations of bedding, faults, and other structures are calculated from the HiRISE DEM using the commercial software Orion (® Pangaea Scientific). This software is used to calculate a best-fit plane through multiple points (defined by two horizontal coordinates and elevation) along a feature of interest. Five points are used to determine a single structural orientation (e.g., strike and dip of bedding or faults). The chord length of each line of five points is approximately 50 m to 100 m, and several hundred orientations are typically measured within each mapped area just for bedding alone. Hundreds of additional measurements are made for faults, fractures, unconformities, and other structural discontinuities.

Initial results: Each mapped area is defined by the extent of stereo coverage, which is ~20.6 km x 5.2 km for map 1. The layered deposits within this map area are interpreted by [3] to be Late Hesperian to Middle Amazonian in age. The mapped area crosses the general location of a major down to the north normal fault associated with the formation of west Candor Chasma [4]. The mapped area also traverses the contact between layered deposits and the foothills of the south wall of west Candor Chasma.

Away from apparent deformation and sedimentation associated with folds, faults, and unconformities, the dip of bedding in the local layered deposits is generally < 20° and commonly < 10° (e.g., Fig. 1b). Bedding commonly dips toward the south in Avme and dips toward the north in the lower-most (oldest) exposed strata of Hvl. Bedding is contorted in Avfs due to a large landslide off the chasma wall.

Structural mapping reveals evidence of two buried impact craters, along with two other morphologically similar landforms, along the upper boundary of the Hvl section, just below the contact with Avme. These putative infilled craters and crater-forms are expressed as conical mounds that are 300 m to 800 m in diameter at their bases. Bedding dips inward at several tens of degrees around the periphery of these features and becomes subhorizontal at higher levels, consistent with an infilled crater (rather than spring mounds or mud volcanoes). CRISM spectral summary products produced from HRL000033B7 show that these mounds have a spectral response that is similar to the surrounding, subhorizontal layered material. Thus diagenesis does not appear to have been localized within these mounds and these mounds are likely composed of Hvl, Avme or both.

Regional through-going normal faults that have the requisite attitudes and displacement directions to be attributed to chasma-related faulting are not observed within map 1. Chasma-related faulting in this area is likely to occur within Hvl (Fig. 1). Bedding within the local Hvl is well exposed and largely conformable, aside from a few disconformities and displacements across isolated km-scale faults. This suggests that deposition of the local Hvl postdated any normal faulting related to chasma formation in this area.

A 5.36-km-long section of a roughly 15.5-km-long normal fault is observed in the mapped area (Fig. 1B). This fault is concave toward the south and exhibits down to the south displacements. Regional CTX coverage shows that this fault is part of a previously unrecognized array of normal faults with similar attitudes and displacement directions. The geometry of this fault array is suggestive of a ~40 km-wide landslide complex within Hvl. These faults are present in erosional exposures, and their primary surface morphologies are no longer apparent.

Erosion of these concave to the south normal faults has revealed that the traces of the faults are in fact comprised of arrays of sinuous ridges that form zones that are up to ~60 m wide. Analysis of the three-dimensional orientations of these ridges shows that they represent the internal structure of damage zones surrounding the normal faults and that the damage zones consist of deformation bands. While deformation bands have been previously documented on Mars [5,6], this finding is very significant because it is the first recognized example of fault-related, *deformation band damage zones* on Mars. This discovery opens the way for a new (for Mars) field of structural studies using Earth-based methodologies for gaining more detailed insight into the mechanics of faulting and its implications for regional groundwater flow within the layered deposits.

Future work: Efforts are underway to quantify and map all of the major faults, folds, and other structures in map 1. These results will then be used to reconstruct the stress history and geologic evolution of the area. Initial submission of this first map for review is planned for fall 2011.

References: [1] Kirk, R. L. et al. (2008), *JGR*, *113*, E00A24. [2] USGS (2011), http://webgis.wr.usgs.gov/pigwad/tutorials/socetset/SocetSet4HiRISE.htm. [3] Witbeck, N. E. et al. (1991), *USGS Map I-2010*. [4] Schultz, R. A., and Lin, J. (2001), *JGR*, *106*, 16549–16566. [5] Okubo, C. H. (2010), *Icarus*, *207*, 210–225. [6] Okubo, C. H. et al. (2009), *GSA Bull.*, *121*, 474–482.

INTEGRATED SPECTRAL, THERMOPHYSICAL, AND GEOMORPHOLOGIC MAPPING RESULTS IN LIBYA MONTES AND TYRRHENA TERRA, MARS. A. Deanne Rogers[1], Kimberly D. Seelos[2], and James A. Skinner, Jr.[3], [1]Stony Brook University, Department of Geosciences, Stony Brook, NY, adrogers@notes.cc.sunysb.edu, [2]Johns Hopkins University Applied Physics Laboratory, Laurel, MD, [3]U.S. Geological Survey, Astrogeology Science Center, Flagstaff, AZ.

Overview: As described in a companion abstract [1], a 1:1M scale mapping project of the geologic landforms and materials within the Libya Montes and Tyrrhena Terra regions (MTMs 00282, -05282, -10282, 00277, -05277, and -10277) is underway. A unique aspect of this mapping effort is that we integrate both morphologic and spectral information in unit delineation/description and construction of a geologic history. This integration is critical to test and, where necessary, refine the prevailing lithologic and formational interpretations of massifs, intermediate (cratered) plains, and low-standing palus regions of the Martian highlands. This abstract describes results from spectral analyses within the study region.

General Approach: Initially, units were independently delineated by each author using 1) geomorphologic information from the THEMIS daytime IR mosaic (100 m/pixel), 2) spectral information from THEMIS multispectral decorrelation stretch (DCS) mosaics (100 m/pixel) and TES spectral indices, and 3) CRISM summary parameters (231 m/pixel). This allowed each investigator to identify unique units within their respective data sets and to form initial hypotheses about unit relationships and origin. Then the primary geomorphologic base map (led by J. Skinner) was distributed to the spectral data set leads (K. Seelos and D. Rogers), and compositional information for geomorphological units was retrieved and used to answer outstanding questions that arose during geomorphologic mapping. For more details, see [1].

Data and Methods: The CRISM, THEMIS and TES spectral instruments view differing wavelength regions and have different but complementary sensitivities to surface compositions. The CRISM instrument acquires visible/near-infrared (VNIR) spectra in 544 channels. Iron- and OH/H2O-bearing minerals exhibit diagnostic absorptions in this range, allowing for detection of a wide variety of minerals, with the exception of a few silicates such as feldspar. CRISM is sensitive to mineral abundances as low as ~4% [2]; however, estimating mineral abundances is challenging (though advances have been made recently [e.g., 3]). The TES instrument acquires thermal infrared (TIR) spectra in 143 channels. Nearly all minerals exhibit diagnostic absorptions in this range; and, for coarse-particulate surfaces, quantitative mineral abundances may be retrieved with accuracy between 5-15%. The coarse spatial resolution (~3 km/pixel) is a major limitation for delineating units at the 1:1M scale; however, the THEMIS multispectral imager provides complementary TIR spectral data at a spatial resolution of 100 m/pixel which allows for detailed lithologic mapping.

For each quadrangle within the study region, THEMIS DCS mosaics were generated using three different band combinations displayed as red-green-blue: 8-7-5, 9-6-4, and 6-4-2. A spectral index derived from TES data (the "507 cm^{-1} index"), which is sensitive to the overall olivine and pyroxene content relative to feldspar and high-silica phases [4], was also used. CRISM summary parameter images, which map the strength of key absorptions for a variety of minerals, were also generated. Areas of interest highlighted by THEMIS DCS, TES index or CRISM summary parameter maps were examined in detail using full wavelength-range TES or CRISM spectra. Lastly, thermophysical information from THEMIS nighttime radiance images was used to help delineate and interpret the properties of each unit.

Results: In the independent mapping stage, three major units were identified with the TIR data sets. These units (**Figure 1**), which were also described in a complementary study of Iapygia and Tyrrhena Terra [4-5], are: Unit 1--a relatively low thermal inertia (TI), older intercrater plains unit that is depleted in olivine and pyroxene relative to Unit 2; Unit 2--a relatively high TI, younger intercrater plains unit that is enriched in olivine and pyroxene relative to other units; and Unit 3--a relatively high TI, younger intracrater floor unit that is enriched in olivine and/or pyroxene relative to Unit 1. [4] interpreted Units 2 and 3 to be the same material (discussed below). Units 2/3 have variable spectral character and olivine abundance in TES and THEMIS data (see arrows in **Figure 1**). The most olivine enriched areas tend to correspond with surfaces that exhibit the highest TI; this along with the lack of a distinct morphology or distribution led [4] to suggest that the areas of low olivine concentration within Units 2/3 were likely areas of heavier alteration or sediment deposition from Unit 1, rather than a separate unit. Based on the relatively high TI, higher olivine abundance, resistant morphology, and lack of a bedrock source for olivine-enriched sediment, Units 2/3 were interpreted to be predominantly of volcanic origin, rather than of a sedimentary or impact origin [4].

CRISM-based mapping efforts also identified olivine-bearing surfaces on crater floors and in low-lying

plains. In many regions, these detections coincide with surfaces mapped as Unit 2 or 3 in THEMIS/TES data. Determining the degree to which olivine unit distributions from each data set coincide is a major goal for the upcoming work period. CRISM uniquely identifies numerous phyllosilicate-bearing materials within the study region. These detections primarily occur within crater materials – rims, central peaks, and ejecta. Future work will include detailed TES spectral modeling of these regions to try to place constraints on the modal mineralogy associated with these exposures.

[1] identified several geomorphologic units in the study region, including: a "massif" unit (Nm), two "terra" units (Nt1 and Nt2), in which heavy dissection within Nt2 exposes older Nt1, two younger "palus" units (HNp1 and Hp2), which differ by their location in high-standing areas versus large topographic lows, and a "smooth" crater fill unit (s). We find that (1) unit Hp2 corresponds very strongly with areas mapped as Unit 2, (2) unit "s" corresponds with Unit 3, and (3) units Nm, Nt1 and Nt2 correspond with Unit 1 (**Figure 1**). Unit HNp1 was mapped in some areas as Unit 1 and in others as Unit 2. Some of the questions raised by the geomorphic mapping efforts were: **Q1**) Are the volcanic plains of Syrtis Major, which were mapped as the same unit as the palus filling material Hp2, compositionally distinct from Hp2? **Q2**) Are the HNp1 palus materials compositionally equivalent to Hp2? **Q3**) Are there compositional differences between the terra units (Nt1 and Nt2)? **Q4**) Are there consistently observable compositions in the massif units? and **Q5**) Can the crater filling smooth unit "s" be grouped with any other unit? Each of these questions is addressed below.

Q1. Average TES spectra from 5 locations within palus Hp2 exposures are variable in spectral shape and olivine abundance. In contrast, average TES spectra from 3 locations within Syrtis Major are remarkably consistent. The average palus Hp2 unit is not spectrally distinct from Syrtis Hp2. However, if the variability within palus Hp2 locations is due to varying levels of alteration or sediment from Unit 1, as described by [4] for Units 2/3, then it is appropriate to compare the least altered areas of palus Hp2 with the Syrtis Hp2 plains. We find that the highest TI areas within palus Hp2 are depleted in plagioclase (~10%) and enriched in pyroxene (~30%) and olivine (~5%). If one assumes that these areas are most representative of the palus Hp2 plains, then Syrtis Major is distinct from the palus Hp2 units. **Q2**. In some areas, HNp1 units are spectrally similar to Hp2, whereas in other, HNp1 units are spectrally similar to Nt1 and Nt2. One possible explanation for the inconsistency is that all HNp1 units are compositionally the same as Hp2, but have variable amounts of alteration or sediment cover from Nt1 and Nt2. **Q3**. Despite some morphologic variability, no significant spectral difference is observed between Nt1 and Nt2. **Q4**. Massif units show a consistent spectral shape, and are very similar to Nt1 and Nt2. There is a subtle difference between the massif and terra units; whether or not this difference is significant must be assessed with comparisons between the two units within individual TES orbits. **Q5**. The smooth crater filling unit is spectrally and compositionally identical to Hp2, suggesting that they may have a similar origin.

Future work: Future work will focus on integrating units delineated from the VNIR, TIR, and geomorphologic data sets described here. Surface comparisons within individual TES orbits are needed to constrain whether there are detectable TIR differences between massif and terra units. Crater counts within various exposures of Hp2 ("Unit 2" of [4]) and the smooth unit "s" ("Unit 3" of [4]) will constrain the timing of emplacement of these units and whether they formed contemporaneously (as speculated by [4]).

Acknowledgement: This work was funded by the NASA Planetary Geology and Geophysics Program.

References: [1] Skinner et al. (2011), *this volume*. [2] Bibring, J-P et al. (2006), *Science*, *312,* 400. [3] Poulet, F. et al. (2009), *Icarus, 201*, 69-83. [4] Rogers and Fergason (in press), *JGR-Planets*.

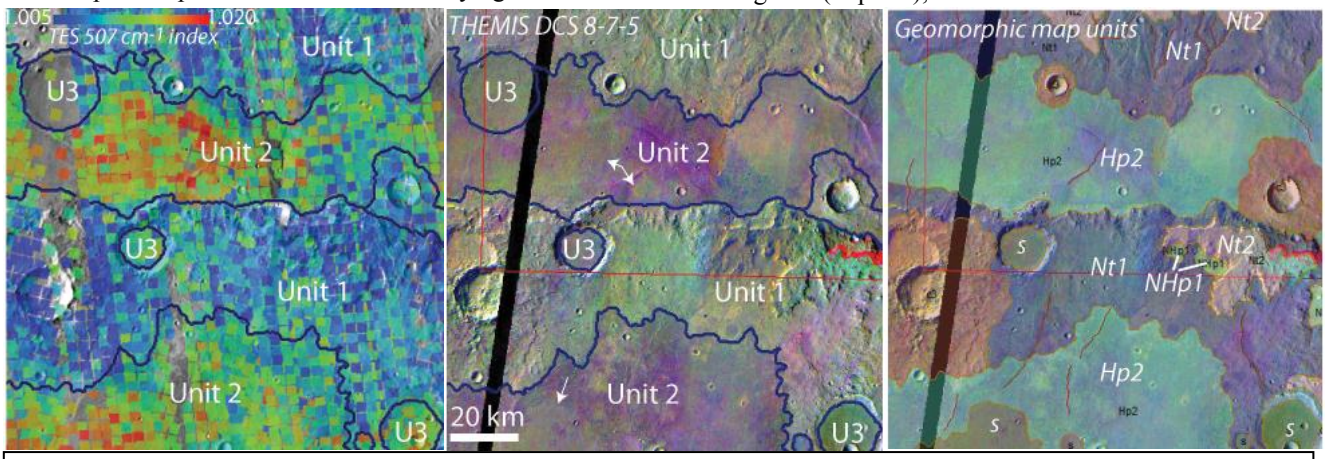

Figure 1. Key units identified using TIR datasets are shown in the left and center panels. Left: TES 507 cm^{-1} index [4]. Center: THEMIS DCS mosaic using bands 8-7-5 displayed as R-G-B. Arrows point to examples of lower TI, lower-olivine regions within Unit 2. The right panel shows geomorphic map units identified by [1]. Area shown is within the SW portion of MTM -10277.

GEOLOGY OF LIBYA MONTES AND THE INTERBASIN PLAINS OF NORTHERN TYRRHENA TERRA, MARS: SECOND YEAR RESULTS AND THIRD YEAR WORK PLAN. J.A. Skinner, Jr.[1], A.D. Rogers[2], and K.D. Seelos[3], [1]Astrogeology Science Center, U.S. Geological Survey, 2255 N. Gemini Drive, Flagstaff, AZ 86001 (jskinner@usgs.gov), [2]Stony Brook University, 255 Earth and Space Science Building, Stony Brook, NY 11794, [3]Johns Hopkins Applied Physics Laboratory, MP3-E140, 11100 Johns Hopkins Road, Laurel, MD 20723.

Introduction: The Libya Montes-Tyrrhena Terra highland-lowland transitional zone of Mars is a complex tectonic and erosional region that contains some of the oldest exposed materials on the Martian surface [1-3] as well as aqueous mineral signatures that may be potential chemical artifacts of early highland formational processes [4-5]. The map region extends from the Libya Montes southward into Tyrrhena Terra and to the northern rim of Hellas basin and includes volcanic rocks of Syrtis Major Planum and a broad low-lying plain that forms a topographic divide between Isidis and Hellas basins. Our 1:1M scale map focuses on six contiguous MTM quadrangles that cover the highland portion of the transitional zone (**Fig.1**). The primary base map is a THEMIS daytime IR mosaic (100 m/px). Compositional supplements include THEMIS and TES thermal infrared and CRISM visible and near infrared data sets (see [6], this volume). Our objective is to detail the geologic history of this region, specifically the evolution of the massifs and intervening intermediate and low-lying plains. Herein, we summarize year 2 results, including (1) nomenclature additions and changes, (2) map unit definitions and temporal relationships, and (3) a preliminary geologic history.

Nomenclature: The use of approved nomenclature is critical for geologic mapping because it allows succinct identification and description of units and features. We requested and received IAU approval for three previously unnamed features within the region of interest (**Fig. 1**). Zarqa Valles are a distributed system of channels that source in the inter-massif terra units of western Libya Montes (1146 m elevation) and debouch into Isidis Planitia (-1500 m elevation). Collectively, the valles are 480 km long, 380 km wide, and are centered at 0.87°N, 81.50°E. Some upslope segments are physically detached from the main system, perhaps buried by Syrtis Major lava flows (mapped as **Hp_2**). Oenotria Plana are a series of plains, each separated by subtle topographic rises (generally <50 m), and characteristically positioned between (and burying) older massif and terra units. The plana are 450 km wide, 750 km long, and are centered at 8.47°S, 79.04°E. Oenotria Plana range from 1000 m to 1400 m elevation and display only a slight southward slope (<<0.1°). Lipany crater is 49.2 km in diameter, centered at 0.25°S, 79.68°E, and likely formed within one of the two terra units (units **Ht_1** or **Ht_2**). The crater has a rugged, well-defined crater rim and ejecta (mapped as **c_3**), the periphery of which is buried by plains material (unit **Hp_2**). The smooth interior floor of Lipany crater is subtly convex in cross-section (rising >200 m) and contains several quasi-radial fractures (<3 km wide) that deflect around an 8-km-wide central pit. These characteristics are not observed elsewhere in the map region.

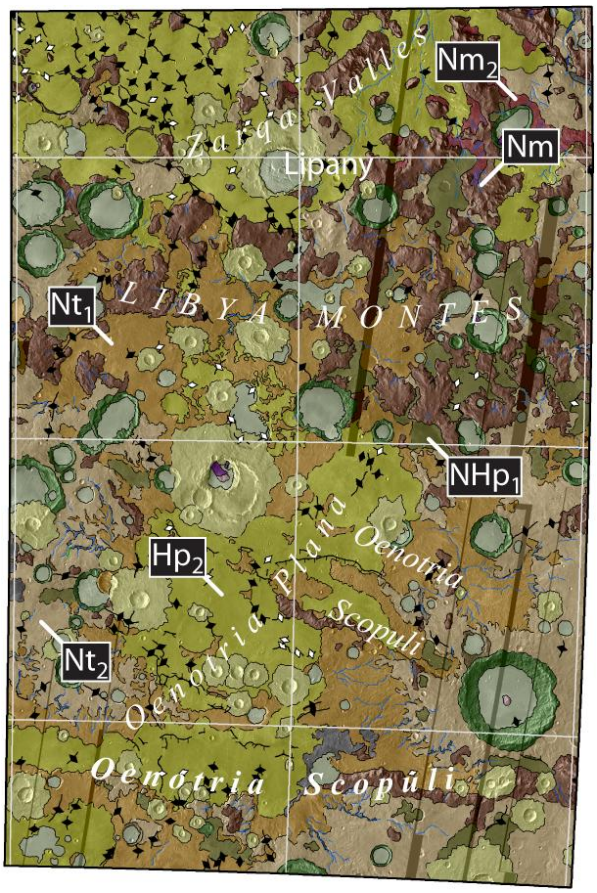

Figure 1. Geologic map showing nomenclature and existing contextual geologic units. Major units indicated in boxes. MTM projection (center longitude of 70°E). Figure is ~600 km wide.

In addition to these newly named features, we requested (and received approval) of a name change. The previously named Oenotria Scopulus identified a 1360-km-long arcuate scarp centered at -10.97°S, 76.90°E and located roughly circumferential to Isidis basin. Post-Viking Orbiter image and topography data sets show the feature to be comprised of several physically detached scarps, each with similar planimetric trends. These occur not only along the originally named feature but also to the north, partitioning Oenotria Plana.

As such, the feature has been renamed Oenotria Scopuli to reflect the plural descriptor term.

Mapping Results: We expanded year 1 mapping efforts, which focused on the materials and landforms that occur within the central and northern quads into the southern two quads to produce a complete set of contextual geologic contacts and units (**Fig. 1**). Contextual geologic units include two "massif" units, two "terra" units, two "plains" units, and five crater/undifferentiated units. System assignments used in geologic symbols are based on crater counts to date and are subject to change.

We identify two material units associated with Libya Montes massifs. The older massif unit (unit **Nm**) is characterized by rugged, mountainous outcrops that rise 800 and 2500 m above inter-massif plains and have mean slopes >10°. Individual outcrops are roughly rectangular in planiform shape, with margins orthogonal to one another (trends ESE-WNW and NNE-SSW). The unit often contains numerous linear channels and gullies near their bases. Unit **Nm** is interpreted as ancient crustal material uplifted during the formation of impact basins, as well as associated impact breccias. The younger massif unit (unit **Nm_2**) is characterized by generally smooth surfaces located at the base of many unit **Nm** outcrops. These sloping outcrops contain numerous linear channels and have mean local slopes <4°. Unit **Nm_2** is interpreted as alluvial/colluvial debris shed from adjacent, higher-standing massifs. These units display low thermal inertia, are depleted in olivine and pyroxene, relative to adjacent units [6-7], and exhibit high CRISM D2300 signatures, suggesting the presence of Fe/Mg-bearing phyllosilicates.

We identify two terra units associated with the intermediate elevation inter-massif regions of Libya Montes and cratered plains located immediately to their south. Both the older and younger terra units (units **Nt_1** and unit **Nt_2**, respectively) are characterized by rolling cratered plains with well integrated channels. These units are differentiated by a regionally traceable topographic scarp, which is interpreted to form the boundary between the two terra units. Compositionally, the mapped terra units are equivalent to unit **Nm**.

We identify two plains units located in the topographic lows between outcrops of massif and terra units. The older plains unit (unit **NHp_1**) occurs in irregularly-shaped depressions between high-standing massif units, where they commonly abut and bury scoured, gullied, or dissected **Nm** surfaces. The younger plains unit (**Hp_2**) is more widely occurring, forming the nearly horizontal Oenotria Plana. Though generally smooth, the unit contains ridges and asymmetric scarps, often in a reticulate pattern. As mapped, unit **Hp_2** is equivalent to flank materials (lavas) of Syrtis Major, though compositional differences exist.

We identify six crater/undifferentiated units within the map region. We discriminate a gradation of crater rim and ejecta materials (units **c_1**, **c_2**, and **c_3**). In addition, we define local crater peak (unit **cpk**) and slide (**cs**) material, each of which shows variable composition [8]. Finally, we define an undifferentiated "smooth" unit (unit **s**), which occupies crater floors as well as shallow, circular depressions in Oenotria Plana. This unit displays high thermal inertia and is enriched in olivine and/or pyroxene [6-7] relative to adjacent units. Occurrence and compositional details will likely result in local grouping with unit **Hp_2**.

Geologic History: We augmented unit mapping efforts with cross-cutting and superposition relationships as well as first-order crater counts to begin regionally correlating map units. Though our observations and the history they implicate will undergo refinement during year 3, our efforts delineate a preliminary geologic history, as follows:

Early to Middle Noachian - Isidis and/or Hellas impact uplifts crustal blocks and superposed regolith (basin ejecta?) through normal faulting, exposing units **Nm**, **Nt_1**, and **Nt_2**. Terra units appear to be displaced by the same faults that uplifted and define massif units.

Late Noachian - Erosion of elevated massif and terra units emplaces unit **Nm_2** (alluvial/colluvial sequences?), which was subsequently dissected, perhaps reflecting decrease in base level. Coincidently or subsequently, regionally widespread fluvial activity dissects unit **Nt_2**, exposing lower (older) unit **Nt_1**. Unit **NHp_1** accumulates in inter-massif basins.

Early Hesperian – Erosion of massif and terra units continues and eventually wanes, resulting in the debouchment of sediments in Oenotria Plana and the accumulation of unit **Hp_2**. Coeval volcanic activity, perhaps related to Syrtis Major, emplaces lavas in similar basins, perhaps resulting in stratigraphic interfingering.

Late Hesperian to Amazonian - Continued surface impacts and impact-related resurfacing/burial. Accumulation of dust in various topographic depressions.

Year 3 Work Plan: The third year of the project is underway and is focusing on the iterative refinement of geomorphic unit boundaries and descriptions through the incorporation of compositional assessments. By year's end, we will refine unit boundaries, complete unit descriptions, and improve temporal correlations.

References: [1] Greeley and Guest (1987), *USGS I-1802-B*, 1:15M scale. [2] Crumpler and Tanaka (2003), *JGR*, 98. [3] Tanaka et al. (2005), *USGS SIM 2888*, 1:15M scale. [4] Bibring et al. (2005), Science, 307. [5] Bishop et al. (2007), *7th Int. Conf. Mars*, #3294. [6] Rogers et al. (2011), this volume. [7] Rogers and Fergason (2011), JGR-Planets, in press. [8] Skinner et al. (2010), NASA/CP-2010-217041.

MARS GLOBAL GEOLOGIC MAP: NEARING COMPLETION. K.L. Tanaka[1], J.M. Dohm[2], R. Irwin[3], E.J. Kolb[4], J.A. Skinner, Jr.[1], C.M. Fortezzo[1], T.M. Hare[1], T. Platz[5], G.G. Michael[5], and S. Robbins[6], [1]U.S. Geological Survey, Flagstaff, AZ, ktanaka@usgs.gov, [2]U. Arizona, Tucson, AZ, [3]Planetary Science Inst., Tucson, AZ, [4]Google, Inc., CA, [5]Freie U., Berlin, [6]U. Colorado, Boulder, CO.

Introduction: We are in the final year of a five-year effort to map the global geology of Mars at 1:20M scale using mainly Mars Global Surveyor and Mars Odyssey image and altimetry datasets. Previously, we reported on details of project management, developments in mapping approaches, and tactics of map unit and unit group delineation, naming, and dating [1-4]. This year we report on recent mapping progress and some adjustments to our approach. We also describe remaining steps to take the map to completion.

Mapping progress: This past year, unit and line feature mapping has been completed as a preliminary draft. This has included comprehensive reviews by Tanaka of all initial mapping. Edits have involved map unit assignments, unit contacts, line features, drafting style, and more. Fortezzo was added as a map author, because he was given the task to map line features in a consistent and systematic fashion (see below). He also is in charge of assembling and editing the master GIS files for the map.

Assignment of unit ages: Platz and Michael have assisted with producing detailed crater counts of selected outcrops of highland units. This work is helping us to determine how to assign ages and thus unit labels to isolated outcrops of highland units. Werner and Tanaka [5] are addressing how to more precisely tie crater size-frequency distributions to the Martian epochs [6] for Hartmann and Neukum crater production functions [7]. In turn, we will need to see how to apply the global crater database of Robbins [8] that has been completed down to 1 km diameter, based on THEMIS IR and other data sets. That data set is in GIS format and thus readily imported into the global map for generation of crater densities for each unit outcrop. Some disparity in ages will result until the proper shape and calibration of the crater production function and cratering rate history are resolved. In any case, our scheme and judgment will be exercised in the assignment of ages to mapped outcrops.

We also find challenging the division and assignment of ages for sequences of lava flows. Across much of Tharsis and Elysium, we map an undivided unit, because discrete patches of flows as defined by relative age and/or source cannot be confidently delineated. Preliminary studies involving detailed crater counts of individual flows in given regions are indicating that lavas can erupt randomly in terms of spatial distribution over time (e.g., sourcing from fissures and lava tubes), and thus major eruptive sequences may be difficult to discern [8-9]. Exceptions that we can and do map are fields of local fissure and small shield vents and their flows. These features tend to be among the youngest eruptive products in several areas and form spatially well-defined outcrops, given that they generally have flows radiating from them of limited extents.

New line-feature scheme: Previous planetary geologic maps generally have included line, point, and sometimes stipple symbols to highlight a wide variety of geomorphic, albedo, and geologic features of interest. We decided that, to extend our efforts to achieve a more objective map product, we would not use interpretive labels on mapped line features, such as fault, fracture, graben, etc. Instead, we are mapping features according to their (a) form (scarp, trough, or ridge), (b) width (greater or less than 10 km), and (c) preservation state (fresh vs. subdued). We also in our geodatabase discriminate secondary geomorphic aspects (e.g., wrinkle-type ridges), probable geologic type(s) or interpretation where clear (e.g., graben, fluvial valley), and geologic process (tectonic, volcanic, erosional, etc.). Within the scope of this project, we are not assigning relative ages to the features; however, this can be achieved using the mapping relationships for temporal constraints as performed previously for Martian structures based on Viking mapping [10].

We also decided that we could not effectively follow the same objective approach for small features traditionally mapped as point features (e.g., small volcanoes), given for example that all hills or mounds in some size range would need to be mapped objectively then assigned to geologic interpretation classes. This is illustrated by a regional mapping study of the Scandia region of the northern plains, where >17,000 knobs were mapped and interpreted (in a synoptic fashion) [11]. The same problem applies to mapping stipple patterns that represent surficial characteristics such as geomorphic textures, albedo patterns, etc.—they would need to be mapped in a consistent, comprehensive, and objective manner that may be impossible or at least difficult to conceive of.

Map completion: We intend to complete the map for submission and review within the next several months. The map will employ the latest submission guidelines [12], including, for the GIS product, organizing mapping layers and creating metadata. In addition to possibly 3 formal reviews, we will seek feedback from the planetary mapping community and others in order to increase its value to the eventual user.

References: [1] Tanaka K.L. et al. (2007) *7th Intl. Conf. Mars* Abs. #3143. [2] Tanaka K.L. et al. (2008) *LPSC XXXIX,* Abs. #2130. [3] Tanaka K.L. et al. (2010) *in* Bleamaster et al. (eds.), *Abs. Ann Mtg. Planet Geol.*

Mappers, San Antonio, TX, 2009, NASA/CP—2010-216680, p. 41-42. [4] Tanaka K.L. et al. (2010) *in* Bleamaster et al. (eds.), *Abs. Ann Mtg. Planet Geol. Mappers, Flagstaff, AZ, 2010, NASA/CP—2010-217041,* p. 46-47. [5] Werner S.C. and Tanaka K.L. (in review) *Icarus.* [6] Tanaka K.L. (1986) *JGR 91, suppl.,* E139-158. [7] Hartmann W.K., and Neukum G. (2001) *Space Sci. Rev., 96,* 165-194. [8] Platz T. and Michael, G.G. (in review) EPSL. [9] Dohm J.M. et al. (2011) *EPSC2011,* abs. [10] Anderson R.C. et al. (2001) *JGR, 106,* 20563-20585. [11] Tanaka K.L. et al. (in press) *Planet. Space Sci.,* doi:10.1016/j.pss.2010.11.004. [12] Tanaka K.L. et al. (2010) *in* Bleamaster et al. (eds.), *Abs. Ann Mtg. Planet Geol. Mappers, San Antonio, TX, 2009, NASA/CP—2010-216680, Appendix,* 21 p.

THE SCANDIA REGION OF MARS: RECENT RESULTS, NEW DIRECTIONS. K. L. Tanaka[1], J. A. P. Rodriguez[2], C. M. Fortezzo[1], R. K. Hayward[1], and J. A. Skinner, Jr.[1], [1]U. S. Geological Survey, Flagstaff, AZ (ktanaka@usgs.gov), [2]Planetary Science Institute, Tucson, AZ.

Introduction: We are in the third year of a four-year project to produce a geologic map of the Scandia region of Mars at 1:3,000,000 scale for publication in the USGS Scientific Investigations Map series. The primary objective of the map is to reconstruct the geologic history of this region of Mars using post-Viking image and topographic data [1-2]. We rely mostly on Mars Orbiter Laser Altimeter (MOLA) digital elevation models, Thermal Emission Imaging Spectrometer (THEMIS) infrared and visual range, and Context Camera images for mapping and topographic analysis.

The study region includes (1) a broad swath of the Vastitas Borealis units [1] (where the Phoenix landing site is located); (2) part of the margin of the north polar plateau, Planum Boreum; and (3) the northern margin of the immense Alba Mons volcanic shield.

Science results: Last year we presented a preliminary geologic map of the study region consisting of 20 map units and various features [3] (Fig. 1). Our mapping results provided geologic context for evaluation of geomorphic features, including the distribution and potential origin of (a) >17,000 knobs throughout the study region and concentrated in Scandia Colles, (b) the Scandia Tholi and Cavi field of round plateaus and irregular depressions, and (c) pronounced, channeled flows emanating from fissures radial to Milankovič crater.

We postulated that the location of Scandia down-slope of Alba Mons could explain the formation of Scandia features due to Alba Mons volcanism, which was active during the Late Hesperian (and perhaps earlier) and Early Amazonian. The associated crustal heating may have resulted in a zone of partial volatile melt [4]. Farther north the zone of partial volatile melt transitioned into a zone of permafrost, which would account for the accumulation of older, ice-rich materials making up the base of Planum Boreum. Scandia Tholi and Cavi occur within a sub-basin within the northern lowlands that would have preferentially accumulated ices, sedimentary fines, and evaporites related to outflow channel activity and perhaps groundwater emergence. We inferred that these conditions led to (a) enhanced surface collapse and gradation to explain many of the knob fields (including Scandia Colles), (b) sedimentary diapirism to form Scandia Tholi and Cavi, and (c) impact-induced mobilization of surface material that resulted in associated flow deposits. In another study, Rodriguez and Tanaka [5] investigated the only extensive northern plains region that does not comprise a topographic sub-basin within the northern lowlands. The region occurs south of Gemini Scopuli on Planum Boreum and north of a zone of highland collapse along the margin of Arabia Terra, and it is *not* located down-slope from outflow channel discharges from the highlands. Widespread landforms in that region include knob fields, degraded wrinkle ridges, and pedestal craters, as well as an area of older plains materials, which contains channels and possible thermokarst features. The geomorphology indicates relatively less dramatic surface gradation than for Scandia; this also occurred during the Late Hesperian and into the Amazonian. The authors postulated that emergence along tectonic fabrics of excess pressured groundwater led to extensive resurfacing of a Late Hesperian cratered landscape. These resurfacing stages contributed to the generation of northern plains sediments and volatile deposits within them. Aquifer pressurization resulted from an elevated hydraulic head produced by aquifers that extend across the regional highland-lowland boundary (HLB).

A third investigation of chaotic terrains within the southern circum-Chryse outflow channels [6] indicates that the Martian cryosphere may contain lenses of briny fluids (cryopegs). Just like in the investigated chaotic terrains, no channels emerge from the similar-sized Scandia Cavi [4], which suggests that both features share a history of gradual devolatilization of upper crustal materials that was not driven by overpressured water systems. In addition, the finding of gypsum aeolian deposits on nearby dunes is consistent with the existence of salt deposits within the regional upper stratigraphy (which would facilitate cryopeg formation).

Summary and implications: These studies indicate that at least two distinct cryo-hydrospheric settings have existed in the Martian northern lowlands, which likely contributed to a complex history of sedimentary and volatile accumulation and subsequent modifications therein. These include: (I) zones where eruptions of groundwater and fluidized sediments in the lowland occurred over trans-HLB aquifers and (II) zones where volcanic heating partially melted permafrost within the cryosphere. The existence (or formation) of fluid lenses within a cryospheric setting could have facilitated some types of volatile-driven resurfacing that apparently affected the northern plains and particularly during low obliquity (colder) conditions.

Next steps: During the next year we will accomplish three tasks. First, we will perform a focused mapping study of the Scandia Tholi and Cavi, given that our regional analysis [4] noted but did not reconstruct complex details in the development of these features. Evident were multiple stages of tholi/cavi development and attendant feature development, including narrow sinuous ridges, polygonal troughs, remnants of

paleosurfaces (as elevated pedestals), and moats. We are also interested in documenting the duration, timing and stages of this activity. Second, we will use the results from the previous task in order to develop geologic models to help assess possible processes and conditions that led to development of Scandia region features, thereby testing hypotheses for their origin. For example, we will test the cryopeg scenario for Scandia Cavi formation, along with others we are currently contemplating. Finally, we will assemble our results and revisit and update our preliminary geologic map [3] and complete it for submission following mappers' handbook guidelines [7]. We plan to follow a more objective approach to line-feature mapping that is being developed for the global map of Mars [8].

References: [1] Tanaka K.L. et al. (2005) *USGS SIM-2888*. [2] Tanaka K.L. et al. (2003) *JGR, 108,* 8043. [3] Tanaka K.L. et al. (2010) *in* Bleamaster et al. (eds.), *Abs. Ann Mtg. Planet Geol. Mappers, Flagstaff, AZ, 2010, NASA/CP—2010-217041*, p. 48-49. [4] Tanaka K.L. et al. (in press) *Planet. Space Sci.*, doi:10.1016/j.pss.2010.11.004. [5] Rodriguez J.A.P. et al. (2010) *Icarus, 210,* 116-134. [6] Rodriguez J.A.P. et al. (2010) *Icarus, 213,* 150-194. [7] Tanaka K.L. et al. (2010) *in* Bleamaster et al. (eds.), *Abs. Ann Mtg. Planet Geol. Mappers, San Antonio, TX, 2009, NASA/CP—2010-216680, Appendix*, 21 p. [8] Tanaka K.L. et al. (this vol.).

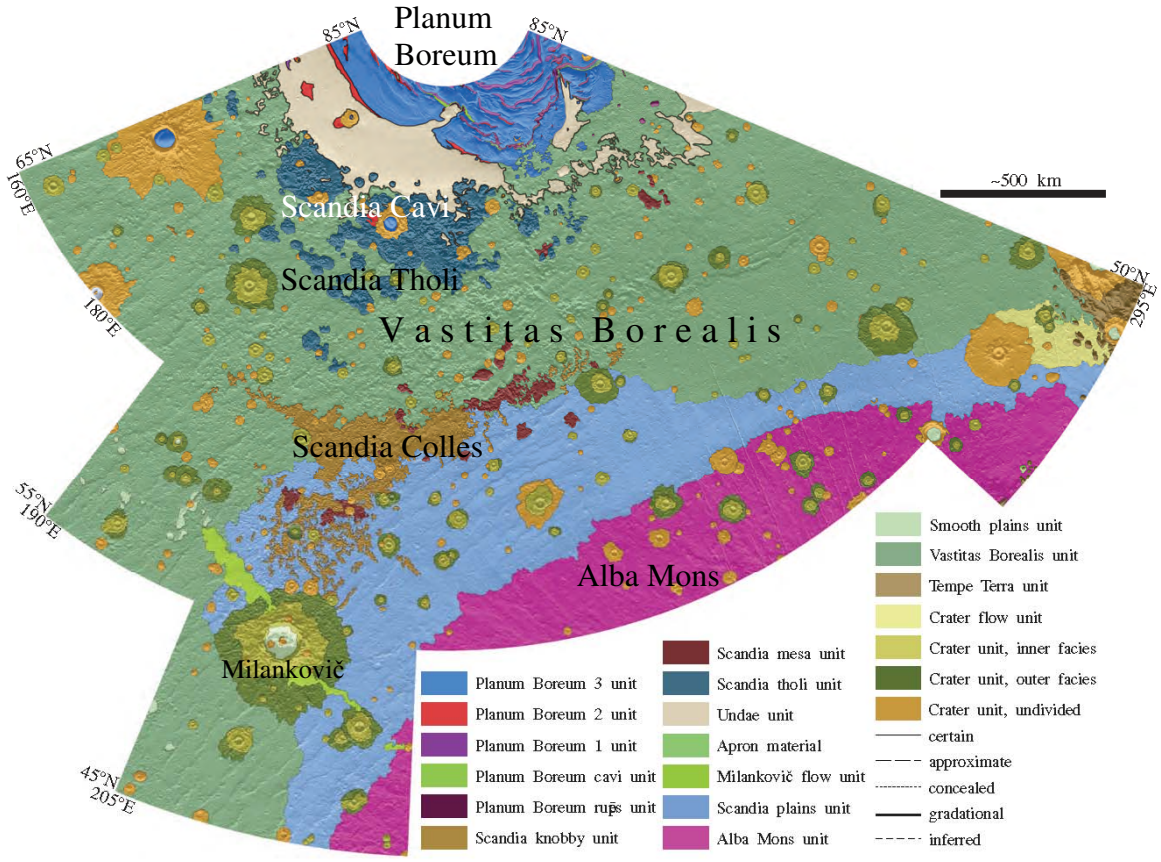

Figure 1: Geologic map of the Scandia region with units and symbols. North is at top and vertical meridian is 230ºE.

GEOLOGIC MAPPING OF NILI FOSSAE, MARS. A.C. Wetz[1,2] and L.F. Bleamaster, III[1,2], [1]Planetary Science Institute, 1700 E. Ft. Lowell Rd., Suite 106, Tucson AZ, 85719, [2]Trinity University Geosciences Department, One Trinity Place #45, San Antonio TX, 78212; lbleamas@psi.edu.

Introduction: Geologic mapping at 1:1 million-scale of Nili Fossae and Mawrth Vallis (Bleamaster et al., this issue) is being used to assess geologic materials and processes that shape the highlands along the Arabia Terra dichotomy boundary. See Bleamaster et al., this issue for objectives, data use, and methodology.

Nili Fossae (MTM quadrangles 20287, 20282, 25287, 25282, 30287, 30282; ***Figure 1***) is located west of Isidis basin and north of Syrtis Major volcano. Nili Fossae contains materials from the Noachian to late Hesperian, with the largest trough of the region containing Hesperian age volcanic flows. The region contains a series of other small curved depressions related to the Isidis basin that cut both the plateau and plains sequences revealing a window into the local stratigraphy provided they have not been completely filled with eolian deposits, which mask the underlying bedrock. Outcrops of phyllosilicate-bearing materials discovered by both the OMEGA and CRISM instruments have been identified in the Nili Fossae region including: smectites, chlorite, prehnite, serpentine, kaolinite, potassium mica, high and low-Fe olivine, high and low-Ca pyroxene, and traces of dunite [1]. These lie mostly within the plateau sequences of the highlands, mostly in exposures along trough walls. The presence of these phyllosilicates provides evidence for the stable presence of water for extended periods of time in Mars ancient history; however, low calcium pyroxene outcrops are also observed in the plateau sequences (brown and green units) and make up the majority of the Isidis plains unit (plains C - blue unit). These mineral signatures, if broadly correlated with morphology and geologic units, may reveal a break in aqueous alteration.

Unit Descriptions: (in order from oldest to youngest as constrained by **preliminary** N16 and N5 counts; ***Figure 2***). Nili Fossae map area consists of three major unit types: plateau sequences, plains sequences, and Syrtis Major flows, which have then been subdivided, as well as several small scale surface deposits, craters, and crater fill units. Formal geographic names have yet to be assigned.

plateau sequence unit A (plA) – Rugged dark-toned deposit with some internal layering and isolated knobs; relatively higher standing than plateau sequence unit B; several secondary crater chains; superposes plateau sequence unit B. *Interpretation:* Deposit of layered material exposed by denudation of overlying sequence. Mineral detections: low Ca-pyroxene.

plateau sequence unit G (plG) – Disarticulated massive outcropping material appearing as isolated plateaus and massifs, knobs and hummocks; relatively lower than the adjacent plateau sequence unit 1. *Interpretation:* Heavily modified highland material; combination of tectonic forces producing plateau and trough (fretted) terrain, possible fluvial dissection and eolian deflation have denuded the surface creating disparate, knobby-like regions, particularly north and east of the dichotomy; may be stratigraphically equivalent with (or lower member of) plateau sequence unit 1; relatively lower position may also be attributed to faulting of the northeast portion of the map area.

plateau sequence unit B (plB) – Rugged dark-toned deposit with internal layering and a jagged, irregular margin; several secondary crater chains; dissected by some fluvial channels near the boundary with plateau sequence unit C; superposes plateau sequence unit C. *Interpretation:* Deposit of layered material exposed by denudation of overlying sequence. Mineral detections: phyllosilicate, low Ca-pyroxene.

Syrtis Major flows, unit 2b (sf2b) – Relatively smooth plains; displays a few flow lobes and terminal scarp; superpose Syrtis Major flow unit 1. *Interpretation:* Volcanic flow materials of relatively low to moderate viscosity delivered from Syrtis Major to the south; flow boundary may represent extent of lava flow in which case the lava may have been considerably more viscous, or margin may be where lava filled a topographic depression and the bounding materials subsequently eroded away leaving the appearance of a steep flow margin.

plateau sequence unit 2 (pl2) – Smooth capping material (almost always defined by low relief scarp) with few secondary craters and crater chains; dissected by orthogonal faults exposing plateau sequence unit 1. *Interpretation:* Deposit of relatively significant strength modified by tectonic forces producing ridge and trough (fretted) terrain. Modified by surface processes occurring within the troughs (possibly glacial) in the northwest; may be stratigraphically equivalent with plateau sequence unit F.

plateau sequence unit 1 (pl1) – Massive outcropping material with secondary craters and crater chains; dissected by orthogonal faults in north and fluvial-like channels to the south. *Interpretation:* Highland material modified by tectonic forces producing ridge and trough (fretted) terrain; possible subsequent glacial processes occurring within the troughs to the north; dissected by channels (of fluvial origin) to the south; eolian deflation and (or) weathering processes have eroded the surface, creating disparate, knobby-like regions, particularly north and east of the dichotomy; may be stratigraphically equivalent with, or upper member of, plateau sequence unit G. Mineral detections: phyllosilicate, low Ca-pyroxene, olivine.

Syrtis Major flows, unit 2a (sf2a) – Relatively smooth plains; superpose Syrtis Major flow unit 1. *Interpretation:* Volcanic flow materials of relatively low to moderate viscosity delivered from Syrtis Major to the south.

plains sequence unit B (pB) – Extremely smooth, relatively light-toned material; fills in topographic lows within plains sequence unit C; superposes plains sequence unit C. *Interpretation:* Eolian sedimentation in topographic lows. Mineral detections: olivine.

plains sequence unit D (pD) – Smooth, relatively light-toned material with distributed and abundant knobs associated with plateau sequence units 1 and G; deformed by small-scale wrinkle ridges in the northwest. *Interpretation:* Plains materials of eolian, fluvial, "marine," and (or) volcanic origin that blanket the northern lowlands subduing the degraded highland plateau remnants.

plains sequence unit C (pC) – Smooth, relatively light-toned material with distributed and abundant knobs; dissected by moderately-sized fluvial channels originating from the west. *Interpretation:* Heavily modified remnant highland materials interspersed with fluvial deposits in local crater basins.

Mineral detections: phyllosilicate, low Ca-pyroxene, ultra low Ca-pyroxene, olivine.

plains sequence unit A (pA) – Extremely smooth, dark-toned material; fills in topographically lowest areas within Isidis Planitia. *Interpretation:* Eolian sedimentation in topographic lows.

plateau sequence unit F (plF) – Smooth material with some knobby regions; abundant secondary craters and crater chains; gradational boundary with plateau sequence unit G. *Interpretation:* Deposit of relatively significant strength modified by tectonic forces producing subtle plateau and trough terrain and knobby appearance; may be stratigraphically equivalent with plateau sequence unit 2, or an intermediate member equivalent to upper plateau sequence unit 1 and lower plateau sequence unit 2. Mineral detections: olivine.

Syrtis Major flows, unit 1 (sf1) – Relatively smooth plains that fill local lowlands including a significant portion of the Nili Fossae trough structure; displays isolated wrinkle ridges. *Interpretation:* Volcanic flow materials of relatively low viscosity delivered from Syrtis Major to the south. Mineral detections: phyllosilicate, ultra low-Ca-pyroxene.

Other units (unconstrained by crater counts):

plateau sequence unit E (plE) – Smooth capping material with few secondary craters and crater chains; dissected by faults and troughs; gradational boundary with plateau sequence unit F. *Interpretation:* Deposit of relatively significant strength modified by tectonic forces producing plateau and trough terrain; may be stratigraphically equivalent with upper plateau sequence unit 2.

plateau sequence unit C (plC) – Rugged light-toned deposit with internal layering and a jagged, irregular margin; occupies local topographic lows; dissected by fluvial channels; superposes plateau sequence unit 1. *Interpretation:* Deposit of relatively significant strength exposed by denudation of overlying sequence; may be stratigraphically equivalent with plateau sequence unit 2. Mineral detections: phyllosilicate, low Ca-pyroxene.

Abbreviated unit descriptions: **crater peak (cp)**–Rugged and massive materials with significant topographic relief relative to surrounding crater floor; located in the center of an impact crater. **crater ejecta (ce)**–Continuous to semi-continuous ejecta blanket and rim displaying relief relative to surrounding surfaces; several craters have channels and mass-wasting features along the interior walls and interior deposits. **crater fill, undivided (cfu)**–Materials with a smooth continuous surface and no observed layering contained completely within an impact crater. **crater fill, lineated (cfl)**–Lineated materials displaying parallel, sub-parallel, and concentric surface ridges contained completely within an impact crater; occurs north of 29° latitude. **crater fill, units 1 and 2 (cf1, cf2)–**Layered materials contained completely within an impact crater; typically located adjacent to a crater rim breech, inlet, or outlet channel. **valley fill, undivided (vfu)**–Materials with a smooth continuous surface and no observed layering contained within isolated topographic depressions. **valley fill, hummocky (vfh)**–Massive and blocky (although highly degraded, deflated, and subdued) materials located on valley floors of "fretted terrain" adjacent to plateau sequence units 1 and 2. **valley fill, units 1 and 2 (lineated) (vf1, vf2)**–Lineated materials displaying parallel, sub-parallel surface ridges contained completely within topographic depressions; occurs north of 29° latitude. **alluvial deposits (al)–**Layered and braided deposits; typically located at the mouth (or terminus) of a channel that has breeched a crater wall. **landslide (ls)–**Massive to blocky surfaces with lobate margins and fronts; typically confined to channels and gullies near regions of significant relief. **dunes (dn)–**Local and isolated landforms with barchan, barchanoid, and transverse geomorphologies; typically located in low-lying areas, especially within craters.

References: [1] Ehlmann et al. (2009) *JGR 114*, doi:10.1029/2009JE003339.

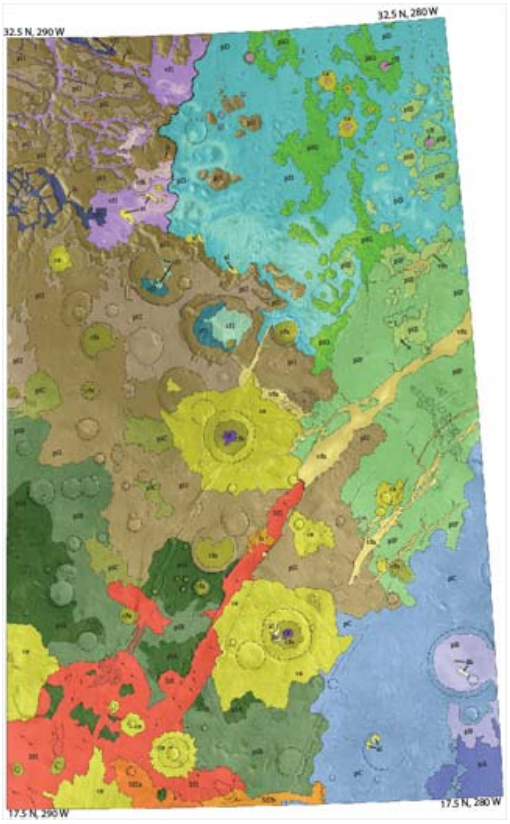

Figure 1. *Nili Fossae. See Bleamaster et al., this issue for global context image.*

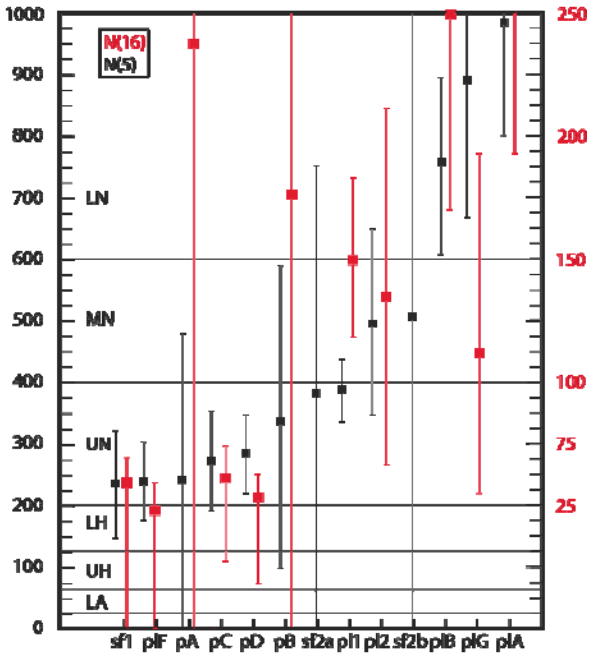

Figure 2. *N5 and N16 crater ages for major units.*

GEOLOGIC MAPPING OF THE THARSIS MONTES. D.A. Williams[1], J.E. Bleacher[2], W.B. Garry[3], [1]School of Earth & Space Exploration, Arizona State University, Tempe, Arizona 85287 (David.Williams@asu.edu), [2]Planetary Geodynamics Division, NASA Goddard Spaceflight Center, Laurel, Maryland, [3]Planetary Science Institute, Tucson, Arizona.

Introduction: We are funded by the NASA Mars Data Analysis Program (MDAP) to produce 1:1,000,000 scale geologic maps of Arsia Mons and Pavonis Mons, as well as conduct mapping of surrounding regions. In this abstract we discuss progress made during year 1 of the project.

Objectives: The *scientific objectives* of this mapping project include: 1) Determining the areal extent, distribution, and age relationships of different lava flow morphologies (**Fig. 1**) on the main flanks, rift aprons, and associated small-vent fields of Arsia and Pavonis Montes to identify and understand changes in effusive style across each volcano, and to provide insight into Martian magma production rates. This work builds on a preliminary study performed by Co-I Bleacher as part of his Ph.D. dissertation [1]. Results will provide insight into the overall volcanic evolution of each structure, enable comparisons between volcanoes, and determine the extent of each shield's contribution to the Tharsis plains; 2) Determining the areal extent and distribution of purported glacial and aeolian deposits on the flanks of each shield and their relationship to the lava flows. Results will establish a volcano-wide understanding of the nature of potential lava-ice interactions and the contribution of aeolian cover to the current form of the shields, enabling comparison among the shields potentially in different stages of development; and 3) Characterizing erosional and tectonic features, such as rift zone graben, flank terraces, and channel networks present on the flanks, rift aprons, and small-vent fields (**Fig. 2**), to determine their relationships to volcanic materials and processes.

Progress: We are completing our year 1 objectives on schedule. Our objectives for year 1 include: 1) Assemble all required data products, provide them to the USGS, and have the USGS produce the Tharsis Montes (TM) map project in ArcGIS™ software to perform the mapping, consistent with current NASA guidelines. This objective has been completed. 2) Begin geologic mapping of the volcano. As of this date (June 1, 2011), we have completed mapping of structural features over both Arsia and Pavonis Montes volcanoes (**Fig. 3a,b**). The next step will be to apply the material unit definition and characterization methodology that Co-I Jacob Bleacher has developed for the Olympus Mons mapping project [2], adapt it to the Tharsis Montes, and begin unit mapping. Material unit mapping will be the primary tasks of years 2 and 3.

References: [1] Bleacher, J.E., R. Greeley, D.A. Williams, S.R. Cave, and G. Neukum (2007), Trends in effusive style at the Tharsis Montes, Mars, and implications for the development of the Tharsis province, *J. Geophys. Res., 112*, E09005, doi:10.1029/2006JE 002873. [2] Bleacher et al. (2011), LPSC 42, abstract # 1805.

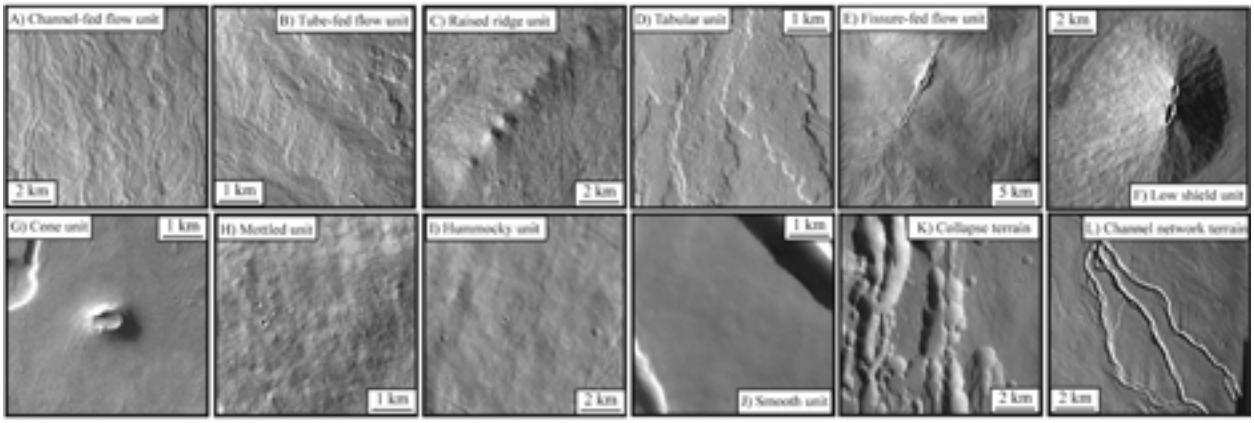

Figure 1. Type examples of volcanic units mapped in the Tharsis Montes, using HRSC and THEMIS data. From left to right, top to bottom: A) channel-fed flows (CFF), B) tube-fed flows (TFF), C) raised ridges, D) tabular flows, E) fissure-fed flow fields, F) low shields, G) cones, H) a mottled unit, I) a hummocky unit, J) a smooth unit, K) collapse of non-impact origin, and L) channel network terrain. Modified from [1].

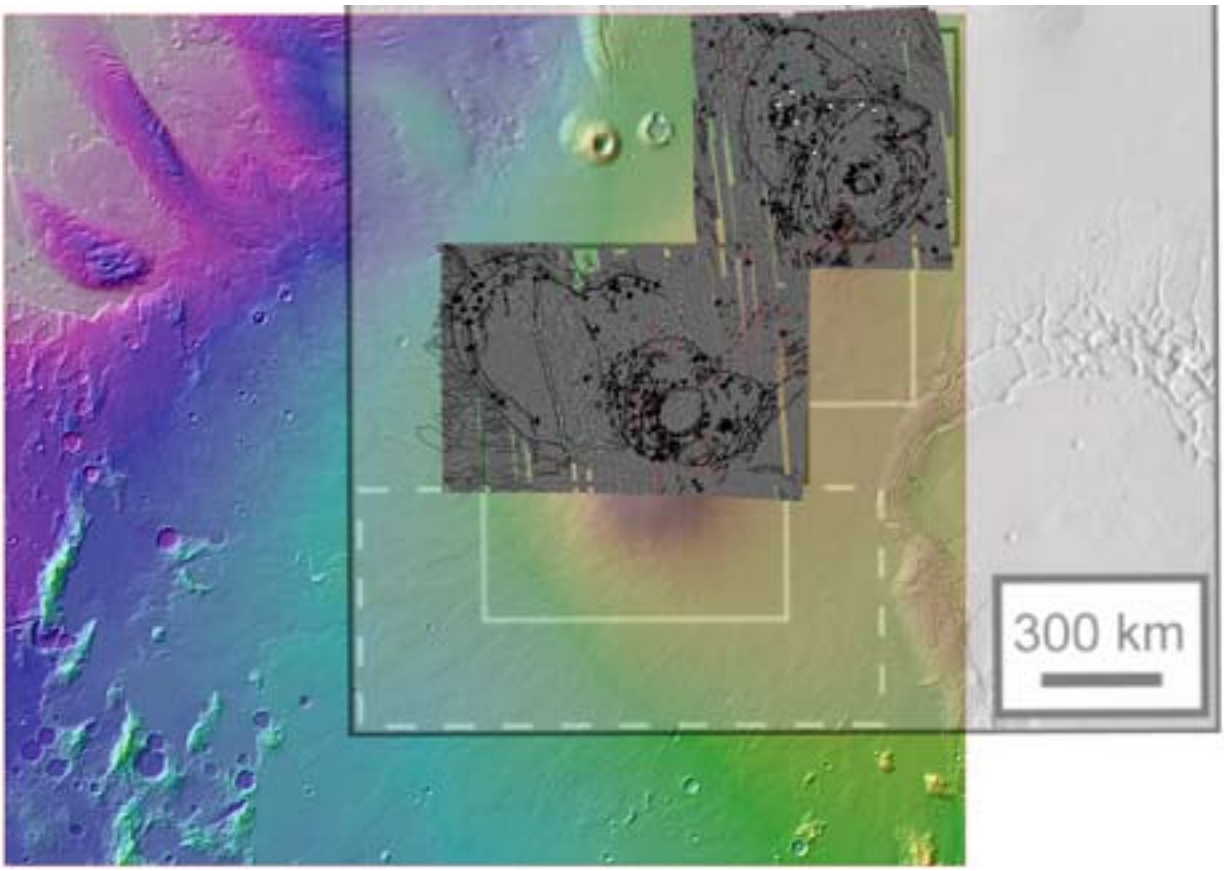

Figure 2. Color-coded altimetry map of the central Tharsis region of Mars showing our mapping regions and the area of our mapping coverage (derived from the ArcGIS™ project provided by the USGS). This map shows superposed CTX coverage (6 m/pixel, bottom image), which almost fully covers the primary mapping regions (smaller solid black rectangles). Supplemental mapping regions include the rift aprons and shield fields (solid white rectangles) and a region of long lava flows (dashed white rectangle).

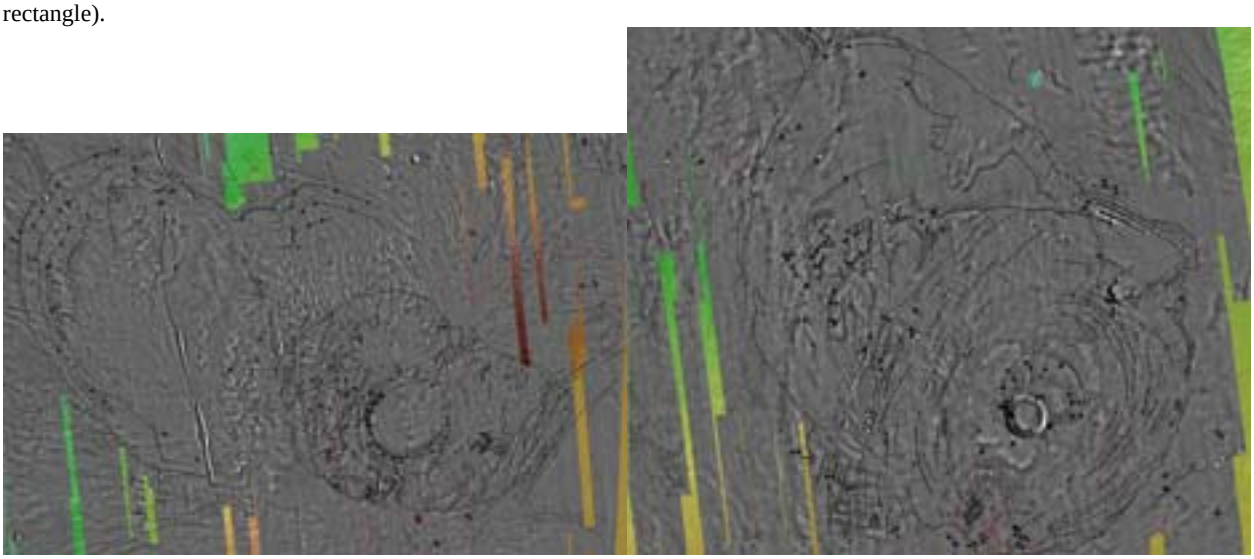

Fig. 3a (left). Structural mapping of Arsia Mons superposed on CTX coverage (6 m/pixel) and MOLA color map. **Fig. 3b (right).** Structural mapping of Pavonis Mons on same basemap. Red lines mark the trace of volcanic lava channels and/or the traces of lava tubes. Linear features with the white diamond symbols mark the locations of eskers in glacial terrains, and possible dikes in volcanic terrain. Figures derived from the ArcGIS™ project provided by the USGS.

ALLUVIAL FANS IN MARGARITIFER TERRA: IMPLICATIONS FOR A LATE PERIOD OF FLUVIAL ACTIVITY ON MARS. S. A. Wilson and J. A. Grant, Center for Earth and Planetary Studies, National Air and Space Museum, Smithsonian Institution, 6th St. at Independence Ave. SW, Washington, DC 20560, purdys@si.edu.

Introduction: The distribution, age and morphology of alluvial deposits within impact craters on Mars provide insight into the hydrologic and climatic history of the planet [1-9]. Many of these deposits occur as alluvial fans within large craters in and around USGS quadrangles -20037, -25037, -30037 and -30032 (Fig. 1). Many fans in southern Margaritifer Terra [5, 8] were assumed to be Late Noachian in age [e.g., 10] based on the Noachian age of their host craters [5]. Crater statistics of the fans based on high resolution MRO data [11-12], however, yield an age near or after the Amazonian-Hesperian boundary, suggesting a late period of water-driven fluvial activity on Mars [13].

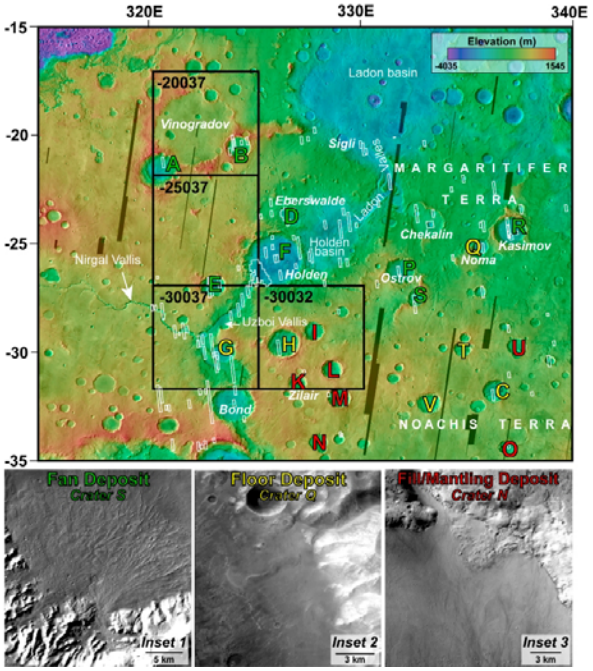

Figure 1. Southern Margaritifer Terra study region. Craters with labels included in study; color of label indicates alluvial fans (green, e.g. Inset 1), floor deposits (yellow, e.g. Inset 2) or fill/mantling deposits (red, e.g. Inset 3). MOLA over THEMIS daytime IR. Black and white boxes indicate USGS quadrangles funded for geologic mapping and HiRISE footprints, respectively.

Classification of Deposits: Based on morphology, 22 crater interiors (D>50 km) in southern Margaritifer Terra were classified as 1) fan deposits, 2) floor deposits, or 3) fill/mantling deposits (Fig. 1). Craters with alluvial fans typically display well-developed alcoves and incised walls, and fan surfaces preserve distributary channels standing ~10-15 m in relief [5, 8, 14]. Other craters with incised walls lack fans but preserve crater floor deposits indicative of past fluvial and/or possible lacustrine activity (e.g., light-toned layers). The remaining craters are filled or mantled by diverse materials.

Methods: Statistics were compiled for craters with fan, floor, and fill/mantling deposits using CraterTools software in ArcGIS [15]. Gaps in CTX data, secondary clusters, dune fields, lava flows and etched surfaces were excluded. Craterstats software was used to derive relative and absolute ages [16] based on the chronology function of [17] and production function of [18]. Similar results were obtained from the variable diameter bin-size plot of [19]. Craters smaller than D~200 m (except in crater N where the largest crater is ~280 m across) were generally excluded from the interpretation of ages.

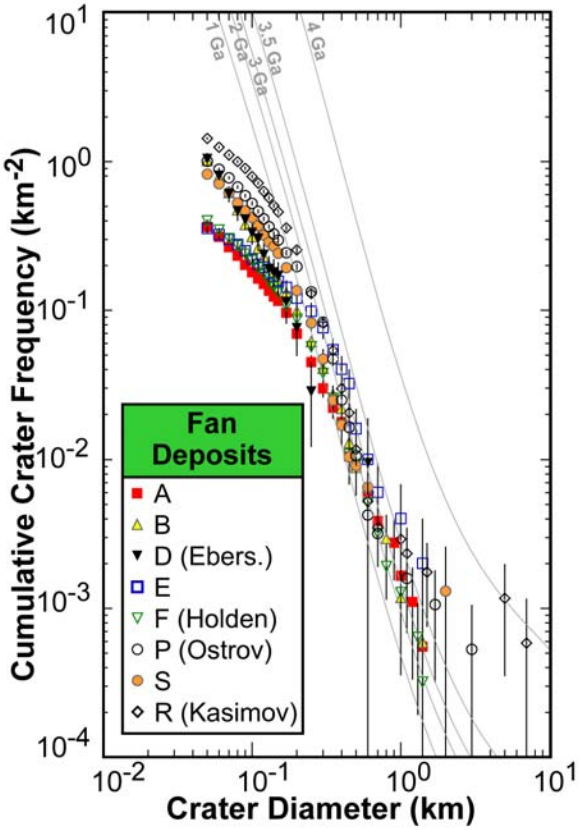

Figure 2. Crater statistics for alluvial fan deposits (craters with green labels in Fig. 1) date to the early Ama-

zonian or near the Hesperian-Amazonian boundary (average age = 1.9 Ga ± 0.5).

Results: In both types of plots, fan deposits date from the Amazonian to near the Amazonian-Hesperian boundary (Fig. 2). Crater floor deposits are likely Hesperian, and fill/mantling deposits are mostly Amazonian except for the Hesperian or Noachian-aged deposit in crater K. Despite variations between individual counts, the clustering of results within each class relative to one another indicates distinct differences in ages. The cumulative and incremental plots yield broadly similar results and are internally consistent, though absolute ages derived from the incremental plot are systematically younger due to differences in the production function and position of hypothesized isochrones [19, 27].

Discussion: Count-to-count variability in the relative ages may relate to both the relatively small areas considered and real differences in age. Nevertheless, a paucity of craters up to ~200 m across is consistent with the erosion required to account for topographic inversion of fan distributary channels. At larger diameters, the statistics show a good match to the expected production population of craters and a paucity of additional inflections suggesting other intervals of burial and/or exhumation. Hence, the statistics appear to record the ages of these materials. The relatively young age of most mantling deposits suggests burial of additional alluvial fan and crater floor deposits is possible.

An Amazonian age for the fans likely requires precipitation (rain or snow [5, 20]) relatively late in Martian history, after most precipitation-driven fluvial activity ended [e.g., 5, 14, 21]. Inferred ages for the crater floor deposits are broadly contemporary with events elsewhere [e.g., 5, 14, 21, 22] and may record an earlier wet period. Formation of the fans near or after the Amazonian-Hesperian boundary, however, likely requires a later period of water driven gradation [13].

Formation of Hale crater (35.7S, 323.6E) in the Amazonian or near the Amazonian-Hesperian boundary is one possible mechanism for triggering fan formation [e.g. 23, 24]. Hale's ejecta is incised by numerous valleys suggesting release of volatiles after formation [24]. Hale does not appear responsible for the alluvial fans, however, because 1) some alluvial fans are 700-800 km away, 2) craters with fans occur at a range of azimuths from Hale, and 3) many craters bearing older floor deposits and mantling deposits are closest to Hale. Other potential crater sources are older [e.g., 25] and less likely to be responsible for the fans.

Late intervals of water-driven erosion on Mars have been suggested [e.g., 21, 26-31] and a possible source of water includes precipitation derived from redistribution of outflow channel discharge [e.g., 27, 32] into the highlands [33]. Therefore, alluvial fans may record late widespread water-driven degradation, perhaps accentuated by topography and/or orbital variations. Because Holden and Eberswalde craters are finalists for the MSL landing site, the age of their fans implies MSL could sample relatively young materials.

References: [1] Cabrol, N. A., E. A. Grin (2001), *Geomorph.*, *37*, 269. [2] Malin, M. C., K. S. Edgett (2003), *Science*, 302, 1931, doi: 10. 1126 / science. 1090544. [3] Moore, J. M., et al. (2003), *GRL*, 30, 2292, doi:10.1029/2003GL019002. [4] Crumpler, L. S., K. L. Tanaka (2003), *JGR*, 108, 8080, doi: 10. 1029/ 2002JE002040. [5] Moore, J. M., A. D. Howard (2005), *JGR*, 110, doi:10.1029/2005JE002352. [6] Irwin, R. P. III, et al. (2005), *JGR*, 110, doi: 10. 1029/ 2005JE002460. [7] Weitz, C. M., et al. (2006), *Icarus*, 184, 436. [8] Kraal, E. R., et al. (2008), *Icarus*, 194, 101, doi:10.1016/j.icarus.2007.09.028. [9] Williams, R. M. E., et al. (2010), *Icarus* doi:10.1016/ j.icarus.2010.10.001. [10] Scott, D. H., K. L. Tanaka (1986), *USGS Misc. Invest*. Ser. Map I-1802-A. [11] McEwen, A. S., et al. (2007), *JGR*, 112, doi:10.1029/ 2005JE002605. [12] Malin, M. C., et al. (2007), *JGR*, 112, doi:10.1029/2006JE002808. [13] Grant, J. A. and S. A. Wilson (2011), *GRL, 38*, doi: 1029/2011GL046844. [14] Grant, J. A., et al. (2010), *Icarus*, doi:10.1016/j.icarus.2010.11.024. [15] Kneissl, T., et al. (2010), *PSS*, doi:10.1016/j.pss.2010.03.015. [16] Michael, G. G., G. Neukum (2010), *EPSL*, doi:10.1016/j.epsl.2009. 12.041. [17] Hartmann, W. K., and G. Neukum (2001), *Space Sci. Rev.*, 96, 165. [18] Ivanov, B. A. (2001), *Space Sci. Rev.*, 96, 87. [19] Hartmann, W. K. (2005), *Icarus*, 174, 294. [20] Howard, A. D., Moore, J. M. (2011), *JGR*, 2010JE003782 (in press). [21] Fassett, C. I., J. W. Head (2008), *Icarus*, 195, 61, doi:10.1016/ j.icarus. 2007.12.009. [22] Grant, J. A., et al. (2008), *Geology*, 36, 195, doi: 10.1130/G24340A. [23] Maxwell, T. A., et al. (1973), *Geology, 1*, 9. [24] Jones, A.P., et al. (2010), *Icarus*, doi: 10.1016/j.icarus. 2010.10.014. [25] Irwin, R. P. III, and J. A. Grant (2010), *USGS Sci. Invest. Map*, scale 1:500,000, (in revision). [26] Gulick, V. C., and V. R. Baker (1990), *JGR*, 95, 14,325, doi:10.1029/JB095iB09p14325. [27] Carr, M. H. (1996), *Water on Mars*, 229p. Oxford Univ. Press, NY. [28] Carr, M. H. (2006), *The Surface of Mars*, 307p, Cambridge Univ. Press, Cambridge, UK. [29] Mangold, N., et al. (2004), *Science*, 305, 78, doi: 10.1126/ science.1097549. [30] Dickson, J. L., et al. (2009), *GRL.*, 36, doi:10.1029/2009GL037472. [31] Fassett et al. (2010), *Icarus*, 208, doi: 10.1016/j.icarus. 2010.02.021. [32] Rotto, S., K. L. Tanaka (1995), *USGS Map I-2441*. [33] Luo, W., and Stepinski, T. F. (2009), *JGR*, 114, doi:10.1029/2009JE003357.

GEOLOGIC MAPPING OF THE MEDUSAE FOSSAE FORMATION, MARS, AND THE NORTHERN LOWLAND PLAINS, VENUS. J.R. Zimbelman and S.P. Scheidt, CEPS/NASM MRC 315, Smithsonian Institution, Washington, D.C., 20013-7012; zimbelmanj@si.edu.

Introduction: This report summarizes the status of mapping projects supported by NASA grant NNX07AP42G, through the Planetary Geology and Geophysics (PGG) program. The PGG grant is focused on 1:2M-scale mapping of portions of the Medusae Fossae Formation (MFF) on Mars. Also described below is the current status of two Venus geologic maps, generated under an earlier PGG mapping grant.

Medusae Fossae Formation, Mars: Work on mapping of the heavily eroded western portions of MFF continues to progress. Attributes of MFF as documented in Mars Orbiter Camera images were used in a reevaluation of the numerous hypotheses about the origin of MFF, with the conclusion that an ignimbrite origin is most consistent with observations [1]. Yardangs are abundant within an intensely eroded component of the lower member of MFF (labeled here as unit Aml_2), and they provide insights into the friable nature of Aml_2 [2], as evidenced by differences in competency resulting from erosion and mass wasting, a result that appears to be most consistent with variable degrees of welding often present within volcanic (ignimbrite) deposits [1]. The geologic map of the **MC-23 NW** quadrangle at 1:2M scale (Fig. 1) covers the southwestern

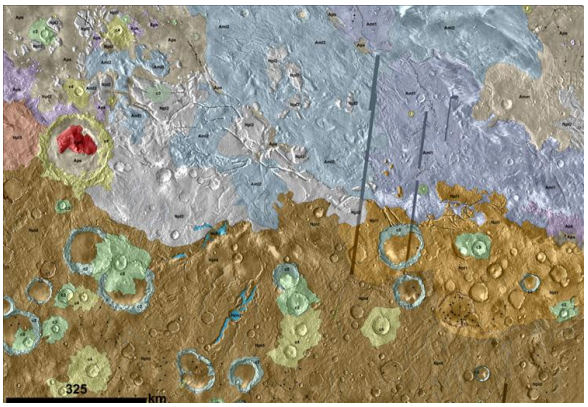

Figure 1. Geologic map for MC-23 NW [4].

margin of the globally mapped large exposures of MFF [3]. Mapping has revealed several outliers interpreted to be isolated remnants of Aml_2 (Fig. 2), suggesting that the previous extent of MFF materials may have been much larger than what is expressed by the present-day MFF exposures [4]; this supports earlier inferences that current MFF exposures do not represent the full extent of the deposits [5-7].

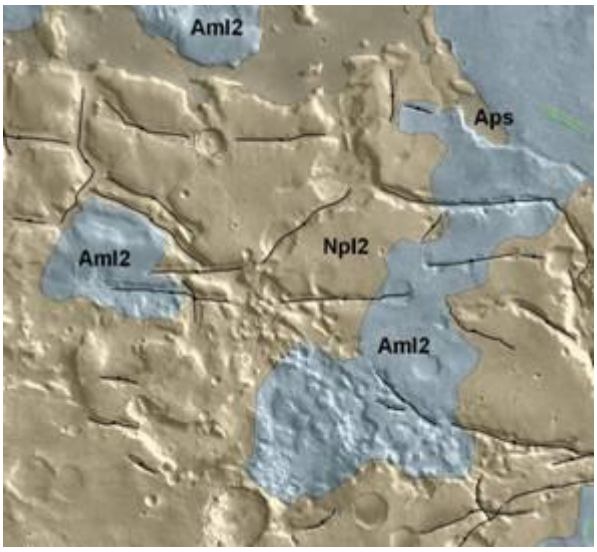

Figure 2. Detail of MC-23 NW map (center-left of Fig. 1) showing outliers of Aml_2 materials, located south and west of the globally mapped Aml_2 exposures.

A distinctive feature thus far restricted to the westernmost MFF exposures is the occurrence of sinuous positive-relief ridges [8], which in MC-23 NW are restricted to the topographically lowest portions of Aml_1, what we interpret to be the lowest stratigraphic component of global unit Aml [2; Aml is described in 3]. These sinuous ridges are interpreted to be inverted paleochannels [8, 9] which may represent prolonged flow of a liquid coincident with the emplacement of the stratigraphically lowest component of MFF [2, 8, 9].

Since early 2009, the PI has been learning to use ArcGIS software, obtained through a licensing agreement with the Smithsonian Institution. The learning curve for ArcGIS has been very steep for the PI, but the crucial assistance of coauthor SPS has greatly facilitated recent progress. The MC-23 NW map is the first geologic map produced by the PI using ArcGIS. The unit contact locations are unlikely to change by much, unless peer review reveals necessary changes.

Mapping of **MC-16 NW** (Fig. 3) has been undertaken primarily by coauthor SPS, with oversight by the PI [10]. This new map will provide important insights into the lower, middle and upper members of MFF [11]. To fully document the stratigraphic relationships evident in this map area, the global units are divided into multiple sub-units based on distinctive textures and layering expressed in erosion of the MFF materials

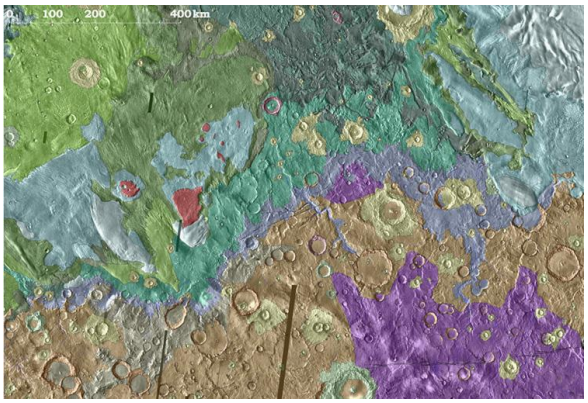

Figure 3. Geologic map for MC-16 NW [10].

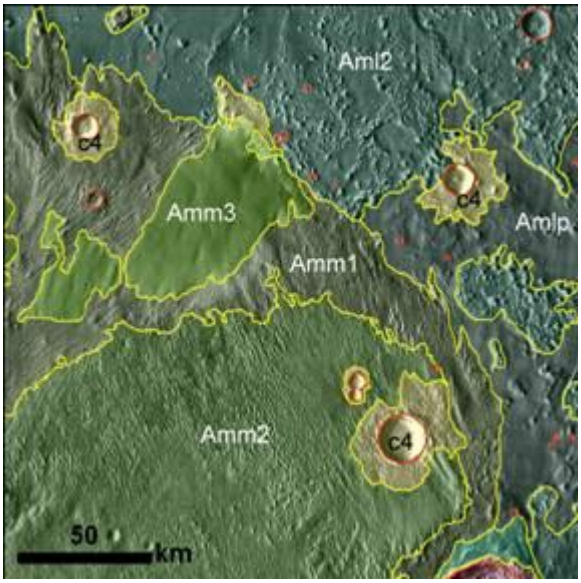

Figure 4. Detail of MC-16 NW map showing subunits of lower (Aml) and middle (Amm) units of the MFF.

(Fig. 4). The lowest MFF unit (Amlp) exhibits remnants of eroded materials mapped as a subunit between the western and eastern portions MC-16 NW, and the middle MFF units can be divided into separate subunits from evidence of layering and aeolian erosion patterns. Results from both MC-23 NW and MC-16 NW are expected to provide valuable new insights into both the emplacement and the erosional characteristics of all three of the globally mapped members of MFF. Once mapping of both MC-23 NW and MC-16 NW is submitted to USGS for review, the PI will work on producing an ArcGIS version of a geologic map for **MC-8 SE**, using an earlier (Illustrator 9) mapping product [12] as a guide to the geology now evident in the latest THEMIS base maps.

Northern Lowland Plains, Venus: The map and text for the Kawelu Planitia quadrangle (**V-16**) have been in review with the USGS for several years [13]. A revised version, addressing all reviewer comments, was submitted to the USGS in 2008, where it became apparent that the linework (which dated from mapping begun on hardcopy base materials) was not uniformly registered to the digital photobase that is the current standard for production of published maps. Careful review of all of the linework revealed that no single shift or warp could correct the situation, due to map revisions that were made at different times to various sections of the map. During 2010, the V-16 linework was manually adjusted to register with the digital photobase, through the helpful assistance of NASM volunteers. We have not yet regenerated the unit polygons in Adobe Illustrator 9, the software used to make the current version of the map, but we intend to do so following submission of the Mars maps. Once the adjusted linework is reconstituted into a map registered to the digital base, V-16 should be able to continue through the approval process. The Bellona Fossae quadrangle (**V-15**) was mapped several years ago [14] under a previous PGG grant, also initiated on hardcopy base materials like V-16. When the V-16 map is through review, the V-15 geology will be done in ArcGIS, using the prior map as a primary guide.

Future Plans: The MC-23 NW and MC-16 NW maps will be submitted to the USGS this summer, followed by production of revised versions of the geologic maps for MC-8 SE and V-15 in ArcGIS.

References: [1] Mandt, K.E., et al. (2008) JGR, 113, E12011, doi: 10.1029/2008JE003076. [2] Zimbelman, J.R., and Griffin, L.J. (2010) Icarus, doi: 10.1016/j.icarus.2009.04.003. [3] Greeley, R., and Guest, J.E. (1987) USGS Misc. Invest. Series Map I-1802-B. [4] Zimbelman, J.R. (2011) LPSC 42, Abs. #1840. [5] Schultz, P.H. and Lutz, A.B. (1988) Icarus, 73, 91-141. [6] Edgett, K.S., et al. (1997) JGR, 102, 21,545-21,567. [7] Hynek, B.M., et al. (2002) JGR, 108, E9, 10.1029/2003JE002062. [8] Burr, D.M., et al. (2009) Icarus 200, 52-76, doi: 10.1016/j.icarus.2008.10.014. [9] Williams, R.M.E., et al. (2009) Geomorphology, 10.1016/j.geomorph.2008.12.015. [10] Scheidt, S.P., and Zimbelman, J.R. (2011) LPSC 42, Abs. #2631. [11] Scott, D.H., and Tanaka, K.L. (1986) USGS Misc. Invest. Series Map I-1802-A. [12] Zimbelman, J.R. (2007) NASA Mappers mtg, ZIMBELMANa2007PGM.PDF. [13] Zimbelman, J.R. (2007) NASA Mappers mtg, ZIMBEMANb2007PGM.PDF. [14] Zimbelman, J.R. (2004) NASA Mappers mtg, ZIMBELMAN2004PGM.PDF.

GLOBAL GEOLOGIC MAP OF IO: FINAL RESULTS. D.A. Williams[1], L.P. Keszthelyi[2], D.A. Crown[3], P.E. Geissler[2], P.M. Schenk[4], Jessica Yff[2], W.L. Jaeger[2], [1]School of Earth & Space Exploration, Arizona State University, Tempe, Arizona 85287 (David.Williams@asu.edu), [2]Astrogeology Science Center, U.S. Geological Survey, Flagstaff, Arizona, [3]Planetary Science Institute, Tucson, Arizona, [4]Lunar and Planetary Institute, Houston, Texas.

Introduction: We have completed a new 1:15,000,000-scale global geologic map of Jupiter's volcanic moon, Io, based on a set of 1 km/pixel combined *Galileo-Voyager* mosaics produced by the U.S. Geological Survey [1]. The map was produced using ArcGIS™ software, has been revised based upon peer-review, and is now being edited by the USGS. In this abstract we present the map (**Figure 1**) and we discuss the geographic distribution of material units and report some of the key insights into the volcanic evolution of Io arising from our mapping results. An *Icarus* manuscript describing in detail the map and derived results is currently in review [2].

Results: The surface of Io was mapped into 19 units based on albedo, color and surface morphology, and is subdivided as follows: plains (65.8% of surface), lava flow fields (28.5%), mountains (3.2%), and patera floors (2.5%). Diffuse deposits (DD) that mantle the other units cover ~18% of Io's surface, and are distributed as follows: red (8.6% of surface), white (6.9%), yellow (2.1%), black (0.6%), and green (~0.01%). Analyses of the geographical and areal distribution of these units yield a number of results summarized below. (1) The distribution of plains units of different colors is generally geographically constrained. Red-brown plains occur >±30˚ latitude, and are thought to result from enhanced alteration of other units induced by radiation coming in from the poles. White plains (dominated by SO_2 + contaminants) occur mostly in the equatorial antijovian region (±30˚, 90˚-230˚W), possibly indicative of a regional cold trap. Outliers of white, yellow, and red-brown plains in other regions may result from long-term accumulation of white, yellow, and red diffuse deposits, respectively. (2) Bright (presumably sulfur-rich) flow fields make up 30% more lava flow fields than dark (presumably silicate) flows (56.5% vs. 43.5%), and only 18% of bright flow fields occur within 10 km of dark flow fields. These results suggest that secondary sulfurous volcanism (where a bright-dark association is expected) is responsible for only a fraction of Io's recent bright flows, and that primary sulfur-rich effusions are an important component of Io's recent volcanism. Additionally, an unusual concentration of bright flows at ~45˚-75˚N, ~60˚-120˚W is perhaps indicative of more extensive primary sulfurous volcanism in the recent past. (3) We mapped 425 paterae (volcano-tectonic depressions), up from 417 previously identified by [3]. Although these features cover only 2.5% of Io's surface, they correspond to 64% of all detected hot spots; 45% of all hot spots are associated with the freshest dark patera floors reflecting the importance of active silicate volcanism to Io's heat flow. (4) Mountains cover only ~3% of the surface, although the transition from mountains to plains is gradational with the available imagery. Forty-nine percent of all mountains are lineated, showing evidence of linear structures supportive of a tectonic origin. In contrast, only 6% of visible mountains are mottled (showing hummocks indicative of mass wasting) and 4% are tholi (domes or shields), consistent with a volcanic origin. (5) Our mapping does not show significant longitudinal variation in the quantity of Io's mountains or paterae. This is because we use the area of mountain and patera materials as opposed to the number of structures, and our result suggests that the previously proposed anti-correlation of mountains and paterae [4] is more complex than previously thought. There is also a slight decrease in surface area of lava flows toward the poles of Io, perhaps indicative of variations in volcanic activity. (6) The freshest bright and dark flows make up about 29% of all of Io's flow fields, suggesting active emplacement is occurring in less than a third of Io's visible lava fields. (7) About 47% of Io's diffuse deposits (by area) are red, presumably deriving their color from condensed sulfur gas, and ~38% are white, presumably dominated by condensed SO_2. The much greater areal extent of gas-derived diffuse deposits (red + white, 85%) compared to presumably pyroclast-bearing diffuse deposits (dark (silicate ash) + yellow (sulfur-rich ash), 15%) indicates that there is effective separation between the transport of pyroclasts and gas in many Ionian explosive eruptions. Future improvements in the geologic mapping of Io can be obtained via (a) investigating the relationships between different color/material units that are geographically and temporally associated, (b) better analysis of the temporal variations in the map units, and (c) additional high-resolution images (spatial resolutions ~200 m/pixel or better). These improvements would be greatly facilitated by new data, which could be obtained by proposed future missions (*Io Volcano Observer*, *Jupiter Europa Orbiter*).

References: [1] Becker, T. and P. Geissler (2005), *LPS XXXVI*, Abstract #1862. [2] Williams, D.A. et al. (2011), *Icarus*, in review. [3] Radebaugh, J., et al. (2001), *JGR 106, E12*, 33,005-33,020. [4] Schenk, P., et al. (2001), *JGR 106, E12*, 33,201-33,222. [5] Wil-

liams, D.A. et al. (2007), *Icarus*, *186*, 204-217. [6] Rathbun, J.A. and S.E. Barrett (2007), *LPS XXXVIII*, Abstract #2123. [7] Williams, D.A. et al. (2008), *LPS XXXIX*, Abstract #1003. [8] Williams, D.A. et al. (2009), *LPS XL*, Abstract #1403.

Figure 1. Final ArcGIS™ version of the global geologic map of Io as submitted to the USGS for publication. For additional information on basemap mosaics, mapping strategy, Io database, areal coverage of map units, and stratigraphic correlation of map units, see [1, 2, 5, 6, 7, 8].

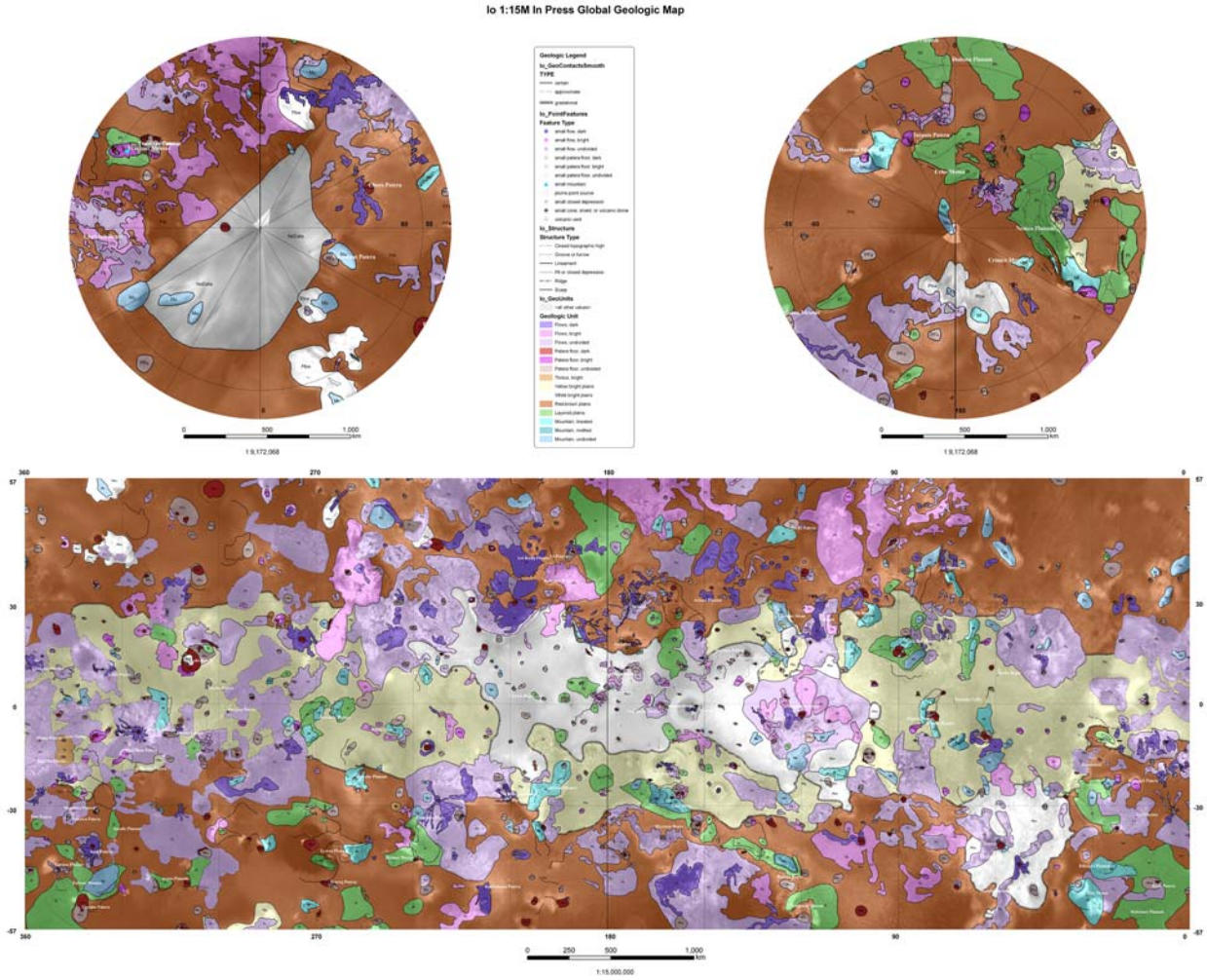

A GIS TOOLSET FOR THE RAPID MEASUREMENT AND CATALOGING OF MORPHOLOGIC FEATURES IN PLANETARY MAPPING. R. A. Nava and T. M. Hare, Astrogeology Science Center, U. S. Geological Survey, 2255 N. Gemini Dr., Flagstaff, AZ 86001 (rnava@usgs.gov).

Introduction: Geographic Information Systems (GIS) technologies are becoming an integral component of planetary geologic research and mapping [1]. Aside from the collection and visualization of spatially referenced data, GIS offers many analytical and measurement capabilities that can be used in conjunction with mapping for the efficient extraction and storage of ancillary information pertinent to geographic features.

Last year we introduced *Crater Helper Tools* for ArcGIS 9.3, a toolset for automating the measurement and cataloging of topographic and albedo features in a map projection-independent environment. The toolset is distributed as an ArcMap Add-In and was originally developed to assist the mapping efforts of the USGS in maintaining the International Astronomical Union (IAU) Gazetteer of Planeraty Nomenclature [2]. Since its introduction, a new version of the hosting program, ArcGIS 10, has been released. Herein, we present the rationale, technical methods, and workflow behind *Crater Helper Tools* for ArcGIS 10.

Rationale: Surficial planetary data are often made available to the planetary community in the form of spatially registered images compatible with GIS software. These images are either referenced to the spherical or ellipsoidal model of their planetary body (latitude and longitude), or map-projected with reference to those models (x, y). Because map projections introduce the distortion of shapes, distances, areas and directions, they are designed with careful consideration of geographic coverage (e.g., *Polar* for north and south pole images) and purpose (e.g., *Azimuthal* for measuring directions). This leads to a proliferation of spatial reference systems with map projections not always suited for a particular measurement type, and can quickly impose challenges when deriving spatial data from inherently distorted base images.

Another minor but important difficulty that often emerges in mapping is the time-consuming implementation of a large number of spatial operations during feature digitizing. Morphologic feature extraction from base images usually takes place in two steps: one related to the storage of geometric shapes, and another to the attribution of non-geometry-related properties to individual features (i.e., qualitative information) [3]. When numerous digitizing tasks are implemented separately, the amount of time required to accomplish the generation of shapes, measurements, and attributes for a large number of features can be substantial.

To overcome both of these challenges, *Crater Helper* makes ample use of the extensibility options in ArcGIS software to (1) maintain a standardized measurement methodology consistent across map-projected coordinate systems, and (2) provide a limited number of digitizing tools that encapsulate several GIS routines into a single operation. For example, when capturing a crater, the rim's geometry is generated from three points and stored along with its diameter, latitude and longitude, perimeter, area, etc., all in one operation (**Fig. 1**).

Technical Methods: The toolset utilizes both unprojected and projected systems when computing feature geometries and their measurement information. Projected systems distort properties of real-world features by the process of representing a curved surface on a plane [4]. Although not all, some of these properties can be shown accurately at the expense of others [5]. When projected space is required, localized map projections are designed specifically for the areal extent, and centered about the feature being generated in order to reduce distortion. Distances and areas are determined by spherical and ellipsoidal formulae.

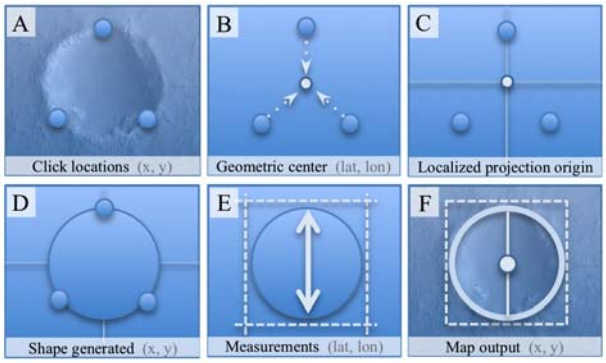

Figure 1. Internal coordinate transformation process used to generate geometries and perform measurements in projected (x, y) and unprojected (lat, lon) space respectively.

The process begins with the capture of map locations determined by user mouse clicks (**Fig. 1-A**). Map-clicks (x, y) are transformed into their latitude and longitude equivalents and used in the generation of localized Transverse Mercator and Azimuthal-Equidistant projections, where the 'projection origin' is established from calculating the geometric center of all click locations for a single feature (**Fig. 1-B, C**).

Feature (e.g., crater rim) and measurement (e.g., crater diameter) geometries are computed in different spatial reference systems. The Transverse Mercator projection maintains the correct shape of spatial features, and is employed internally for the determination of circles, ellipses, and other polygon type geometries (**Fig. 1-D**). Measurement lines, on the other hand, are given shape and direction in an Azimuthal-Equidistant projection, where azimuths remain true when measured from the center of the projection [5]. Next, another switch to unprojected space allows for the geodesic measurement of distances and areas (**Fig. 1-E**). To do this, lines are unprojected from their localized projections and their lengths calculated using ellipsoidal formulae, where the latitude and longitude pairs of line endpoints are input to equations that yield distances in metric units. Areas are determined by utilizing the geometric shape of the unprojected feature as input to spherical formulae. The final stage in the process transforms all geometries back to the map's spatial reference.

After the new features and their measurement lines are created, they are automatically added to the map as temporary graphics and distorted in the same way as the base image to help the user visually determine if measurements were performed correctly (e.g., the computed crater diameter is contained inside its rim) (**Figs. 1-F, 2-B**). Optionally, feature shapes can be stored permanently in a *line* database layer. If this is the case, geometries are transformed into the spatial reference of the layer and stored in the layer's database.

Process automation. Automation is achieved by bundling several digitizing tasks into a single operation and, in some instances, by reducing the number of clicks required to perform that operation. When digitizing a feature, several 'measurement types' may be selected prior to click locations being defined (**Fig. 2-A**). Each selected measurement is internally chained along with others and the entire chain executed once input from the map has been captured.

Workflow: Spatial data in a GIS are often conceptualized as having two components: coordinate information, describing the geometry of objects, and attribute information, which describes other properties about those objects [3]. While ArcGIS is able to store both components in the same database record, *Crater Helper* stores measurement information as attributes in a *point* database layer (**Fig. 2-C**), and feature geometries as *lines* in a separate layer. The workflow when using the toolset is as follows: (1) select the *point* and *line* database layers where measurements and shapes will be stored, (2) check any number of measurement types available, (3) select a tool to perform measurements with, and (4) click on the map to digitize and measure the feature (**Fig. 2**).

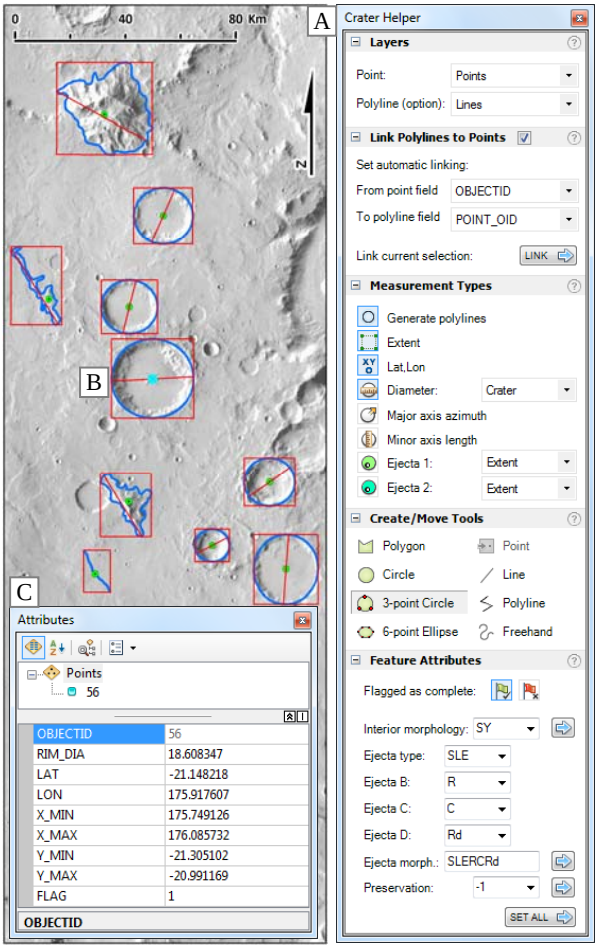

Figure 2. Feature measurement example using *Crater Helper*. (A) 'Dockable' window with controls grouped into different collapsible panels. (B) Feature geometry in blue, measurement lines in red. (C) Point attribute information for crater feature in B.

Availability: *Crater Helper Tools* for ArcGIS 10 is available for download from the PIGWAD (http://webgis.wr.usgs.gov) and ESRI Resource Center (http://resources.arcgis.com/gallery/file/arcobjects-net-api) websites. The download package includes the installation Add-In file, a reference manual, and this abstract. Once downloaded, the Add-In can be simply double-clicked and installed.

References: [1] Hare, T. (2010) LPSC XLI, abs. #2728. [2] Gazetteer of Planetary Nomenclature, http://planetarynames.wr.usgs.gov/. [3] Bolstad, P. (2005) GIS Fundamentals: A First Text on Geographic Information Systems. [4] Lo, C.P. and Yeung, A.K.W. (2007) Concepts and Techniques of Geographic Information Systems. [5] Snyder, J.P. (1987) Map Projections- A Working Manual.

Planetary Geologic Mapping Handbook – 2011

K.L. Tanaka, J.A. Skinner, Jr., and T.M. Hare
U.S. Geological Survey, Astrogeology Science Center
2255 N. Gemini Dr., Flagstaff, AZ 86001

Endorsed by:

The Geologic Mapping Subcommittee (GEMS) of the NASA Planetary Cartography and Geologic Mapping Working Group (PCGMWG)

M.S. Kelley[1], L.F. Bleamaster III[2], D.A. Crown[2], T.K.P. Gregg[3], S.C. Mest[2], and D.A. Williams[4]

[1]NASA Headquarters, Washington, DC
[2]Planetary Science Institute, Tucson, AZ
[3]University at Buffalo, Buffalo, NY
[4]Arizona State University, Tempe, AZ

TABLE OF CONTENTS

WHAT'S NEW: This addition includes instructions on formatting maps for official USGS submission, including required map components, file structures and formats, and digital templates (tables, correlation of map units). Because information and guidelines provided herein may be refined, readers are encouraged to check for and use the most recent version of this mapping handbook.

1. INTRODUCTION

Geologic maps present, in an historical context, fundamental syntheses of interpretations of the materials, landforms, structures, and processes that characterize planetary surfaces and shallow subsurfaces (e.g., Varnes, 1974). Such maps also provide a contextual framework for summarizing and evaluating thematic research for a given region or body. In planetary exploration, for example, geologic maps are used for specialized investigations such as targeting regions of interest for data collection and for characterizing sites for landed missions. Whereas most modern terrestrial geologic maps are constructed from regional views provided by remote sensing data and supplemented in detail by field-based observations and measurements, planetary maps have been largely based on analyses of orbital photography. For planetary bodies in particular, geologic maps commonly represent a snapshot of a surface, because they are based on available information at a time when new data are still being acquired. Thus the field of planetary geologic mapping has been evolving rapidly to embrace the use of new data and modern technology and to accommodate the growing needs of planetary exploration.

Planetary geologic maps have been published by the U.S. Geological Survey (USGS) since 1962 (Hackman, 1962). Over this time, numerous maps of several planetary bodies have been prepared at a variety of scales and projections using the best available image and topographic bases. Early geologic map bases commonly consisted of hand-mosaicked photographs or airbrushed shaded-relief views and geologic linework was manually drafted using mylar bases and ink drafting pens. Map publishing required a tedious process of scribing, color peel-coat preparation, typesetting, and photo-laboratory work. Beginning in the 1990s, inexpensive computing, display capability and user-friendly illustration software allowed maps to be drawn using digital tools rather than pen and ink, and mylar bases became obsolete.

Terrestrial geologic maps published by the USGS now are primarily digital products using geographic information system (GIS) software and file formats. GIS mapping tools permit easy spatial comparison, generation, importation, manipulation, and analysis of multiple raster image, gridded, and vector data sets. GIS software has also permitted the development of project-specific tools and the sharing of geospatial products among researchers. GIS approaches are now being used in planetary geologic mapping as well (e.g., Hare and others, 2009).

Guidelines or handbooks on techniques in planetary geologic mapping have been developed periodically (e.g., Wilhelms, 1972, 1990; Tanaka and others, 1994). As records of the heritage of mapping methods and data, these remain extremely useful guides. However, many of the fundamental aspects of earlier mapping handbooks have evolved significantly, and a comprehensive review of currently accepted mapping methodologies is now warranted. As documented in this handbook, such a review incorporates additional guidelines developed in recent years for planetary geologic mapping by the NASA Planetary Geology and Geophysics (PGG) Program's Planetary Cartography and Geologic Mapping Working Group's (PCGMWG) Geologic Mapping Subcommittee (GEMS) on the selection and use of map bases as well as map preparation, review, publication, and distribution. In light of the current boom in planetary

exploration and the ongoing rapid evolution of available data for planetary mapping, this handbook is especially timely.

2. PURPOSE OF THIS HANDBOOK

The production of high-quality geologic maps is a complex process involving a wide range of data, software tools, technical procedures, mapping support specialists, review steps, and publication requirements. This handbook provides a comprehensive 'how to' mapping guide that covers each of these topics to clarify the process for map authors. This guide emphasizes the production of planetary geologic maps in a digital, GIS format, because this format is required by NASA PGG for maps beginning in (1) 2011 that are submitted for technical review and (2) 2013 that are finalized for publication. Because of continual changes in data availability and mapping techniques, it is understood that the geologic mapping process must remain flexible and adaptable within time and budgetary constraints. Users are advised to seek the latest edition of this handbook, which will be updated periodically as an appendix to the annual abstracts of the Planetary Geologic Mappers' (PGM) meeting (downloadable at the PGM web page; see below for a complete list of web links). Other updates, including recently published maps, will be posted on the USGS Astrogeology Science Center's (ASC) PGM web page.

First, we describe the steps and methods of map proposal, creation, review, and production as illustrated in a series of flow charts (Figs. 1-4). Second, we include basic formatting guidelines for each map component. Third, we provide a list of web sites for useful information and download.

3. MAP PROCESSING

Planetary geologic maps as supported by NASA and published by USGS are currently released under the 'USGS Scientific Investigations Maps' (SIM) series. In this section, we summarize the process of completing USGS SIM series planetary geologic maps from proposal submission to publication (Figs. 1-4; note that the SIM series was formerly named Geologic Investigations Series and Miscellaneous Investigations Series and both used "I" for the series abbreviation for published maps; all I and SIM series share a common, progressive numbering scheme). These processing steps are subject to change as they are dictated in many cases by higher-level organizational policies, budget constraints, and other circumstances. Planetary geologic mapping support personnel are listed in Section 7; these are subject to change on an annual basis.

a. Proposals. Planetary geologic maps published by USGS have been sponsored largely by the NASA PGG program. Thus, maps submitted to USGS for publication must have been accepted under a NASA PGG grant (see the NASA research opportunities web page) and/or have the approval of the NASA PGG Discipline Scientist. Map publication and printing costs are covered by separate PGG funding and thus are not included in PGG research proposals. The proposal submission deadline is generally during the spring, and selections are usually announced by the following winter (depending on when funds can be released from NASA). Those considering proposing for a grant to perform planetary geologic mapping should visit the USGS Planetary Geologic Mapping web page, where information on current mapping programs and projects, map preparation guidelines, and links to published maps can be found. While a variety of map areas,

scales, and projections are potentially feasible for publication, some issues may make a conceived map untenable for publication (e.g., NASA PGG has a limited budget and multiple and oversized map sheets may be prohibitive in cost). Mappers are highly encouraged to contact the USGS Map Coordinator (MC) regarding the maps to be proposed for prior to proposal submission to ensure that preparation of the desire map base and publication of the final product are feasible. (See table in Section 7 listing PGM personnel names and email addresses). Generally, proposals should address:

1) Digital production: Will the map be generated in GIS software compatible with ESRI's ArcGIS® software (the USGS standard)?
2) Map base: The proposal should include a description and justification of the desired map base that addresses the following questions. What data set is desired for the map base (which forms the map background) and are all the needed data released? Does USGS have the capability to generate the map base with available capability and resources? (Consult with the USGS Map base Specialist to find out.) What other data sets are desired and can they also be imported into the GIS geodatabase? Does the work plan allow for adequate time for USGS to construct the base (usually within 6 months after the USGS is notified by the PGG Discipline Scientist of the proposal's award), depending on complexity?
3) Map printing: At the proposed scale and projection, will the map be oversized (i.e., >40x56 inches)? Will multiple sheets be required for a given map area? (Consult with the USGS Map Coordinator for estimates of potential extra costs.) Proposer should be aware that increased complexity adds considerable time for preparation, review, and publication.
4) Map reviews: Proposers should be prepared to review two other planetary geologic maps for each intended map publication. It is appropriate to budget your time to review maps in each new mapping proposal that you submit.
5) Supplemental digital products: Digital map supplements may be proposed. These can include helpful figures and ancillary GIS raster and vector layers that can greatly enhance the map product but may not fit on the printed map.
6) Additional analyses and products: Detailed and interpretative analyses outside of the scope of the map product may be desired (for example, to test existing and construct new hypotheses, model observations, etc.), but these should be expressed as tasks independent of map generation (best suited for publication in science journals). Maps will no longer contain such material.
7) Attendance at mappers meetings: Proposal budgets must include funding for attendance at the annual Planetary Geologic Mappers' meetings and possible GIS workshops.

b. Map base package *(Fig. 1).* The map base forms the background image (usually in reduced contrast form) upon which the drafted geologic map units, symbols, and nomenclature are superposed. It is a geometrically controlled product that is the fundamental data set upon which map drafting is performed. In some cases, there are adequate data available from a particular data set, but the map base itself does not yet exist when the mapping proposal is submitted. Thus USGS must generate the map base. (In special cases, the proposer may construct the base, with advance permission from the USGS Map Coordinator). Sometimes, data gores can be filled in with other lower-quality yet useful data. Even if a desirable data set is released, there may be as-yet unresolved issues in radiometric and geometric processing and/or in data volume that prevent

USGS from producing a map base with that particular data set. For example, the number and volume of images may be too large to generate a map base with available resources. Alternatively, such data may be readily viewable as individual frames by using image-location footprints as GIS shapefiles having web links to data repositories. Other ancillary data in various forms may be provided at the request of the author if there is a demonstrated need for the data and if they can be readily integrated into a GIS geodatabase. The USGS Map base Specialist is tasked by PGG to produce the digital map base and ancillary data products and to satisfy reasonable and tractable mapping requests by map authors.

Typically, the USGS must generate several map base packages in a given year; these are generally compiled in order of increasing complexity and/or areal extent. Map bases for Venus quadrangles are usually the simplest and are thus generated first during each funding cycle. Map bases for Mars quadrangles may require mosaicking of many individual image frames that must be compared visually and stacked in order of quality and then collectively processed for tone balance. More complex maps may require several months to complete after USGS is notified to produce them.

For GIS mapping projects, the USGS GIS Project Specialist generates a GIS map template after quality-checking and collating GIS data layers. The template includes map bases and a map-ready geodatabase with pre-populated symbols. These products are compiled and delivered using ESRI's ArcGIS® software. (USGS can import shapefiles produced from other software in some cases, but authors should consult with USGS GIS specialists *prior* to mapping to ensure that their map files will be usable.) In addition, a variety of GIS thematic maps can be downloaded and imported into the project, as well as other GIS tools, as administered by the USGS GIS PIGWAD Specialist (see PIGWAD web site). For Mars, Moon, and Venus maps, the mapping projects will include a stand-alone DVD volume (or equivalent compressed, digital file) of global datasets that can be incorporated into the project-specific GIS template.

c. Digital mapping. Mappers presently are mapping mostly in Adobe Illustrator or ArcGIS. For proper building of polygons in Illustrator layers, see the help web site. For ArcGIS, contact and structure mapping is generally done first as polyline shapefiles. Vertex snapping is important for later generation of polygons. Point shapefiles can be used to indicate unit identification for each outcrop. At an advanced stage in mapping, the contacts can be cleaned, smoothed, and converted to polygons. We recommend that the final GIS linework have a vertex spacing of ~0.3 mm at map scale (equivalent to 300 m for a 1:1,000,000-scale map). We also recommend that a consistent scale is used to digitize linework, usually a factor of 2 to 5 larger than the published map to ensure adequate precision but not overkill (e.g., map at 1:200,000 to 1:500,000 for a 1: 1,000,000 map). GIS tools can be applied to generalize and smooth linework to achieve the desired result, such as rounded corners. Also, outcrops should generally be at least 2 mm wide at map scale. Reasonably sized cutoffs should also be defined for line feature lengths (for example, 1 or 2 cm long at map scale). Point features can be used to show the distribution of important features such as craters and shields that are too small to map (their size ranges should be indicated). For clarity and completeness, we encourage the compilation and summary of digital mapping approaches and settings for inclusion in the map text.

d. Mappers' meetings and GIS workshops. These meetings are announced by the GEMS Chair and are also posted on the NASA Mars Exploration Program Analysis Group (MEPAG) calendar web page and the Planetary Exploration Newsletter (PEN) calendar of events. While under

active NASA mapping grants, mappers are expected to submit and present abstracts for the Annual Meeting of Planetary Geologic Mappers typically held in late June each year. Others are encouraged to attend as a means to benefit from various aspects of the program. At these meetings, mappers demonstrate their progress and discuss mapping issues and results. Preliminary map compilations are also displayed and informally reviewed by other attendees during poster sessions. In addition, programmatic issues, mapping standards and guidelines, and related scientific issues are presented and discussed. Expert-led GIS workshops and/or geologic field trips to nearby localities of interest are commonly attached to the mappers' meeting. When possible, associated GIS workshops are held prior to or immediately following mappers' or other appropriate workshops (and occasionally as stand-alone meetings) throughout the year. These GIS workshops are customized to assist planetary geologic mappers in developing proficiency in GIS software and tools as applied toward planetary geologic maps published in the USGS SIM series. Abstracts and related reports are published in an abstract volume in either a USGS or NASA publication series, and they can be downloaded from the USGS Planetary Geologic Mappers web page.

e. Submission and technical review *(Fig. 2).* Mappers are expected to prepare maps in accordance with guidelines herein (see Map Contents section below) as well as with those posted on the USGS Planetary Geologic Mappers web page. Once the map is produced according to required guidelines, it is submitted in digital form to the USGS Map Coordinator (MC). The MC reviews the map submission for completeness. If the map is incomplete, the MC returns the map to the corresponding author for revision. If the map is complete, the MC assigns two reviewers, with the approval of the GEMS Chair. The MC fills out an Information Product Review and Approval Sheet (IPRAS; Figure 5) in which all reviewers are listed. Both reviewers must approve (in rare cases, a third reviewer may be assigned to help resolve reviewer conflicts). Maps are returned to authors one or more times until review comments are adequately addressed as determined by the MC. The MC may adjudicate some issues that arise (for more challenging cases and in cases of potential conflict of interest, the MC consults with the GEMS Chair). Normally, initial map reviews are expected to be returned within 1 to 2 months and any additional reviews within 2 weeks.

f. Map Coordinator review *(Fig. 3).* Once the technical reviews are complete, the MC, with assistance from other USGS specialists as needed, performs a review that ensures that (1) the map conforms to the proper scale and projection, (2) final technical reviewer comments were adequately addressed, (3) map materials follow PSC author submission checklist guidelines, (4) map information conforms to established USGS and GEMS conventions, (5) nomenclature is sufficient, given what the map text discusses, and (6) stratigraphic inferences are properly conveyed and supported by observations. Map authors respond to the MC review comments and resubmit the map package. Name requests for mapped or referenced features are made by the author as needed using the online form; these can be made anytime during the mapping process. New name proposals may take 4 to 8 weeks or longer for approval. Proposed names *may not be used* in publications until they have been approved by the International Astronomical Union.

g. Nomenclature review *(Fig. 3).* The USGS Nomenclature Specialist then reviews the map to assess whether the use of nomenclature accurately reflects the current terminology in the IAU Gazetteer of Planetary Nomenclature. The map itself should have a nomenclature layer that

presents all available formal names. Note that some exceptions to this naming requirement may apply in special situations; for example, overly small named features may exist only for a sub-region of the map. (For a brief review of how IAU nomenclature is being managed and developed in the case of the Moon, see Shevchenko and others (2009)).

h. USGS metadata preparation *(GIS maps only; Fig. 3).* Metadata is the necessary ancillary documentation that describes each GIS layer in a geologic map, including rationale, authorship, attribute descriptions, spatial reference, and other pertinent information as required by the metadata standard. This information is archived with and becomes part of the map layer. The USGS GIS specialists will oversee metadata preparation and will tap authors for information when needed. Metadata for a map is comparable to the documentation required by NASA's Planetary Data System for digital planetary data, but it is created specifically for geospatial data sets. USGS GIS specialists will oversee incorporation of metadata for the mapped layers according to USGS publication standards and Federal Geographic Data Standards (FGDC). Metadata and readme files are required when the manuscript is submitted to PSC for publication. The PSC Digital Map Editor reviews general information (such as correct USGS contact information, information in appropriate fields, etc.).

i. ***USGS Publications Services Center (PSC) editing and production*** *(Fig. 3).* The PGM Administrative Specialist works with other USGS staff to ensure that the product is complete for PSC processing, and sends the product and review materials on CD or DVD and hardcopy form according to PSC guidelines (see PSC author submission and Astrogeology submission checklist web pages). PSC contacts the Map Coordinator and estimates costs for PSC editing and production and printing through a contractor selected by the Government Printing Office (GPO). Based on available funds for these costs, maps are put into the editing and production queue for the current or next fiscal year. A USGS PSC Map Editor then is assigned to the map and works with the author to produce the edited copy. Next, the map goes to the PSC Production Cartographer to produce a printable version in Adobe Illustrator®. The author has an opportunity to proof the map before it is finalized for publication; however, no significant content changes are allowed (authors will be responsible for proofing non-standard items such as special characters (small caps, diacriticals, etc.)). Also, if there is room on the map, the author may be notified by PSC that appropriately sized tables and/or figures can be shifted from the pamphlet and/or digital supplement to the map.

j. ***Map printing and web posting*** *(Fig. 3).* The PSC Production Cartographer submits the completed map to GPO for bid and printing. Generally, 100 copies of the map are sent to authors, and 300 copies are received by the USGS Regional Planetary Image Facility (RPIF) in Flagstaff, Arizona, for distribution to other RPIFs and PGG investigators on a mailing list provided by the PGG Discipline Scientist. Extra copies are kept by the USGS RPIF and can be requested by investigators through the Map Coordinator. Digital files of map materials are posted by the PSC Web Master on a USGS server for downloading, including: (a) PDFs of all printed materials produced by PSC, (b) author-provided Adobe Illustrator® files, and (c) GIS database, metadata, readme, and additional data files provided by PSC (a copy of these final files is provided to the author). Minor corrections and cosmetic improvements of the digital map product can be generated by authors as a new digital version of the map and submitted to the Map Coordinator for review, editing, and posting (however, consult first with the MC before

initiating such a product, as authors have to pay for this service). Minor, non-science changes are shown by a decimal number, for example, correcting spelling of a name throughout the publication or correcting a number in a table would generate a version upgrade from 1 to 1.1. Changing science on the map or adding data would generate a version upgrade from 1 to 2.

4. MAP CONTENTS

Planetary geologic maps in the past have varied widely in content and arrangement, largely at the preference of map authors. Though some flexibility is desirable to convey the geologic data and interpretation in ways that are suitable for each particular geologic map, unnecessary divergences and details come at a cost. Highly complex and uniquely assembled maps require more effort from mappers, reviewers, cartographers, and editors to prepare the map for publication. This handbook, under the direction of GEMS, defines a basic content template for planetary geologic maps, so that they become more uniform in format and thus simpler for users to assimilate and use as well as easier and cheaper to produce. In addition, following established USGS style guidelines in initial text preparation will result in less editing and revision. Mappers should refer to recently published geologic maps for examples of proper style in terms of spelling, word usage, grammar, and formatting, as well as the USGS Tips web page that addresses common formatting and editing issues. *Doing so will save time and effort!*

a. Map sheet components. To keep the printed map sheet as small as possible, authors are requested to keep map components to a minimum.

1) Map: Of course, the map itself is the fundamental product. It should be complete with map base at correct scale and projection, outcrops clearly colored and labeled, and structures consistently mapped. (The PSC Production Cartographer will cosmetically fine tune these elements, as well as add the map scale and grid and any notes on base, but cannot be expected to complete or decipher any aspects prepared incompletely or unclearly.) To avoid clutter, highly detailed information may be included in the digital product as a layer (see the digital data products section below). Printed maps normally must be contained within a single sheet having a maximum size of 40 x 56 inches (larger or additional sheets result in significant additional printing costs; authors desiring multiple or oversized sheets may choose to pay for the extra costs, with prior approval via the Map Coordinator).
2) CMU/SMU: Each map will include a Correlation or Sequence of Map Units (CMU/SMU) chart. The chart is organized horizontally left to right showing the following elements:
    a) *Stratigraphic column*: Formal or informal stratigraphic divisions (where available).
    b) *Map units*: Units can be arranged in groups according to location or unit type. Units that form groups closely related in provenance and/or definitive characteristics may have similar unit names and symbols (e.g., Utopia Planitia 1 unit, Utopia Planitia 2 unit) and should be juxtaposed horizontally and/or aligned vertically in the CMU/SMU. Also, younger units and unit groups divided by region or morphologic type generally are placed toward the left, and older and diverse (e.g., ‘undivided highland materials’) and widespread (e.g., ‘crater material’) units are placed to the right. If more complex relations are portrayed, such as unconformities, time transgressive contacts, and other juxtaposition relations, they may be explained using

a key (e.g., Young and Hansen, 2003; see also GEMS guidelines for Venus SMUs and Appendix D in Tanaka and others, 1994).

c) *Major geologic events (optional)*: Juxtaposed chart to the right of the CMU/SMU showing inferred episodes of geologic activity (such as deposition, erosion, deformation, etc.; e.g., Tanaka and others, 2005).

d) *Crater density scale (where data are available)*: Cumulative density of craters larger than specified diameter(s) (e.g., Tanaka and others, 2005). Supporting text should be provided in the 'age determinations' text section (see below).

3) Nomenclature: Published USGS maps are expected to display nomenclature completely (with minor exceptions, such as features that are spatially insignificant at map scale) and accurately according to the International Astronomical Union (IAU) Gazetteer of Planetary Nomenclature. For adding nomenclature labels in ArcGIS, see tutorial on Annotation & Nomenclature. Whenever named features are mentioned anywhere in the map, including the text, they should be properly capitalized and spelled (including the Latin plural forms for descriptor terms). In this regard, the IAU recommends that the initial letters of the names of *individual* astronomical objects be capitalized (e.g., "Earth is a planet in the Solar System"). Also, 'crater' is not capitalized: "Mie crater occurs in northeastern Utopia Planitia, north of Elysium Mons and Albor and Hecates Tholi." Informal terrain terms (e.g., 'Utopia basin' and 'dark lava plains') should not be capitalized and non-IAU-approved proper names should not be introduced. If a feature needs a name or name redefinition, the USGS Nomenclature Specialist can assist with a name proposal. Nomenclature needs can be addressed at any time over the course of mapping, but keep in mind that it generally takes one to two months for a name to be approved. Informal names should be identified clearly as such (e.g., 'the feature dubbed Home Plate…'). Formal names proposed to the IAU should not be used in maps or publications until the approval process is complete. Name proposals should be based on the need to single out for identification as-yet unnamed features in the map area (a need for names for use in journal articles may also qualify). Consult with the USGS Map Coordinator and Nomenclature Specialist when nomenclature issues arise.

4) Geologic sections: A limited number of geologic sections can be shown on the map. These must be drafted in ArcGIS® or Illustrator®. Unit colors and symbols and other symbology and nomenclature should be identical to those on the map. The sections should be at the same horizontal scale as the map, and the amount of vertical exaggeration should be indicated and minimized.

5) Map symbol legend: The legend is a chart on the map sheet that includes all line, point, and stipple symbols, with a feature type name and brief explanation (see recently published maps for examples). Where possible, the features should follow official, published USGS cartographic symbols (see FGDC web page as well as examples recently published in planetary geologic maps). The Production Cartographer will assist with converting symbols into final forms when necessary (e.g., when converting from GIS format to Illustrator®). See Tanaka and others (in press) for a discussion of types of tectonic structures found on particular planetary bodies.

6) Unit legend: The unit legend is a list of map units organized by the unit groupings as illustrated graphically in the CMU/SMU. The units include a box showing the unit color (perhaps overlying the base) and are ordered from youngest to oldest exactly as in the Description of Map Units (DMU; see Tanaka and others, 2005). The only text shown is

the unit name (this is a new policy); all unit information is included in the DMU table. However, if the DMU can be included on the map sheet, the unit legend will not be necessary, and colored unit boxes will be added to the DMU.

7) Selected figures, tables, and text: During the map sheet layout construction phase, the USGS Production Cartographer may determine that there is room for additional material on the map sheet, and he/she will notify the author. The author then selects appropriate figures and tables from already submitted material that will fit. For smaller maps with brief text, all the material may fit on the map sheet (e.g., Price, 1998).
8) Map envelope: The map sheet (sometimes accompanied by a pamphlet with descriptive text) is contained within an envelope. In addition to standard publication citation information, the envelope may include an index map showing the map region typically on a hemispherical view of the planet. Digital data generally will be provided on-line only, as inclusion of a DVD in the map envelope is cost prohibitive.

b. Text components. Text will appear in a pamphlet or, when room is available, on the map sheet. Note that unit and feature descriptions are to be put into tables (i.e., delimited text files or other GIS compatible formats), which will encourage concise presentation and easier conversion to metadata for GIS maps.

1) Introduction and background: This section of the map text introduces the map area, including its geography and general geologic setting. It also acknowledges previous work for the map area, particularly any published geologic maps. However, it should not expound on existing scientific controversies. The rationale and purpose of the map are also described here. If the description of geography is extensive, a separate section devoted to it may be provided.
2) Data: Data sets should be described that were used to construct the map base and that were needed to identify and discriminate elements of map units and features critical to the mapping. Additional data sets that were consulted should also be mentioned, along with how they benefitted the mapping (or not). Relevant parameters and descriptions that affect mapping-related understandings should be stated, including what particular subsets of data were particularly useful for mapping; examples of such include pixel or other spatial resolution, solar incidence angle, solar longitude, wavelength bands, night vs. day time acquisition of thermal data, look-direction for synthetic aperture radar data, etc. Many of the most useful data sets for planetary mapping are available from the USGS PIGWAD and Map-a-Planet web sites. Where appropriate, key data sets may be shown in supplemental figures or as GIS layers as digital products. Also, data measurements applicable to the mapping might be shown in tables (e.g., morphometric measurements of landforms, radar properties of map units, etc.).
3) Mapping methods: A variety of techniques can be employed in showing unit names, groupings, symbols, colors, and contact and feature types. The actual methods used should be clearly described and consistently applied.
    a) *Unit names:* Popular approaches to unit naming include morphologic type (e.g., 'corona material,' 'crater material'), geographic names ('Utopia Planitia material'), relative age/stratigraphic position ('lower/older crater material') and combinations thereof. Closely-related units (e.g., units in a sequence or morphologic variations of otherwise similar units) may be mapped as members (e.g., 'lower member of the

Utopia Planitia material') or units having names showing their close association with other units ('Utopia Planitia 1 unit, Utopia Planitia 2 unit…').

b) *Unit groups*: Units commonly are grouped by their geographic occurrence (e.g., 'highland materials') or morphologic type (e.g., 'lobate materials'). Capitalize only proper nouns in unit and group names (e.g., 'Alba Patera Formation,' 'Utopia basin unit,' 'western volcanic assemblage').

c) *Unit symbols:* These can indicate chronostratigraphic age (e.g., 'A' for 'Amazonian'), unit group (e.g., 'p' for 'plains materials'), specific unit designations (including morphology, albedo/reflectivity, and associated geographic feature name), and unit member (commonly as subscripts; may include numbered sequences, as in 'member 1,' 'member 2'…). Small capital letters have been used for unit groupings (e.g., 'E' for 'Elysium province'). Also, capital letters have been used for geographic names on Venus (e.g., 'fG' for 'Gula flow material'). On the geologic map, some symbols may be queried to show that the unit assignment is highly uncertain. For adding unit symbols in ArcGIS, see tutorial on Annotation & Nomenclature.

d) *Unit colors:* Unit color hues may be applied according to suitable precedents, or they may reflect the group they are in (e.g., warm colors for volcanic materials, cool colors for sedimentary rocks, yellows for crater materials, browns for ancient highland materials), or their relative age using a color spectrum for scale (e.g., Tanaka and others, 2005). Also, color saturation can reflect general areal extent of unit outcrops (low saturation for extensive units and high saturation for small units), which assists in finding smaller units. Colors must follow USGS publication guidelines, which ensure that they will print well. Generally, colors should not be changed after submission to PSC.

e) *Contact types:* The quality of contacts varies considerably on most maps. Definitions for contact types are not precisely expressed in most geologic maps, including terrestrial ones. Thus, contact types should be used as consistently as possible for a given map and they should also be defined (e.g., Tanaka and others, 2005). For example, (1) a 'certain' contact may indicate that the contact is confidently located; (2) an 'approximate' contact indicates that the confidence is not well defined (perhaps due to data quality or the surface expression of the juxtaposed units being unclear); (3) a 'buried' contact indicates that surficial material buries the contact but morphologically the contact is still traceable, although subdued; (4) a 'gradational' contact means that the contact is broadly transitional at map scale (which may reflect a gradually thinning, overlapping unit or a unit margin expressed by gradually thinning out of numerous outcrops too small to map, as in the margin of a dune field or of a field of relict knobs); and (5) an in 'inferred' contact, which may be used to delineate map units where the validity of the map unit or distinction between the units is hypothetical (e.g., the contact between the Vastitas Borealis interior and marginal units in Tanaka and others (2005) was drawn as inferred, because the marginal unit may be or may not be the same material as the interior unit).

f) *Feature types:* Mapped geologic features involving line and point symbols and stipple patterns are listed in the map symbol legend. Also, the feature table (see below) provides a format to systematically describe the features and their geologic relationships and interpretations.

g) *Drafting parameters:* Note minimum sizes of outcrops and linear features mapped, as well as the size range of features mapped with point symbols. For GIS maps, note the vertex spacing, digitizing scale, line smoothing methods, and any other important digital controls and processing applied.

4) Age determinations: Techniques and reliability of relative and absolute-age determinations for map units should be discussed, as they vary widely according to data quality and preservation and exposure state of key features. These include superposition and cross-cutting relations and crater densities. For quantitative approaches, error analysis should be included. As absolute-age models are based both on cratering theory, lunar sample dating, and empirical data on bolide populations, they are subject to high uncertainty. Appropriate references should be used throughout. Where possible, crater statistics can be summarized in the unit stratigraphic relations table described below.
5) Geologic history: A summary of the geologic history of a map region serves to provide a context for the entire geologic map and is encouraged. The synthesis is intended to be a brief yet informative review of unit development, tectonic deformation, and erosional and other modifications of the surface and shallow subsurface, with first-order interpretations on geologic and climate process histories as appropriate. However, lengthy considerations of previous and new hypotheses and other interpretive discussions that go beyond immediate mapping results and implications are to be left out.
6) References: The list of references and reference citations in the text follows USGS style guidelines; see published maps and this handbook for examples. Note that for more than 5 authors in a reference, only the first 3 are listed and "and x others" substitutes the number of unlisted authors for their names (see reference for Tanaka and others, 1994). Also, note formats for commonly used conference publications in the reference list below, as follows: *American Geophysical Union meeting abstract*: Banerdt, 2000; *Lunar and Planetary Science Conference abstract*: Skinner and Tanaka, 2003; *NASA Technical Memorandum abstract*: Grant, 1987; *edited NASA Special Publication*: Howard and others, 1988; *book chapter*: Wilhelms, 1990; *web-posted geologic map*: Young and Hansen, 2003.
7) DMU table: To simplify map texts, the Description of Map Units (DMU) table now forms a concise description of the map units, their stratigraphic relations, interpretation, and other pertinent information (previously, most planetary geologic maps provided a separate, stratigraphic narrative resulting in redundant information in the two sections). The DMU table will consist of four columns of information for each unit:
   a) *Unit symbol and name*
   b) *Definition:* Defining, primary characteristics essential to identifying and delineating each map unit from all others. In most cases, 2 to 5 characteristics define a unit, including aspects such as morphology/texture, albedo/reflectivity/spectral character, stratigraphic position or relative age, relative elevation, regional occurrence, and source feature. Where not obvious, mention the critical data sets. Type localities are optional and should be placed at the end of the definition.
   c) *Additional characteristics:* Brief discussion of additional aspects such as relation to units in previous and adjacent maps, local anomalies in unit character, and prominent secondary features (that may obscure or be partly controlled by primary features).
   d) *Interpretation:* Interpreted unit origin focusing mainly on origin of primary features and stratigraphic relationships; secondary features may also be discussed as they

relate to the unit (i.e., fracture systems related to contraction, compositional information relating to surface alteration, etc.); and model crater absolute age (optional). As maps are meant to be enduring products, the interpretations should be inclusive of all reasonably possible alternatives, and wording should reflect the degree of uncertainty (e.g., 'lava flows' vs. 'possible lava flows' vs. 'uncertain; may be lava flows, pyroclastic or impact-related deposits, or tabular sedimentary deposits').

8) Unit stratigraphic relations table: For each unit, show total areal extent in map area and relative-age relations (younger, older, similar in age, or younger and older) for every adjacent unit. Where crater density data are available, show helpful crater density values, including standard deviations. Additional columns can be used for assigned chronologic units and model crater absolute ages. Use footnotes to explain abbreviations used and other important details.
9) Feature table(s): Additional tables can be added as needed to describe the characteristics, relationships, and interpretation of other mapped features, such as tectonic structures, volcanic features, erosional and modificational features, surficial materials, and impact craters.
10) Additional tables: Other useful map information can often be summarized in a table for easier reference and comparisons, such as quantitative aspects of map units, their appearance in specific image data sets, etc.
11) Figures: Figures typically will not be included in the pamphlet. See digital data and map sheet components sections for formatting and possible placement.
12) Digital supplement table: All materials appearing in a digital supplement should be listed in a summarized fashion, such as data and mapping layers, measurements and statistics, and figures.

c. Digital data products. Authors are encouraged to make use of digital repositories for useful ancillary data products and figures. When in GIS form, the products are more accessible to researchers via digital tools and methods. Map authors should follow all guidelines, so that modifications using the original digital files by the USGS Production Cartographer and perhaps other specialists will be minimal in order to meet publication standards.

1) Supplemental figures: These may include, for example, a few reduced-scale images of the map region showing key data sets, distributions of key features, contact relationships, and geologic cross sections. However, additional, digital-only figures can be used generously to show unit characteristics, superposition relations, crater size-frequency distributions, and secondary features as desired. Images, image mosaics, and thematic maps should include in the caption or on the figure as appropriate the data source, type, and resolution (e.g., 'THEMIS daytime infrared mosaic at 100 m/pixel'), solar/incoming energy incidence angle and azimuth, north direction, scale bar (or image width), and latitude/longitude grid. Figures should be prepared at intended publication size with consistent label font types and sizes.
2) GIS layers: For GIS maps, authors can construct raster and vector data layers that are georegistered to map bases as digital-only supplements. These can be used to effectively show ancillary data sets and detailed feature mapping.

3) GIS maps: USGS GIS specialists will convert map files and supplemental figures and GIS layers as needed to conform to USGS geodatabase and FGDC metadata standards. GIS data supplements will be served via the web.
4) On-line map: The map, text, and supplemental figures will be converted to pdf format and made available for download via a USGS server and web page by the USGS PSC. GIS products, if available, will also be included for download.

5. REFERENCES

Banerdt, W.B., 2000, Surface drainage patterns on Mars from MOLA topography: Eos, Transactions of the American Geophysical Union, fall meeting supplement, v. 81, no. 48, Abstract #P52C–04.

Grant, J.A., 1987, The geomorphic evolution of eastern Margaritifer Sinus, Mars, *in* Advances in planetary geology: Washington, D.C., National Aeronautics and Space Administration Technical Memorandum 89871, p. 1–268.

Hackman, R.J., 1962, Geologic map and sections of the Kepler region of the Moon: U.S. Geological Survey Miscellaneous Geologic Investigations I-355 (LAC-57), scale 1:1,000,000.

Hansen, V.L., 2000, Geologic mapping of tectonic planets: Earth and Planetary Science Letters, v. 176, p. 527-542.

Hare, T.M., Kirk, R.L., Skinner, J.A., Jr., and Tanaka, K.L., 2009, Chapter 60: Extraterrestrial GIS, *in* Madden, Marguerite, ed., Manual of Geographic Information Systems: Bethesda, The American Society for Photogrammetry and Remote Sensing, p. 1199-1219.

Howard, A.D., Kochel, R.C., and Holt, H.E., eds., 1988, Sapping features of the Colorado Plateau—A comparative planetary geology field guide: Washington, D.C., National Aeronautics and Space Administration Special Publication, NASA SP-491, 108 p.

Price, K.H., 1998, Geologic map of the Dao, Harmakhis, and Reull Valles region of Mars: U.S. Geological Survey Geologic Investigations Map I-2557, scale 1:1,000,000.

Shevchenko, V., El-Baz, F., Gaddis, L., and 5 others, 2009, The IAU/WGSPN Lunar Task Group and the status of lunar nomenclature [abs.], *in* Lunar and Planetary Science Conference XV: Houston, Tex., Lunar and Planetary Science Institute, Abstract #2016, [CD-ROM].

Skinner, J.A., Jr., and Tanaka, K.L., 2003, How should planetary map units be defined? [abs.], *in* Lunar and Planetary Science Conference XXXIV: Houston, Tex., Lunar and Planetary Science Institute, Abstract #2100, [CD-ROM].

Tanaka, K.L., Moore, H.J., Schaber, G.G., and 9 others, 1994, The Venus geologic mappers' handbook: U.S. Geological Survey Open-File Report 94-438, 66 pp.

Tanaka, K.L., Skinner, J.A., Jr., and Hare, T.M., 2005, Geologic map of the northern plains of Mars: U.S. Geological Survey Science Investigations Map 2888, scale 1:15,000,000.

Tanaka, K.L., Anderson, R., Dohm, J.M., and 5 others, in press, Planetary structural mapping, *in* Watters, T., and Schultz, R., eds., Planetary Tectonics: New York, Cambridge University Press.

Varnes, D.J., 1974, The logic of geological maps, with reference to their interpretation and use for engineering purposes: U.S. Geological Survey Professional Paper 837, 48 pp.

Young, D.A., and Hansen, V.L., 2003, Geologic map of the Rusalka Planitia quadrangle (V–25), Venus: U.S. Geological Survey Geologic Investigations Series, I–2783, scale 1:5,000,000 [http://pubs.usgs.gov/imap/i2783/].
Wilhelms, D.E., 1972, Geologic mapping of the second planet: U.S. Geological Survey Interagency Report, Astrogeology, v. 55, 36 pp.
Wilhelms, D.E., 1990, Geologic mapping, *in* Greeley, R, and Batson, R.M., eds., Planetary Mapping: New York, Cambridge University Press, p. 208-260.

6. USEFUL WEB PAGES

FGDC (Federal Geographic Data Committee) Digital Cartographic Standard for Geologic Map Symbolization: http://ngmdb.usgs.gov/fgdc_gds/geolsymstd.php
IAU Gazetteer of Planetary Nomenclature home page: http://planetarynames.wr.usgs.gov/
IAU Gazetteer of Planetary Nomenclature descriptor terms: http://planetarynames.wr.usgs.gov/jsp/append5.jsp
IAU Gazetteer of Planetary Nomenclature feature name request form: http://planetarynames.wr.usgs.gov/jsp/request.jsp
NASA MEPAG calendar: http://mepag.jpl.nasa.gov/calendar/index.html
NASA research opportunities: http://nspires.nasaprs.com
USGS Planetary Geologic Mapping: http://astrogeology.usgs.gov/Projects/PlanetaryMapping/
USGS Planetary Interactive GIS on-the-Web Analyzable Database (PIGWAD): http://webgis.wr.usgs.gov/
USGS Map-a-Planet: http://www.mapaplanet.org/
USGS PSC author submission checklist for planetary maps: http://astrogeology.usgs.gov/Projects/PlanetaryMapping/guidelines/PSC_author_checklist_7-20-09.pdf
USGS Astrogeology manuscripts to PSC submission process: http://astrogeology.usgs.gov/Projects/PlanetaryMapping/guidelines/AstroSubmitProcess_june2009.pdf
USGS tips and information for preparation of astrogeology maps: http://astrogeology.usgs.gov/Projects/PlanetaryMapping/guidelines/preparationTips.pdf
USGS instructions on building polygons in Illustrator: http://astrogeology.usgs.gov/Projects/PlanetaryMapping/guidelines/layersexample_small.pdf

7. PLANETARY GEOLOGIC MAPPING SUPPORT PERSONNEL

Position/Function	Name	Email	Institution
Map Coordinator	Ken Tanaka	ktanaka@usgs.gov	USGS ASC
GIS Data Specialist	Trent Hare	thare@usgs.gov	USGS ASC
GIS Project Specialist	Jim Skinner	jskinner@usgs.gov	USGS ASC
Map base Specialist	Bob Sucharski	bsucharski@usgs.gov	USGS ASC
Nomenclature Specialist	Jen Blue	jblue@usgs.gov	USGS ASC
PGM Administrative Specialist	Jen Blue	jblue@usgs.gov	USGS ASC
Regional Planetary Image Facility Director	Justin Hagerty	jhagerty@usgs.gov	USGS ASC
Regional Planetary Image Facility Manager	David Portree	dportree@usgs.gov	USGS ASC
Digital Map Editor	Jan Zigler	jzigler@usgs.gov	USGS PSC
Production Cartographer	Darlene Ryan	dryan@usgs.gov	USGS PSC
Map Submission Editor	Carolyn Donlin	cdonlin@usgs.gov	USGS PSC
GEMS Chair	Leslie Bleamaster	lbleamas@psi.edu	NASA PGG
Discipline Scientist	Michael Kelley	Michael.S.Kelley@nasa.gov	NASA PGG

8. ABBREVIATIONS

ASC	Astrogeology Science Center (part of USGS)
CMU	Correlation of Map Units
DMU	Description of Map Units
FGDC	Federal Geographic Data Committee
GEMS	Geologic Mapping Subcommittee (of PCGMWG)
GIS	geographic information system
GPO	Government Printing Office
IAU	International Astronomical Union
MC	Map Coordinator
NASA	National Aeronautics and Space Administration
PCGMWG	Planetary Cartography and Geologic Mapping Working Group (part of PGG)
PEN	Planetary Exploration Newsletter
PGG	Planetary Geology and Geophysics Program
PGM	planetary geologic mapping
PIGWAD	Planetary Interactive GIS on-the-Web Analytical Database
PSC	Publications Services Center
SMU	Sequence of Map Units
USGS	U.S. Geological Survey

Figure 1 - GIS MAPPING TEMPLATE PREPARATION

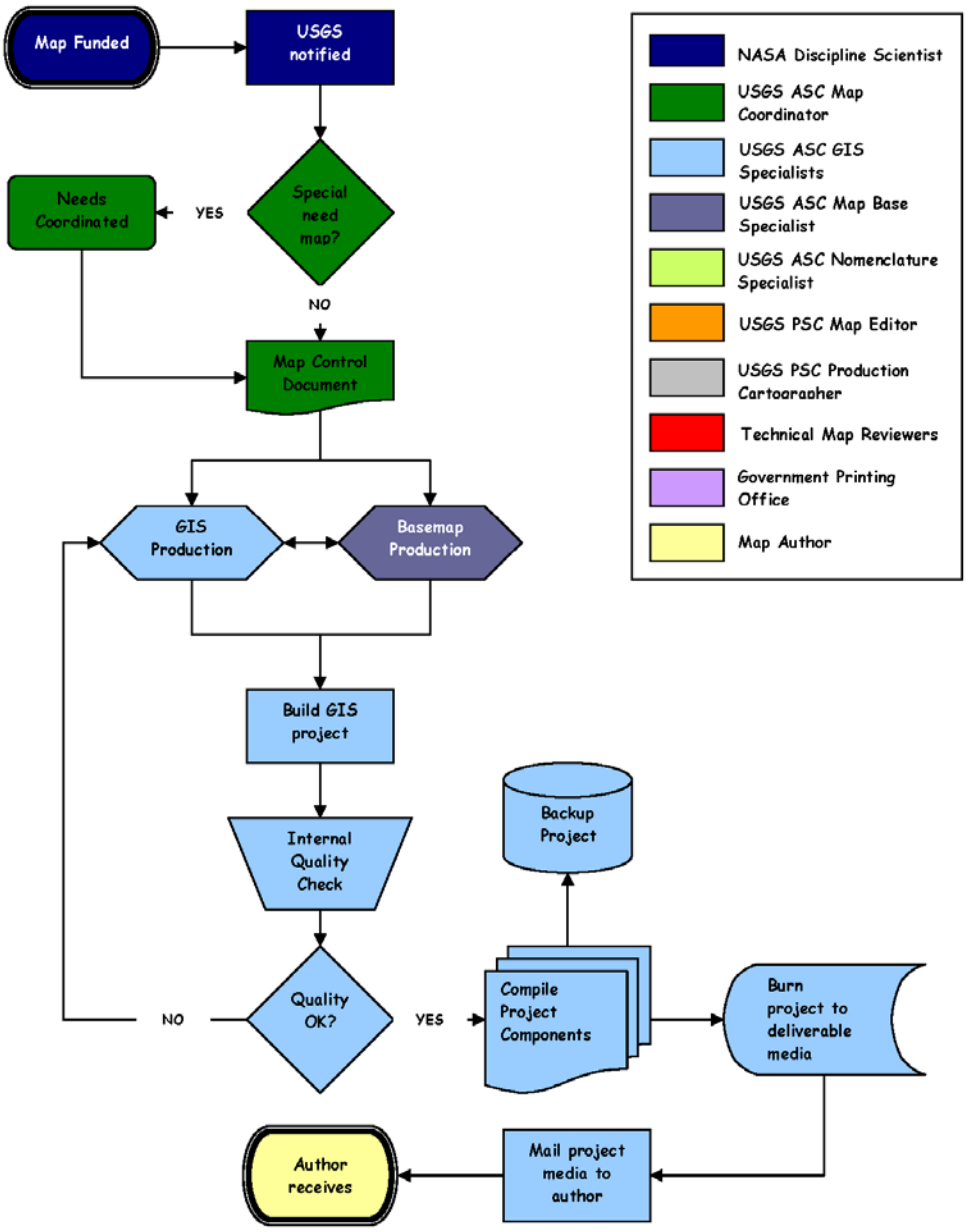

Figure 2 – SUBMISSION AND TECHNICAL REVIEW

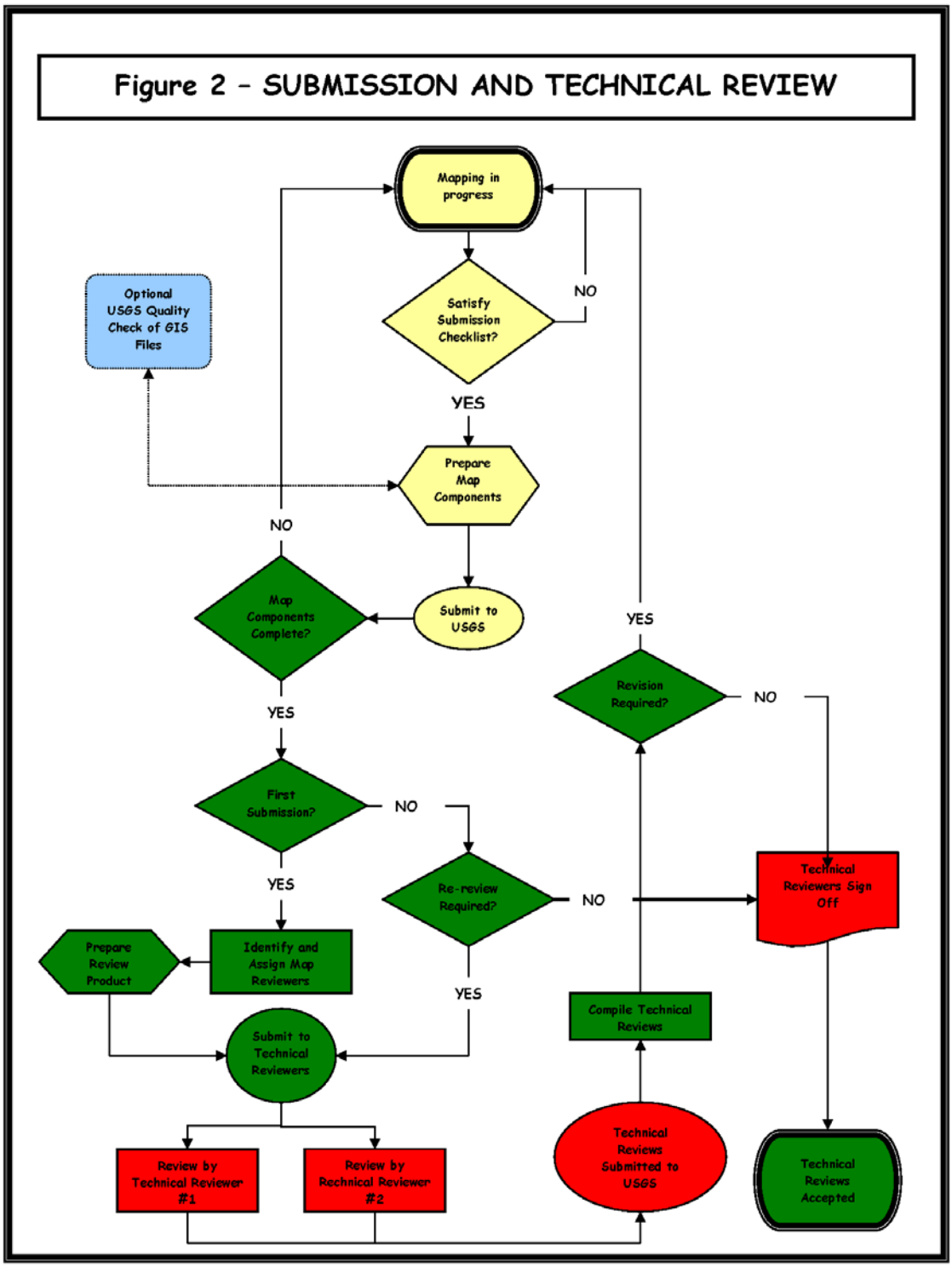

Figure 3 – USGS REVIEW AND PRODUCTION

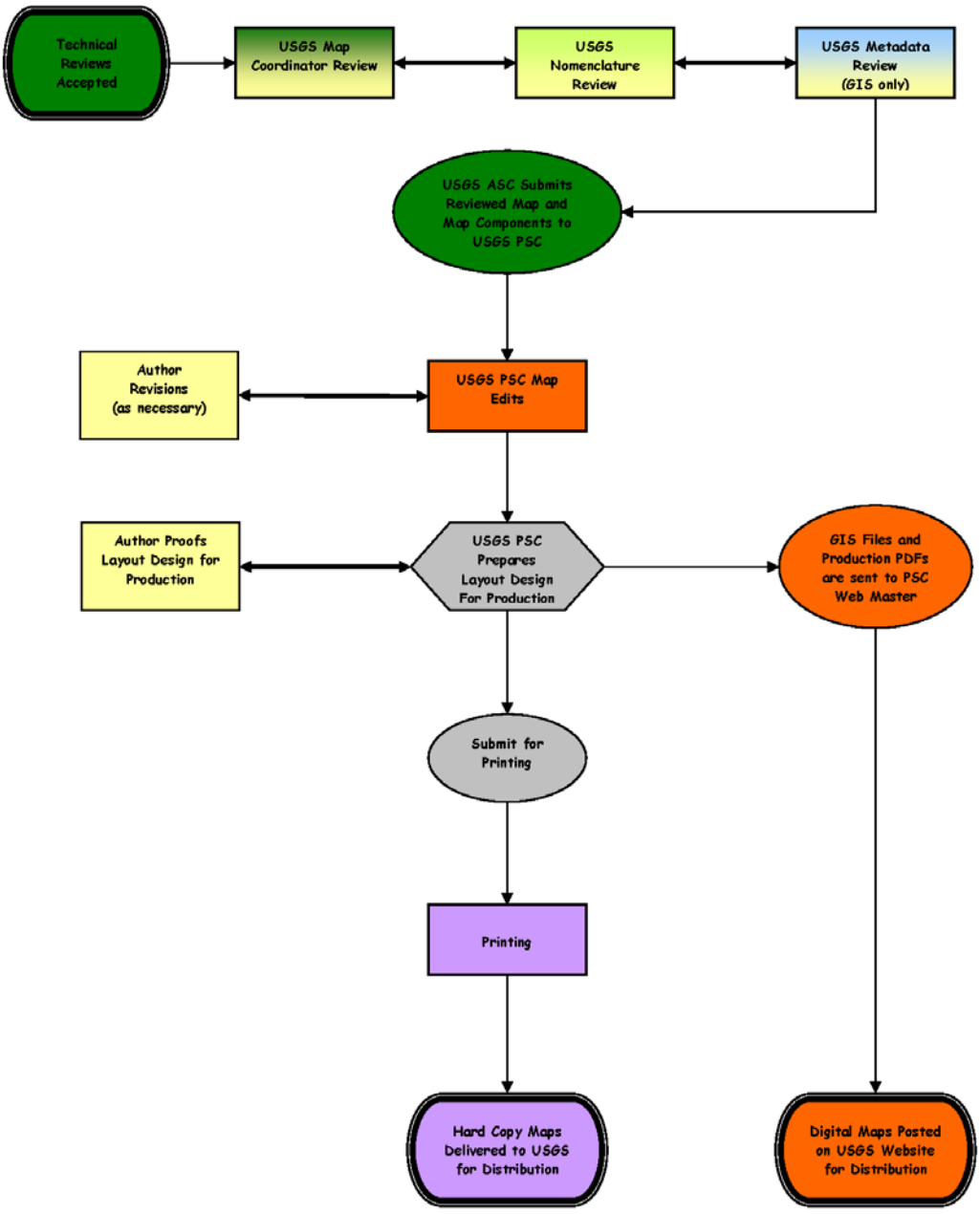

Figure 4 – FLOWCHART SYMBOL DEFINITIONS

Symbol	Symbol Name	Symbol Description and Example Activity
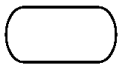	Terminator	Terminators show the start and stop points in a process flow. *A proposed map is accepted for funding.*
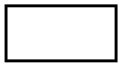	Process	A process or action step, perhaps comprised of multiple segmented actions. *Layout and proofing of final map.*
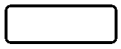	Alternate Process	A process or action step that is an alternate (or option) to normal process flow. *Preparation of non-standard map base.*
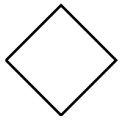	Decision	Indicates a critical question or branch in the process flow. *Does the submitted map adhere to submission requirements?*
	Preparation	Any step that is substantially comprised of preparation and/or collation of digital and/or hard copy product. *Creation of map base.*
	Manual Operation	Any step that is substantially comprised of manual (non-automated) input. *Map reviews.*
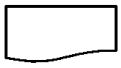	Document	Any process flow step that results in the creation of a critical document. *Map Control Document.*
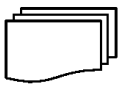	Multi-document	Any process flow step that results in the creation of a critical package of documents. *Prepare Review Package.*
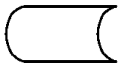	Copy to digital media	Any process flow step that results in the creation of (transitory) digital copy. *Copy to DVD for review.*
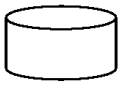	Back-up	Any process flow step that results in the creation of permanent digital copy. *Copy to map base to USGS hard-drive.*
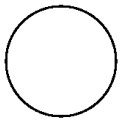	Shipping/Delivery	Denotes process step comprised of packaging, shipping, or delivery. *Submit map project to USGS.*

Form 9-1325
(revised, August 2006)
USGS

INFORMATION PRODUCT REVIEW AND APPROVAL SHEET

SCIENCE CENTER
Yucca Mountain Project Branch

INFORMATION PRODUCT TRACKING NO.
IP-

AUTHOR(S): (last name first; show first name and(or) initials as shown in manuscript)

TEMPLATE! SAVE AS: your document filename_RAS
in X: Publications/From Authors folder (write access granted)

SCIENCE CENTER CONTACT:
(name, address, telephone, fax, email)
Pamela B. Daddow
U.S. Geological Survey
Box 25046 MS 421 DFC Building 53
Denver, Colorado 80225
303-236-5050, ext. 249 Fax 303-236-5047
pbdaddow@usgs.gov

TITLE:

FORM OF PUBLICATION

USGS series
- ☐ Administrative Report
- ☐ Circular
- ☐ Data Series
- ☐ Fact Sheet
- ☐ General Information Product
- ☐ Open-File Report
- ☐ Professional Paper
- ☐ Scientific Investigations Map
- ☐ Scientific Investigations Report
- ☐ Techniques and Methods
- ☐ Outside information product
  - ☐ Edit requested
  - ☐ No edit requested
- ☐ Abstract

PUBLISHER, JOURNAL, OR MEETING:

Format
- ☐ Print
- ☐ CD-ROM
- ☐ WWW
- ☐ Video
- ☐ Print on Demand
- ☐ Other

Check all of above that apply

_____ **TOTAL PAGES** (including title page and all page-size figures and tables)

_____ **TABLES COVERING** _____ **PAGES**

NUMBER OF ILLUSTRATIONS:

Color	*B&W*	
_____	_____	Line drawings
_____	_____	Photographs
_____	_____	Plates

IF PART OF A MULTICHAPTER USGS PUBLICATION:
Total number of chapters ☐ To be published ☐ Together ☐ Separately

DEADLINE:

ARE GEOLOGIC NAMES USED? IF YES, REVIEW REQUIRED. Yes ☐ No ☐

SUPERSEDES OPEN-FILE REPORT? No ☐ Yes, number: _____

REMARKS: (with initials, add additional pages if needed)

PUBLICATION CONTENTS
- ☐ New interpretive
- ☐ Previously approved interpretive
- ☐ Noninterpretive

NAME, TITLE, AFFILIATION	DATE IN	DATE OUT (indicate hours spent)	CHECK PROCESSING STEP WITH "X"									SIGNATURE (or attach e-mail)
			Author Submission	Supervisor Approval	Peer Review	Technical Specialist Review	Office of Communications Review	Science Center Approval	Editorial Review	PSC Approval	Bureau Approval	

CONTINUE ON ADDITIONAL FORMS IF NECESSARY

Figure 5: USGS Information Product Review and Approval Sheet.

INSTRUCTIONS FOR AUTHORS

- Map Submission -

In an effort to continue refining and streamlining the geologic map review and publication process, the NASA Planetary Geology and Geophysics (PGG) Program's Geologic Mapping Subcommittee (GEMS), in conjunction with the USGS Astrogeology Science Center, provides guidelines and checklists for formal map submission. For detailed explanations of the following map components, please see the most recent version of the GEMS-endorsed Planetary Geologic Mapping Handbook:
http://astrogeology.usgs.gov/Projects/PlanetaryMapping/guidelines/

COVER LETTER – A signed and dated cover letter should be included addressed to USGS Map Coordinator Ken Tanaka to serve as the indicator of formal map submission. The map title, author, and scale should be indicated therein.

COVER INFORMATION – A cover page should be included with the map text that denotes map title, authors, USGS SIM series, scale, contact, and lineage (*e.g.*, date submitted, date re-submitted). Below is an example of the cover information.

Geologic Map of the Willy Nilly Region (MTM 12345), Mars

By John A. Smith and Jane B. Jones

U.S. Geological Survey Scientific Investigations Map SIM xxxx (TBD)

Scale 1:1,000,000

Contact:
John A. Smith
Planetary Research Institute
1234 Elm Street
Sunny, CA 12345

EXAMPLE

LIST OF COMPONENTS – The cover page should be followed by a page listing text and map components that are being submitted. Below is an example of the component list, which should be used as a guide for compiling the text and map.

Geologic Map Text
- Introduction
- Physiographic Setting
- Map Base and Data
- Methodology
- Geologic Summary
- References
- Description of Map Units

Table(s)
Figure Captions

Map Sheet
Colored and annotated geologic map
Correlation of Map Units (COMU)
Explanation of Map Symbols (EOMS)
Pamphlet Cover/Geologic map context [optional]
Figure(s)
Cross-sections [optional]

EXAMPLE

NOMENCLATURE – Map author is encouraged to include IAU-approved nomenclature as a GIS layer to the geologic map prior to map submission. Please contact USGS for assistance (Jen Blue, jblue@usgs.gov).

FILE FORMATS – Text components should be submitted for external and editorial review as Word documents (*.doc or *.docx preferred) or some other editable digital format. Map components should be submitted as Adobe PDF documents (*.pdf) and ArcGIS files (see example below). Please contact USGS for assistance.

FILE NAMES – Consistent file names assist with organization, review, and lineage tracking. Each text and map component file should be identified by (1) **component**, (2) **author initials**, and (3) **date**. For example, for a Correlation of Map Unit submitted by John A. Smith on May 15, 2011, the file should be in Microsoft Word format (*.doc or *.docx) and named "COMU_JAS_5-15-11". Below is an example list of file structures and naming conventions.

FILE STRUCTURE – Files should be organized into an intuitive directory tree for delivery to USGS for external and editorial review. These should include not only the text and map components but also the complete set of GIS files. An example structure is located below (folders are shown in **bold**).

MTM12345_500K_GEOMAP <top level folder>
- **Geologic_Map_Text** <second level folder>
  - DOMU_JAS_5-15-11.docx <file>
  - MapText_JAS_5-15-11.docx <file>
  - Table1_JAS_5-15-11.docx <file>
  - Table2_JAS_5-15-11.docx <file>
  - FigureCaptions_JAS_5-15-11.docx <file>
- **Map_Sheet** <second level folder>
  - **COMU** <third level folder>
    - COMU_JAS_5-15-11.pdf <file>
  - **EOMS** <third level folder>
    - EOMS_JAS_5-15-11.pdf <file>
  - **Figures** <third level folder>
    - Figure1_JAS_5-15-11.pdf <file>
    - Figure2_JAS_5-15-11.pdf <file>

Figure3_JAS_5-15-11.pdf <file>
GeoMap <third level folder>
MTM85200_500K_JAS_5-15-11.pdf <file>
GIS_Files <third level folder>
BaseMaps <fourth level folder>
LayerFiles <fourth level folder>
MTM12345_1M.gdb <ArcGIS geodatabase>
MTM12345_1M.mxd <ArcGIS project>

EXAMPLE

SUBMISSION PACKAGE – The author is responsible for compiling the full map submission package, as outlined above and in the Planetary Geologic Mapping Handbook, and conveying that package in full to the USGS Map Coordinator. Map packages can be delivered either via FTP sites or as a CD/DVD. Delivery method should be worked out in connection with the USGS Map Coordinator. No hard-copy maps are required, as these will be printed and delivered to reviewers by USGS as needed.

DIGITAL TEMPLATES – Digital templates are available as guidelines for tables and the Correlation of Map Units. These can be downloaded at the following link:

http://astrogeology.usgs.gov/Projects/PlanetaryMapping/

USGS CONTACT INFORMATION - Please contact the USGS Astrogeology Science Center using information provided below for assistance or clarification.

Map Coordinator: Ken Tanaka (ktanaka@usgs.gov)
GIS Data Specialist: Trent Hare (thare@usgs.gov)
GIS Project Specialist: Jim Skinner (jskinner@usgs.gov)
GIS Project Specialist: Corey Fortezzo (cfortezzo@usgs.gov)
Nomenclature Specialist: Jen Blue (jblue@usgs.gov)